The Ministry of Education and Science of Russian Federation
Federal state autonomous educational institution of higher education

«NATIONAL RESEARCH
TOMSK POLYTECHNIC UNIVERSITY»

Institute of High technology physics
Specialization Material science and technology of materials
Department Material science in mechanical engineering

Master thesis

Research subject
Investigation of Lamb wave ultrasonic technique for non-destructive evaluation of aluminum alloys

Student

Group	Name	Signature	Date
4BM4I	Shah Ronak Tushar		

Scientific adviser

Position	Name	Degree	Signature	Date
Professor in the Department of Material science in mechanical engineering	Panin Sergey Viktorovich	PhD		

ADVISERS:

Section: «Financial management, resource efficiency and resource saving»

Position	Name	Degree	Signature	Date
Senior Lecturer, Department of Management	Gavrikova Nadezhda Alexandrovna			

Section: «Social responsibility»

Position	Name	Degree	Signature	Date
Professor, Department of ecology and safety	Fedorchuk Yurii Mitrofanovich	PhD		

ADMIT THESIS FOR DEFENSE:

Head of the department	Name	Degree	Signature	Date
Material science in mechanical engineering	Panin V.E.	PhD, Academician of RAS		

Tomsk – 2016

Expected learning outcomes on 22.04.01 Materials Science and Technology of Materials (MSc)

Code of result	The result of study
P1	Research, analyze and summarize scientific and technical information in the field of materials science and materials technology with the use of modern information and communication technologies, global information resources
P2	Work with patent law and copyright law when preparing documents for patenting and design know-how
P3	Perform market research and analysis process as a management object, to develop a feasibility of study for innovative solutions in the professional activity
P4	Led the team in their professional activities, tolerant perceiving social, ethnic, religious and cultural differences
P5	Introduce technology in the production of ceramic, metal materials and products, including Nano-materials, be ready for the professional use of modern equipment and devices, allowing to receive and diagnose the materials and products for various purposes.
P6	To develop new and upgrade existing technology for ceramic, metal materials and products, including nano-materials
P7	Implement quality management system in the field of materials, operate equipment to diagnose materials and products, including nano-materials
P8	To act in unusual situations, to bear the social and ethical responsibility for their decisions, to choose the most rational ways of protection and order in the actions of a small team in emergency situations
P9	Oral and written Communicate in the official language of the Russian Federation and foreign language to meet the challenges of professional activity, to prepare and submit the presentation for plans and results of own and team activities, build and defend their own opinions and scientific positions
P10	Independently learn new research methods, change of scientific opinion, pedagogical and production profile of their professional activities
P11	Apply the principles of rational use of natural resources, the basic terms and methods of social, humanitarian and economic approaches in solving professional problems, taking into account the consequences for society, economy and ecology.
P12	Use general categories and general production and management concepts in professional activity

The Ministry of Education and Science of Russian Federation
Federal state autonomous educational institution of higher education

**«NATIONAL RESEARCH
TOMSK POLYTECHNIC UNIVERSITY»**

Institute of High technology physics
Specialization Material science and technology of materials
Department Material science in mechanical engineering

APPROVED:
Head of the department
__________ _________ Panin V.E.

Task
for research work of master degree

Type of work:

Master thesis

Student:

Group	Name
4BM4I	Shah Ronak Tushar

Aim of the work:

Investigation of Lamb wave ultrasonic technique for non-destructive evaluation of aluminum alloys	
Approved by order of the Director IHTP	Order №1332/c from 19.02.2016

Completion date for the work:	

TECHNICAL TASK:

Initial data for work	Specimens of AA2024 and AA7068, ultrasonic transducers, equipment for generating and receiving the ultrasonic signals, consumables for specimen preparation, testing machines for static and fatigue tension tests, digital image correlation stereo system, personal computers.
The list of task for research, design and development	Perform an analytic review on following subjects: fatigue and fracture of structural materials, non-destructive testing, structural health monitoring, digital image correlation, Lamb waves, ultrasonic testing. Prepare specimens with glued ultrasonic transducers and perform cyclic and static tests, during which assess the state of specimens using ultrasonic Lamb waves. Record specimen deformation process using digital image correlation method in order to obtain additional information about the processes of deformation and

	fracture. Study the features of change (decay) of ultrasonic signals propagated through gage length of the sample during the tests, analyze the parameters that are sensitive to the stress-strain state and the processes of nucleation and propagation of fatigue cracks. Compare the main stages of deformation and fatigue crack nucleation according to the digital image correlation method and the data obtained by the ultrasonic method using Lamb waves.
List of graphic material	

Advisers on sections of the work

Section	Adviser
Financial management, resource efficiency and resource saving	*Gavrikova Nadezhda Alexandrovna, Senior Lecturer, Department of Management*
Social responsibility	*Fedorchuk Yurii Mitrofanovich, PhD, Professor, Department of ecology and safety*
Research technique and results	*Burkov Mikhail Vladimirovich, PhD, Associate Professor of Department of Material science in mechanical engineering*

The section titles, which must be written in Russian and foreign languages:

All section must be written in English

Completion date on a calendar plan:	

Task is issued by scientific adviser:

Position	Name	Degree	Signature	Date
Professor in the Department of Material science in mechanical engineering	Panin Sergey Viktorovich	PhD		

Task is accepted by student:

Group	Name	Signature	Date
4BM4I	Shah Ronak Tushar		

The Ministry of Education and Science of Russian Federation
Federal state autonomous educational institution of higher education

«NATIONAL RESEARCH
TOMSK POLYTECHNIC UNIVERSITY»

Institute of High technology physics
Specialization 22.04.01 Material science and technology of materials
Level of education magistracy
Department Material science in mechanical engineering
Implementation period (spring semester of 2015/2016 year)

Type of work:

Master thesis

CALENDAR PLAN
for research work of master degree

Completion date for the work:	

Date of control	The section name (module) / type of work (study)	Max. points
10.02.16	*Literature review*	*10*
20.02.16	*Preparation of the specimen, establishing of testing technique*	*10*
10.03.16	*Testing of AA2024*	*15*
25.04.16	*Testing of AA7068*	*15*
25.05.16	*Writing of Management section*	*5*
27.05.16	*Writing of Social responsibility section*	*5*
30.05.16	*Analysis of results, conclusion on the research*	*20*
20.06.16	*Writing of final version of thesis*	*20*

Prepared by scientific adviser:

Position	Name	Degree	Signature	Date
Professor in the Department of Material science in mechanical engineering	Panin Sergey Viktorovich	PhD		

APPROVED:

Head of the department	Name	Degree	Signature	Date
Material science in mechanical engineering	Panin V.E.	PhD, Academician of RAS		

Abstract

Master thesis consists of 110 pages, 54 Figures, 27 tables, with 60 references, 0 appendixes.

Keywords: Ultrasonic testing/Inspections, Lamb wave, Structural health monitoring, AA2024, AA7068, Static & Fatigue testing, Digital Image correlation, NDT & E.

Subject of research – Ultrasonic Inspection on Aviation Grade aluminium using ultrasonic Lamb Wave principal and algorithms

Aim of study – Is to investigate the ultrasonic technique and to establish the data processing algorithms in order to improve reliability and quality prospects in aviation industries with subject to online monitoring of structures for crack growth sensing through operation.

During the research we investigated static and fatigue testing on dogbone shape specimens of AA2024 & AA7068 (aviation grade aluminum alloys) with weld joints and without weld joints and as well as ultrasonic impact treated.

After the research there were obtained epoxy accessibility for bonding of PZT transducers, understanding of Lamb wave propagation, the change in parameters of signals during different stage of loading of specimens and fatigue crack growth.

Main technological, technical and operational parameters: Piezoelectric transducers, surface mounting, activating and receiving of lamb waves, universal testing machines, digital image correlation studies and analysis of result through different software specially designed and commercially available (Cool edit pro), Origin pro for analysis of different obtained data: stress-strain curve, maximum envelope, second momentum (variance) & normalize cross correlation.

The degree of implementation: the developed technique is now at the stage of laboratory experiments. Further experiments on special structure-like specimens are needed in order to implement it for Structure health monitoring, as well as for Nondestructive testing and evaluation.

Application area: the results can be used for development of robust structural health monitoring systems to be applied in different industries especially in the aerospace

Cost-effectiveness/value of work: the proposed laboratory technique being used for the development of working structural health monitoring systems can decrease the cost and time of inspection of aircrafts, as well as different mechanical engineering structures.

Future plans are focused on the research of structure-like specimens for the development of SHM technique for commercial as well as defense aviation industry.

Contents

Introduction

Main (relevance) Development of Materials in Aerospace Industry
Design optimization of mechanical properties is one of the most challenging tasks in the design and development of new materials for diverse machining applications. Mechanical properties of material play a crucial role during the entire life of component.

Aerospace and space industry has traditionally been a pacemaker for development and introduction of new materials systems and production technologies. The key driving forces for materials development are weight reduction, application-specific performance improvement, and reduced costs. Application of advanced engineering materials has significant impact on both economic and ecological issues. Polymer matrix composites combine high stiffness and strength with low density and are therefore widely used for lightweight structural applications. Aluminum alloys essentially cover cryogenic and moderate elevated temperature range applications. Fiber reinforcements are used where high stiffness and/or wear resistance are required. Titanium alloys are presently used in the temperature range up to 500–550 °C. Fiber reinforcement offers dramatically improved strength and creep resistance, while Titanium aluminides may well push the temperature limit another 200 °C. Super alloys are capable of service temperatures up to 1150°C. Long-term application requires protective coatings against hot corrosion and oxidation. Thermal barrier coatings have been introduced to further expand the useful temperature range of highly loaded components. Ceramics have only seen limited usage so far, but improvement of damage tolerance by fiber reinforcement will presumably broaden their application range at temperatures beyond 1100 C in the future [1,2].

The aerospace and space sector has traditionally been a promoter for the development and application of advanced engineering materials. The demand for these materials is generally spurred by the performance requirements of a component, which is usually an integral part of a complex technical system. The key issues to be addressed by advanced material development are material properties, material fabrication and finally costs. Component performance in this sector is primarily determined by mechanical properties such as strength, stiffness, and damage tolerance as well as by physical and chemical properties such as density, corrosion resistance at ambient and high temperatures. The availability of suitable fabrication methods plays a crucial role with regard to both material properties and costs and may therefore finally determine whether an advanced material will find application. Recently life cycle costing has been recognized as an important tool to assess the economic viability of the material. The key driving forces for engineering materials development in the aerospace and space industry are weight reduction and increased temperature capability. Weight reduction is most effectively done by reducing density. Furthermore, weight reduction of an individual component can generate a snowball effect if, for example, the airframe and the engine of an aircraft are re-optimized allowing the use of less stringers, a down-sized engine, a smaller wing, etc. As a rule of thumb, each pound of direct weight saved in a primary structure results in nearly another pound saved indirectly in another part of the aircraft. A reduced take-off weight of an aircraft, space vehicle or satellite directly affects the amount of fuel burned, indicating the enormous economical and ecological benefits associated with lightweight design. For aircraft, similar benefits associated with a reduction of fuel consumption are achieved by increasing the efficiency of the engines via higher turbine inlet temperatures [3].

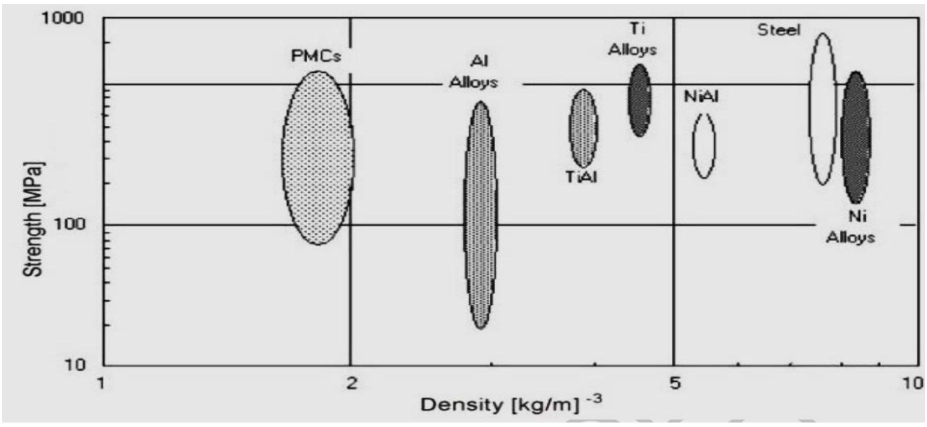

Figure 1. Strength and Density plot for Structural Materials

Although a number of additional criteria is stressed for each individual application, materials are often classified by using property charts such as shown in Figure 1. Considering their strength and density, it becomes quite obvious why aluminum and titanium alloys are the classical lightweight aerospace alloys

Aluminum alloys have been used at normal temperature and in cryogenic applications in aerospace engineering, and researchers have focused on the further reducing density, improving the elevated temperature capabilities and the corrosive resistance of the alloys. The polymer matrix composites offer even higher strength at lower density and have, up to some extent, which will replace metallic materials in specific applications. Titanium alloys are used where lighter aluminum alloys with the no longer meeting strengths, corrosion resistance and elevated temperature requirements. A major effort has been to increase service temperature of titanium alloys. Nearly-alpha type alloys with improve elevated temperature resistance have been introduced and there is more promising are titanium aluminides [4].

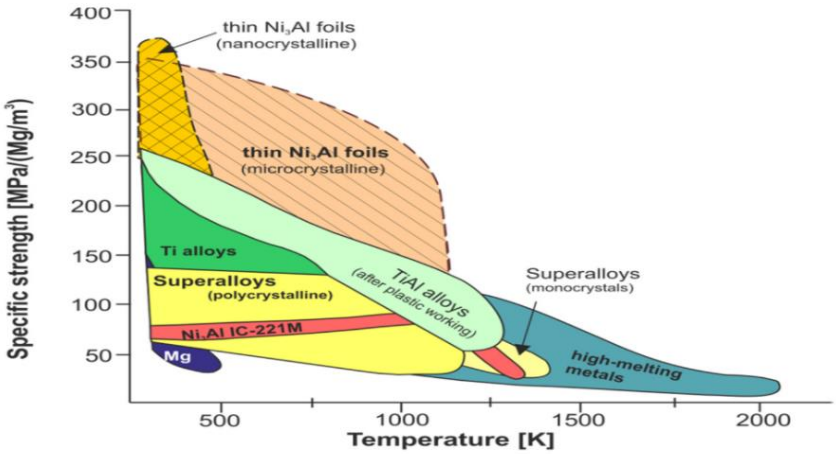

Figure 2. Specific Strength vs. Temperature for Structural Materials

With use temperatures of the order of 800 degrees centigrade showing above figure, these intermetallic have the potential to replace Ni-base super alloys. Ni-base super alloys are the prime choice materials in aero-engines, in the environment where the high temperature capabilities and high strength are required. Single-crystal turbine blades represent today’s advanced technology. Despite their potential for high temperature applications, ceramic components have not been introduced into advanced aero-engine design to a large extent, but the future may see an increasing number of ceramics material for structural parts, mainly when reinforced to enhance toughness.

For high strength aluminum alloys many times strength, stiffness and the toughness increase with fall in temperature. Example of low-temperature applications are the aircraft’s operating at heights beyond 12 km (220 K), structures in space (120 K), storage of liquid cryogenic fuels such as oxygen or hydrogen for propulsion launch systems such as Ariane or the space shuttle. Currently, the huge cryogenic aluminum composition is the expendable tank for the space shuttle [5].

Purpose of investigation - Failure of an Aircraft Structure

Failure of an aircraft structural component can have catastrophic consequences, with resultant loss of life and of the aircraft. The investigation of defects and failures in aircraft structures is, thus, of vital importance in preventing further incidents.

There are many examples of component failures and defects that were detected before an accident could occur, i.e. during routine maintenance and inspection operations. Many in-service aircraft are now required to operate beyond their original design life, partly as a result of the accelerating costs of replacement and also the ability to upgrade systems in old airframes.

Historically, the majority of the structural failures examined have been in metallic materials, reflecting the predominance of metallic structures in aircraft. However, since the mid-1980s an increasing number of aircraft manufacturers have been making use of fiber-reinforced polymer composites for structural components,

What causes failure?

In general, failures occur when a component or structure is no longer able to withstand the stresses imposed on it during operation. Commonly, failures are associated with stress concentrations, which can occur for several reasons including:

- Design errors, e.g. the presence of holes, notches, and tight fillet radii.
- The microstructure of the material may contain voids, inclusions etc.
- Corrosive attack of the material, e.g. pitting, can also generate a local stress concentration.

From our records and case histories data, an assessment can be made of the frequency of failure modes (Table 1). This reveals that the incidence of fatigue failure dominates the distribution in aircraft. This would suggest, therefore, that fatigue is the predominant failure mode in service. The detection and rectification of corrosion damage on in-service aircraft, however, consumes more effort than the repair of fatigue cracking. The high occurrence of fatigue failure observed probably reflects the destructive nature of this failure mode, while corrosive attack is generally slower than fatigue, and usually more easily spotted and rectified during routine maintenance.

Table 1. Failure modes

Failure mechanisms	Percentage of Failures	
	Engineering Components	Aircraft Components
Corrosion	29	16
Fatigue	25	55
Brittle fracture	16	–
Overload	11	14
High temperature corrosion	7	2
SCC/Corrosion fatigue/HE	6	7
Creep	3	–
Wear/abrasion/erosion	3	6

Fatigue is a process whereby cracking occurs under the influence of repeated or cyclic stresses, which are normally substantially below the nominal yield strength of the material. Components that fail by fatigue usually undergo three separate stages of crack growth, which are described as follows:

- Initiation of a fatigue crack. This can be influenced by stress concentrations such as material defects or design.
- Propagation of the fatigue crack. This is progressive cyclic growth of the crack.
- Final sudden failure. Eventually, the propagating crack reaches a critical size at which the remaining material cannot support the applied loads and sudden rupture occurs.

Fatigue failures generally leave characteristic markings on the fracture surface of cracks from which the failure investigator can deduce a great deal of information. The most obvious are the classic ‘beach marks’, which are commonly observed macroscopically. Beach marks indicate successive positions of the advancing crack front and are usually the first telltale signs that the mode of crack growth is fatigue. Fatigue fractures tend to be relatively smooth near the origin and show slight roughening of the surface as the crack progresses. There tends to be little or no macroscopic ductility associated with fatigue cracking.

Detailed examination of the fracture surface in a scanning electron microscope (SEM) usually shows evidence of fatigue striations (dependent on the material), which represent one cycle of load and crack propagation. If the magnitude of load cycle remains constant, the striations normally appear closer near the origin, gradually increasing in spacing as the crack front progresses due to the increasing stress at the crack tip. By taking measurements of striation spacing at various distances from the origin to the end of the crack, it is possible to estimate the total number of load cycles to cause failure. If the cause of the loading can be determined, the number of cycles to failure can then be used to estimate the time required for crack growth.

Table 2. Summary of fatigue initiation sites observed in aircraft.

Initiation Site	Number of Accidents	
	Fixed Wing	Rotary Wing
Bolt, stud or screw	108	32
Fastener hole or other hole	72	12
Fillet, radius or sharp notch	57	22
Weld	53	3
Corrosion	43	19
Thread (other than bolt or stud)	32	4
Manufacturing defect or tool mark	27	9
Scratch, nick or dent	26	2
Fretting	13	10
Surface or subsurface flaw	6	3
Improper heat treatment	4	2
Maintenance-induced crack	4	N. A
Work-hardened area	2	N. A
Wear	2	7

Fatigue cracking is the most common cause of structural failure in aircraft, even though the laboratory fatigue behavior of most metals and alloys is well understood. Materials and their design can be taken into consideration so that the probability of fatigue cracks occurring can be reduced, but it is often the case that the possibility cannot be removed completely. Therefore, many aircraft structural components are designed with a safe or inspection-free life, below which fatigue cracking should not be a cause for concern. The fact that fatigue failures still occur, however, indicates the complex nature of this problem. There are many variables that influence fatigue, some of which are the mean stress, peak stress, frequency of loading, temperature, environment, material microstructure, surface finish, and residual stresses. Many of these factors are taken into account when determining the safe life of a component and, therefore, the majority of fatigue failures in aircraft causing catastrophic failure tend to be those that initiate as the result of unforeseen circumstances.

Material surface defects such as forging laps or surface cracking can increase the local stress, producing a concentration at these points that could initiate fatigue much quicker than would be expected. However, many aircraft components are thoroughly inspected by non-destructive techniques after manufacturing and these types of defects are usually detected and rectified. Stress concentrations caused by surface defects such as scratches and wear tend to be more common as these may not be present at build, but can be introduced during service. Another common cause of stress concentration is corrosion, which can lead to fatigue crack initiation.

Ductile or overload failure occurs when a material has been exposed to an applied load at a relatively slow rate to the breaking point of the material. This results in a ductile fracture of the material, with the fracture surface exhibiting tearing of the metal and plastic deformation. On rapid application of a load, fast fracture or brittle failure can occur. Microscopic examination of brittle fractures reveals intergranular or transgranular facets on the fracture surface.

Corrosion is the chemical degradation of metals as a result of a reaction with the environment. It usually results in failure of components when the metal wastes to such an extent that the remaining material cannot support the applied loads or the corrosion renders the component susceptible to failure by some other mode (e.g. fatigue). Extensive work has been carried out on the rates and types of corrosion observed in different materials so that selecting a suitable material in terms of corrosion resistance for a known environment is relatively straightforward. In aircraft structures, however, the strength to weight ratio can be a more desirable property than corrosion resistance and in these circumstances the most suitable material cannot always be used. In cases like this, measures must be taken to limit corrosion, which most commonly involve the use of a coating, such as a paint system, to act as a barrier to the environment. There are various forms of corrosion that exist, each of which poses different problems to aircraft structures. The most common types of corrosion observed are discussed below

Uniform corrosion, as its name suggests, is corrosion that occurs without appreciable localized attack, resulting in uniform thinning.

Pitting corrosion is a localized form of attack, in which pits develop in a material causing localized perforation of the material. Pitting corrosion occurs when one area of a metal surface becomes anodic with respect to the rest of the surface of the material. The pits formed by this type of attack are generally very small and, therefore, difficult to detect during routine inspection. Pitting attack can cause failure by perforation with very little weight loss to the material.

Crevice corrosion occurs when localized changes in the corrosive environment exist and lead to accelerated localized attack. These changes in the localized corrosive environment are generated by the existence of narrow crevices that contain a stagnant environment, which results in a difference in concentration of the cathode reactant between the crevice region and the external surface of the material. Crevices can be formed at joints between two materials, e.g. riveted, threaded, or welded structures, contact of a metal with a non-metallic material, or a deposit of debris on the metal surface.

Galvanic corrosion occurs when dissimilar metals are in direct electrical contact in a corrosive environment. This results in enhanced and aggressive corrosion of the less noble metal and protection of the more noble metal of the bimetallic couple. This type of corrosion can be recognized by severe corrosion near to the junction of the two dissimilar metals, while the remaining surfaces are relatively corrosion-product free. Galvanic corrosion is generally a result of poor design and materials selection.

Stress corrosion cracking is a mechanical-environmental failure process in which tensile stress and environmental attack combine to initiate and propagate a fracture. Failure by stress corrosion cracking is frequently caused by simultaneous exposure to an apparently mild chemical environment and to a tensile stress well below the yield strength of the material. The stress required for failure can originate from in-service conditions or from residual stress during component manufacturing.

Hydrogen embrittlement is a failure process that results from the retention or absorption of hydrogen in metals, usually in combination with applied tensile or residual stresses. It most frequently occurs in high-strength steels (>1100 MPa). For aircraft components, the common source of hydrogen embrittlement is hydrogen absorption during manufacturing processes such as pickling and electroplating [6,7,8].

Investigation tasks

Aluminum seems to be king in aircraft construction, though in recent years some new alloys have been applied. These super alloys are still quite expensive for the aircraft homebuilder. With its good strength to weight and cost ratio, aluminum is still used very widely in the industry.

Aluminum is the third most abundant element in the Earth's crust after oxygen and silicon. It appears as a silverfish white metal that has a strong resistance to corrosion and like gold, it is also rather malleable. Perfect for our applications in aviation.

The main object is to develop a technique for investigation of structural life of aircraft aluminum using Lamb wave principle and to establish a signal processing algorithms for evaluation of ultrasonic results. We were conducted investigations on aviation grads aluminums mainly on AA2024T3 and AA7068, through static tensile testing and cyclic testing. The specimen was divided in three main categories.

1) Without weld joint
2) With weld joint,
3) With Ultrasonic Impact treatment (only apply on AA7068 alloy)

The research consists main three investigations tasks:

Task 1 – To make the preparation of specimen where modifications of specifications with cleaning, grinding, polishing on emery papers and welding, heat treatment, dimensions of specimen, PZT transducer, surface mounting of the transducer on the specimens (including different positions of transducer on different specimens), wave activator & receiver, and arrangement of Digital Image correlations

Task 2 – the development of the technique, arrangement of all equipment for static and fatigue testing and the analysis of the acquired data output were illustrating with different software used for this investigations like acquired data form static and fatigue testing through inbuilt software from manufactures, cool edit pro used for signal analysis and origin pro used for Graphical generation of analyzed data.

Task 3 – The discussions of the analyzed data for development of techniques, this task are presented in different publications.

Scientific and practical originality. The work deals with novel research of technique for structural health monitoring of aluminum alloys. There is a comprehensive investigation of different aluminum alloy specimens (with or without welding joints) subjected to static and fatigue loading with registration of ultrasonic and optical data in order to establish a technique for evaluation of stress-strain state.

Scientific and practical value. The results can be used for development of robust structural health monitoring systems to be applied in different industries especially in the aerospace.

1 Review on NDT and SHM of structural materials

1.1 Aluminium alloys

The 2xxx, 6xxx and 7xxx Aluminium series as well as some Al-Li alloys enjoy the widest use in aircraft structural applications.

The 2xxx series alloys contain copper as the primary alloying element, which produces high strength but reduced corrosion resistance. The 2024 alloy is probably the most widely used alloy in aircraft applications

The 6xxx series contains magnesium and silicon, which form the magnesium silicide (Mg2Si). The alloys of this series offer a good balance be- tween corrosion resistance and strength along with a good weldability.

In the 7xxx group the primary alloying element is zinc. In this group two types of alloys exist: The Aluminium –zinc –magnesium alloys and the Aluminium –zinc-magnesium-copper alloys, with the second type being less corrosion resistant

1.1.1 Fatigue of Aircraft Aluminium Alloys

Damage tolerance analyses and reliable prediction of crack growth under fatigue loading rely heavily on experimental data and the comprehensive understanding of the underlying crack growth mechanisms [9]

Fatigue dam-age in the material can be divided into a number of subsequent phases characterized by cyclic slip, crack nucleation, micro-crack growth and macro-crack growth up to the final material failure. The different physical processes, which prevail in the gradual fatigue damage accumulation during the fatigue life of a metallic component, are complex and interrelated. They develop with increasing number of fatigue cycles from atomic to macro-scale damage mechanisms and also entail a host of material, geo-metric and loading parameters [10]. It assumes that failure occurs in a critical element when the volume energy density reaches a certain threshold.

Crack growth is dependent to crack closure, which is correlated to several features, such as fracture surface roughness, residual plasticity in the wake or ahead of the crack tip, oxide debris etc. Herein, the role of microstructure and material properties ahead of the crack tip is important.

Authors used material in the experimental investigation was aluminum alloy 2024 T351 in plate and sheet product configuration with a thickness of 15 and 3.2 mm respectively. Both plate and sheet materials were tested in conventional and high purity (HP) composition, which refers to the 2024 material with reduced Fe-rich and Mg2Si phases. The grain morphology obtained for the plate and sheet product is the result of the different degree of rolling process in order to achieve the required thickness (15mm and 3.2 mm respectively). As a result, a different grain microstructure was obtained which corresponds to larger, elongated grains for the plate materials compared to the fine equiaxed grains in the sheet microstructure

The fatigue tests carried out were constant amplitude fatigue crack growth tests as well as constant amplitude fatigue crack growth experiments including single and periodic tensile overloads

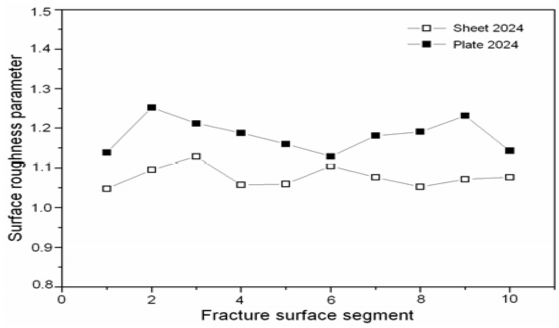

Figure 1.1. Amplitude fatigue

In Fig. 1.1 constant amplitude fatigue crack propagation curves of the materials tested are displayed in terms of half crack length versus stress intensity factor range. The higher crack growth resistance for specimens taken from plate product is reflected through the lower crack growth rates com- pared to the sheet material.

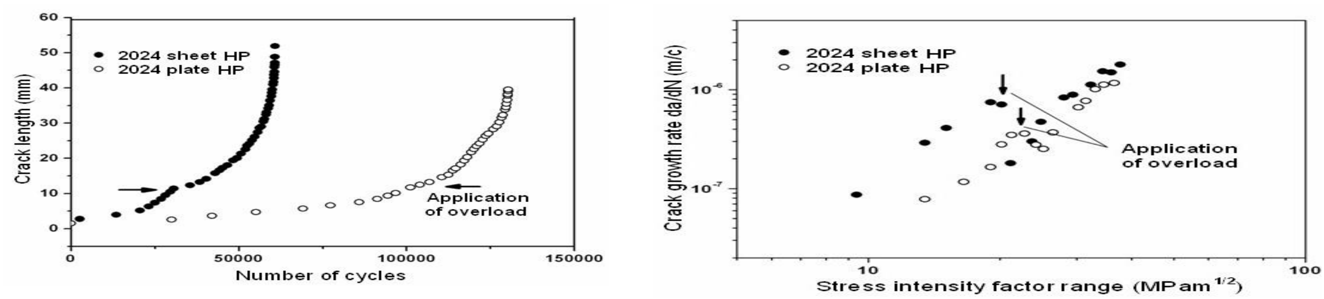

a) b)

Figure 1.2.Crack length (a) and fatigue crack growth rates (b) after tensile overload for sheet and plate material.

The plate product the fractured surface region which is perpendicular to the load is smaller and the developed shear lips are wider in comparison to the sheet material. On the fracture surfaces of the plate materials pronounced black debris could be observed, which according to [11] could be evidence of increased lower and upper crack surfaces contact during fatigue crack growth. By careful examination of fractured surfaces in Fig. 6 it can be observed that crack surface contact marks are more pronounced on the shear lips of plate material specimens. The described mechanism can lead to increased crack closure.

In the case of single and multiple overloads the load interaction phenomena present lead to significant plasticity effects. Thus, crack growth mechanisms become more complex and the results obtained cannot be discussed solely under the viewpoint of pronounced crack closure effects due to fracture surface characteristics.

Concluding Remarks

The fatigue crack growth behavior of 2024 T351 aircraft aluminium alloy with variation in microstructural characteristics

(1) The effect of microstructural features (e.g. grain size and morphology), as well as variations in purity composition can influence fatigue crack propagation in the medium ΔK region, which is of high technological interest for damage tolerance design.

(2) Plate microstructure with elongated grain morphology induced by the rolling process exhibited higher crack growth resistance than the micro- structure of the sheet material with smaller equiaxed grains. This behavior could be attributed to pronounced roughness induced crack closure effects in the plate microstructure [12,13].

1.1.2 Welding opinion for aluminium alloys

Effect of welding processes on tensile properties of AA6061 aluminium alloy joints by A. K. Lakshminarayanan & V. Balasubramanian & K. Elangovan

Aluminium alloys find wide applications in aerospace, automobile industries, railway vehicles, bridges, offshore structure topsides and high speed ships due to its light weight and higher strength to weight ratio.

In joining methods difficulties are associated with this kind of joint process, mainly related to the presence of a tenacious oxide layer, high thermal conductivity, high coefficient of thermal expansion, solidification shrinkage and, above all, high solubility of hydrogen, and other gases, in the molten state [14] Further problems occur when attention is focused on heat-treatable alloys, since heat, provided by the welding process, is responsible for the decay of mechanical properties, due to phase transformations and softening.

The preferred welding processes for these alloys are frequently gas tungsten arc welding (GTAW) and gas metal arc welding (GMAW) due to their comparatively easier applicability and better economy.

Friction stir welding (FSW) is an innovative solid phase welding process in which the metal to be welded is not melted during welding, thus the cracking and porosity often associated with fusion welding processes are eliminated [15]. Therefore, the FSW process can also be used to weld heat-treatable Aluminium alloys in order to obtain high-quality joints FSW gives rise to softening in the joints of the heat-treatable Aluminium alloys such as 7075-T651 and 7475-T76 because of the dissolution or growth of strengthening precipitates during the welding thermal cycle, thus resulting in the degradation of mechanical properties of the joints. [16] reported a comparative study on the corrosion resistance of AA6060-T5 and AA6082T6 jointed surfaces via FSW and GMAW process respectively and found friction stir welded sample has a better behavior concerning the pitting corrosion than that of the GMAW sample [17]. Investigated the contrasting difference of fatigue behaviour of joints made from the traditional process of metal inert gas (MIG) welding, and the emerging process of friction stir welding. yield strength of friction stir welded and gas tungsten arc welded joints are decreased 20% and 50 % respectively compared to the base metal.

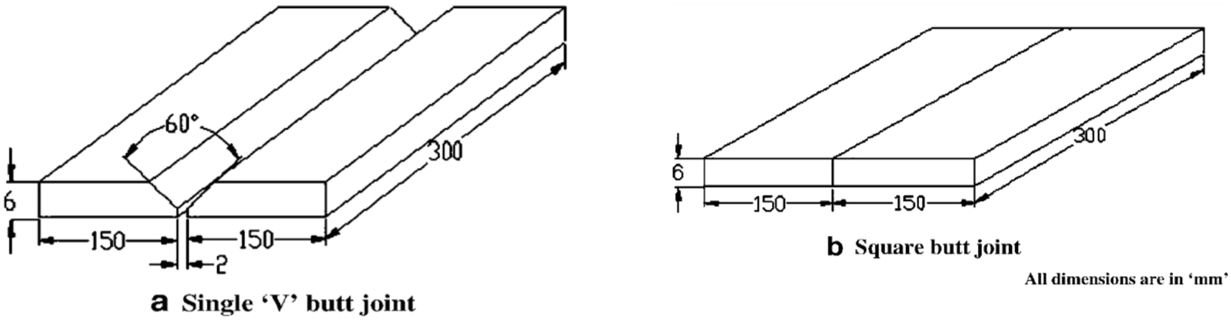

Figure 1.3. Dimensions of joint configuration

The rolled plates of AA6061 Aluminium alloy were machined to the required dimensions (300 mm×150 mm). Single ‘V’ butt joint & square butt joints configuration, as shown in Fig. 1a, was prepared to fabricate GTA and GMA welded joints. The direction of welding was normal to the rolling direction.

High purity (99.99%) argon gas was the shielding gas.

Table 1.1. Mechanical properties of base metal and all weld metals

Type of Material	Yield Strength (MPa)	UltimateTensile Strength (MPa)	Elongation (%)	Reduction in c/s	Hardness (VHN)
Base Metal (AA 6061)	302	334	18	12.24	105
Weld Metal (GTAW)	160	230	8	5.45	65
Weld Metal (GMAW)	150	220	6	4.5	60
Weld metal (FSW)	245	295	14	10.2	85

Tensile properties

The transverse tensile properties such as yield strength, tensile strength, percentage of elongation, notch tensile strength, and notch strength ratio of AA6061 Aluminium alloy joints were evaluated.

Table 1.2. Transverse tensile properties of welded joints

JointType	Y.strength (MPa)	U.T (MPa)	Elon. (%)	Red. c/s (%)	Notch U.T. (MPa)	N.S. Ratio (NSR)	Joint Efficient (%)	W.R.H (VHN)
GMAW	141	63	.4	.80	75	1.073	48.80	58
GTAW	188	11	1.8	.26	28	1.091	62.57	70
FSW	224	48	4.2	56	79	1.125	74.25	85

The average of the three results is presented in Table 1.1. The yield strength and tensile strength of unwelded parent metal are 302 MPa and 335 MPa, respectively. However, the yield strength and tensile strength of GMAW joints are 141 MPa and 163 MPa, respectively. This indicates that there is a 51% reduction in strength values due to GMA welding. Similarly, the yield strength and tensile strength of GTAW joints are 188 MPa and 211 MPa, respectively which are 37% lower compared to parent metal.

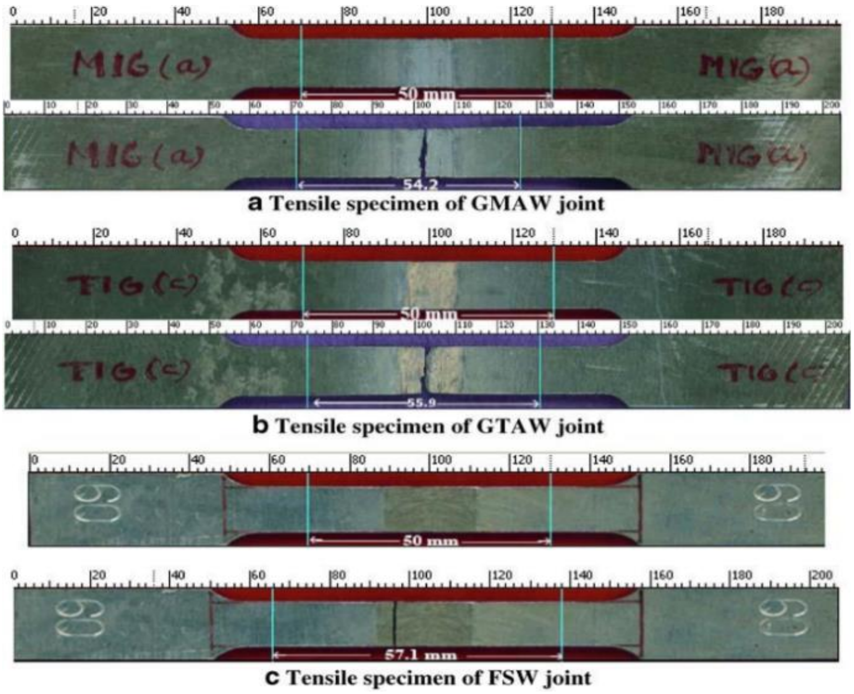

Figure 1.4. Comparison between different weld processes

The hardness across the weld cross section was measured using a Vickers Micro-hardness testing machine, and the values are presented in Table 1.2. The hardness of base metal. This suggests that the hardness is reduced by 47 VHN and 35 VHN in the weld metal region of GMAW and GTAW joints, respectively due to welding heat and the usage of lower hardness filler metal

Fig. 1.4 indicates that the weld region is comparatively weaker than other regions and hence the joint properties are controlled by weld region chemical composition and microstructure [18].

1.1.3 Academic View for Ultrasonic impact treatment

The use of Ultrasonic Impact Treatment to Extend the Fatigue Life of Integral Aerospace Structures by Chris A. Rodopoulos and James Bridges

The fatigue crack propagation in welding direction or perpendicular to it, found more or less pronounced effects of the residual stresses especially in the case of near threshold loading as a result damage tolerance methodologies based on material data can lead to unprecedented errors. In many works the problem was attributed to the presence of residual stresses [19,20,21]. Tensile residual stresses have been found to be responsible for the premature initiation of fatigue cracks, the mitigation of the crack initiation sites, the increase in the number of catastrophic cracks and hence the probability for crack coalescence, etc. In order to minimize the harmful effects of the tensile residual stresses, surface engineering treatments have been employed, it was found that surface treatments can redistribute the residual stresses to the level of obtaining reversal of their direction.

The Ultrasonic Impact Treatment (UIT) [22] is a technique that directly deforms the surface of materials using ultrasonic impacts. This technique fundamentally differs from contact methods of ultrasonic deformation treatment.

The process is mainly controlled by the output of the ultrasonic transducer (frequency), the selected pressure, the feed rate and the number of passes (coverage). The process can induce on request different amounts of cold work and residual stress profiles. The depth of the latter can range from 0.8 to 4mm in Aluminium alloys. [23]

Experimental Investigations & Discussion

The panels were made of 6056-T651 and 2024-T3 Aluminium alloys. Joining of the stringers have been made using laser beam welding. Six points have been selected for measuring the residual stresses using X-Ray diffraction,

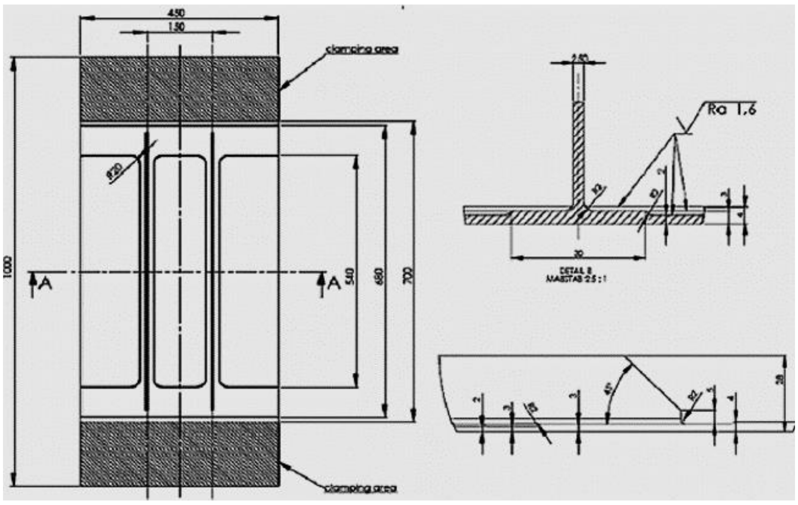

Position	Distance from centre line (mm)	No.
1	10	1
2	50	2
3	70	3
	Distance from Stiffener base	
1	5	4
2	10	5
3	Top	6

Figure 1.4. Schematic representation of the two-stringer testing panel & Position of XRD points

In the case of 6013 point 3 exhibits significant compression while in the case of the 2024 tension has been found. Herein it is important to note that local discrepancies in the residual stress profile will most certainly affect other points. The problem is quite complex and therefore quality control can only be partially sought.

To overcome such problem and in order to induce residual stresses: (a) uniform and (b) having a profile able to enhance the fatigue resistance of the panels Esonix Ultrasonic Impact Treatment was selected.

The panels prior to treatment were cleaned in nitride-free detergent and degreaser suitable for aerospace components. Cleaning is imperative to prevent any residues from machining and handling entering the surface. Uniform clamping of the panels was performed using a vacuum table. The exerted clamping pressure was 50MPa. The parameters have been selected in such way as to smooth the signal from the transducer and hence protecting the uniform distribution of the residual stresses. In order to treat the fillet section between skin and stringer, the tool was set at a 60 angle.

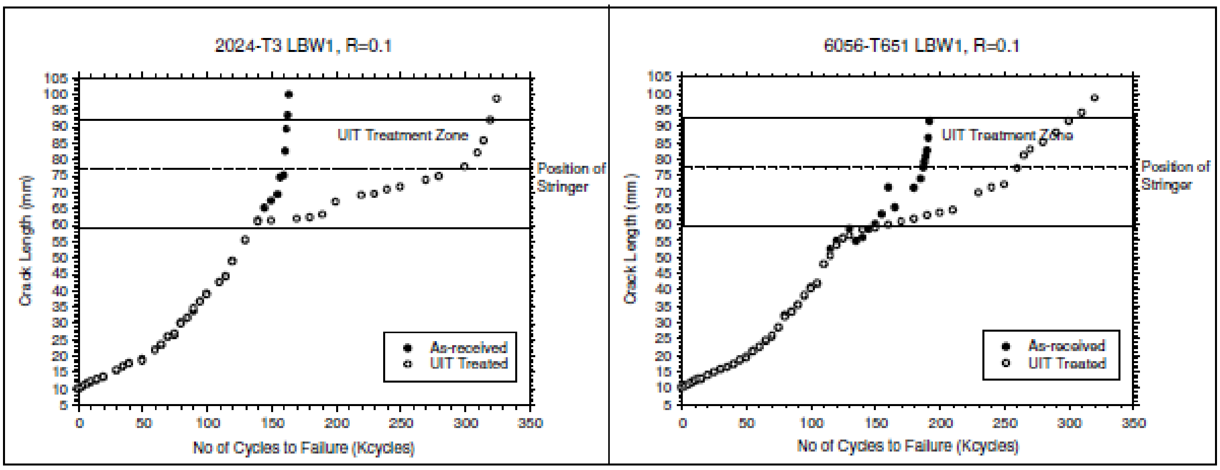

Figure 1.5. Comparison of crack growth rates of 6056-T651 and 2024-T3 LBW

The results indicate that within the UIT treated zone the residual stresses have significantly changed into compression. Their maximum depth is such as to allow enough material for equilibrium without causing tensile peaks

Ultrasonic Impact Treatment has been selected as a process embracing the following benefits: (a) is industrially available, (b) has a process rate similar to that of the joining process, (c) is cheaper that laser shock peening and (d) can offer control over the treatment products [24,25,26].

1.2 NDT&E of structural materials

Nondestructive evaluation is an important method for performance control and condition monitoring. In engineering systems, flaws and especially cracks in the materials of structural systems components can be crucially detrimental to functional performance. For this reason, the detection of defects is an essential part of quality control of engineering systems and their safe successful use. Control techniques are often listed under a variety of headings such as nondestructive testing (NDT), nondestructive evaluation (NDE) or sometimes nondestructive inspection. Applications of NDT techniques, however, are much deeper and broader in scope than just the detection of defects. The determination of various material properties, such as elastic constants of solids or the microstructure and texture of solids are also covered under the NDT title. According to the wide scope of this field, a plethora of physical methods are employed.

Established methods include radiography, ultrasound, eddy current, magnetic particle, liquid penetration, thermography and visual inspection techniques. Applications of NDE in industry are as wide ranging as the techniques themselves and include mechanical engineering, aerospace, civil engineering, oil industry, electric power industry etc.

A large number of components are also in the focus of interest because engineered structures are an integral part of the technological base necessary for our lives and the public infrastructure. The operation of NDT techniques in several industries is standard practice, for example to support condition monitoring for the proper functioning of the daily use of electricity, gas or liquids in which pressure vessels or pipes are employed and where the correct operation of components under applied stress plays a large role for safety and reliability.

1.2.1 Basic Principles of Ultrasonic Testing

Ultrasonic Testing (UT) uses high frequency sound energy to conduct examinations and make measurements. Ultrasonic inspection can be used for flaw detection/evaluation, dimensional measurements, material characterization, and more.

To illustrate the general inspection principle, a typical pulse/echo inspection configuration as illustrated below will be used.

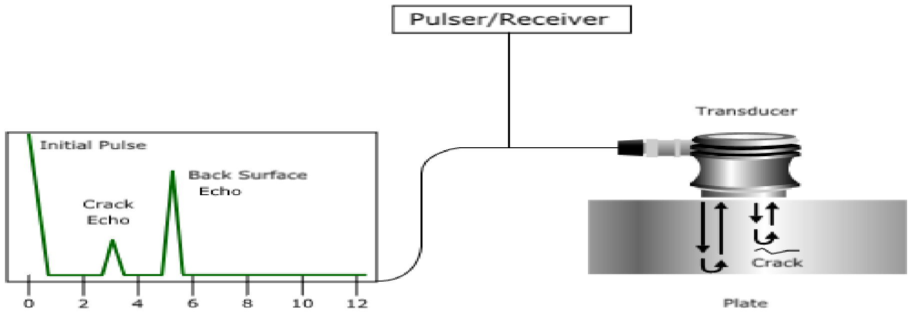

Figure 1.6. Principal of Ultrasonic testing

A typical UT inspection system consists of several functional units, such as the pulser/receiver, transducer, and display devices. A pulser/receiver is an electronic device that can produce high voltage electrical pulses. Driven by the pulser, the transducer generates high frequency ultrasonic energy. The sound energy is introduced and propagates through the materials in the form of waves. When there is a discontinuity (such as a crack) in the wave path, part of the energy will be reflected back from the flaw surface. The reflected wave signal is transformed into an electrical signal by the transducer and is displayed on a screen. In the applet below, the reflected signal strength is displayed versus the time from signal generation to when a echo was received. Signal travel time can be directly related to the distance that the signal traveled. From the signal, information about the reflector location, size, orientation and other features can sometimes be gained.

Ultrasonic Inspection is a very useful and versatile NDT method. Some of the advantages of ultrasonic inspection that are often cited include:

- It is sensitive to both surface and subsurface discontinuities.
- The depth of penetration for flaw detection or measurement is superior to other NDT methods.
- Only single-sided access is needed when the pulse-echo technique is used.
- It is highly accurate in determining reflector position and estimating size and shape.
- Minimal part preparation is required.
- Electronic equipment provides instantaneous results.

- Detailed images can be produced with automated systems.
- It has other uses, such as thickness measurement, in addition to flaw detection.

As with all NDT methods, ultrasonic inspection also has its limitations, which include:

- Surface must be accessible to transmit ultrasound.
- Skill and training is more extensive than with some other methods.
- It normally requires a coupling medium to promote the transfer of sound energy into the test specimen.
- Materials that are rough, irregular in shape, very small, exceptionally thin or not homogeneous are difficult to inspect.
- Cast iron and other coarse grained materials are difficult to inspect due to low sound transmission and high signal noise.
- Linear defects oriented parallel to the sound beam may go undetected.
- Reference standards are required for both equipment calibration and the characterization of flaws.

The above introduction provides a simplified introduction to the NDT method of ultrasonic testing. However, to effectively perform an inspection using ultrasonic, much more about the method needs to be known. The following pages present information on the science involved in ultrasonic inspection, the equipment that is commonly used, some of the measurement techniques used, as well as other information [29].

1.2.2 Basic Principles of Eddy Current Inspection

Eddy current inspection is one of several NDT methods that use the principal of electromagnetism as the basis for conducting examinations. Several other methods such as Remote Field Testing (RFT), Flux Leakage and Barkhausen Noise also use this principle.

Eddy currents are created through a process called electromagnetic induction. When alternating current is applied to the conductor, such as copper wire, a magnetic field develops in and around the conductor. This magnetic field expands as the alternating current rises to maximum and collapses as the current is reduced to zero. If another electrical conductor is brought into the close proximity to this changing electromagnetic field & current will be induced in this second conductor. Eddy currents are induced electrical currents that flow in a circular path. They get their name from eddies that are formed when a liquid or gas flows in a circular path around obstacles when conditions are right. One of the major advantages of eddy current as an NDT tool is the variety of inspections and measurements that can be performed. [30] In the proper circumstances, eddy currents can be used for: crack detection, material thickness measurements, coating thickness measurements, conductivity measurements, material identification, heat damage detection, case depth determination, heat treatment monitoring.

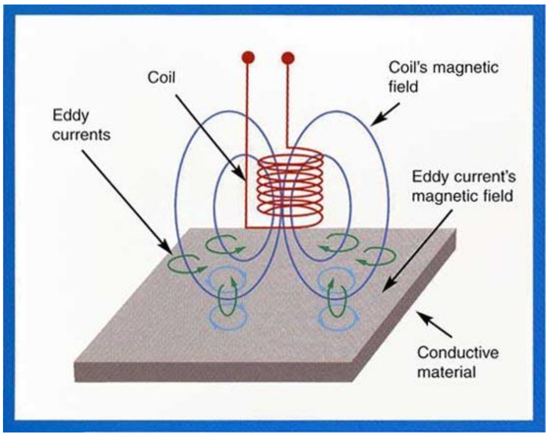

Figure 1.7. Eddy current method

Table 1.3. Features of eddy current inspection:

Advantages	Disadvantages
Sensitive to small cracks and other defects	Only conductive materials can be inspected
Detects surface and near surface defects	Surface finish and roughness may interfere
Inspection gives immediate results	Depth of penetration is limited
Method can be used for much more than flaw detection	Flaws such as delamination that lie parallel to the probe coil winding and probe scan direction are undetectable
Minimum part preparation is required	Skill and training required is more extensive than other techniques
Test probe does not need to contact the part	Surface must be accessible to the probe
Equipment is very portable	Reference standards needed for setup

1.2.3 Radiographic Testing

Industrial radiography involves exposing a test object to penetrating radiation so that the radiation passes through the object being inspected and a recording medium placed against the opposite side of that object. For thinner or less dense materials such as Aluminium, electrically generated x-radiation (X-rays) are commonly used, and for thicker or denser materials, gamma radiation is generally used.

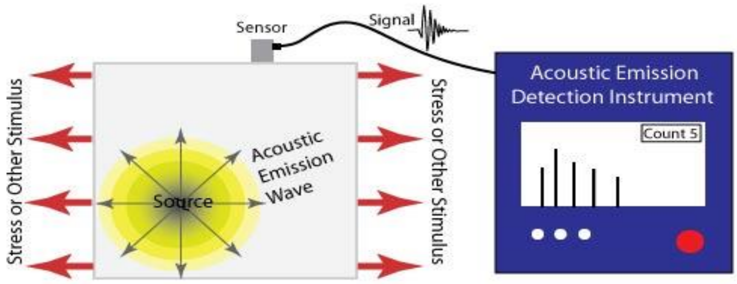

Figure 1.8. Arrangement of RT

Gamma radiation is given off by decaying radioactive materials, with the two most commonly used sources of gamma radiation being Iridium-192 (Ir-192) and Cobalt-60 (Co-60). IR-192 is generally used for steel up to 2-1/2 - 3 inches, depending on the Curie strength of the source, and Co-60 is usually used for thicker materials due to its greater penetrating ability.

The recording media can be industrial x-ray film or one of several types of digital radiation detectors. With both, the radiation passing through the test object exposes the media, causing an end effect of having darker areas where more radiation has passed through the part and lighter areas where less radiation has penetrated. If there is a void or defect in the part, more radiation passes through, causing a darker image on the film or detector, as shown in Fig 1.8 [28].

1.2.4 Acoustic Emission Testing (AE)

Acoustic Emission Testing is performed by applying a localized external force such as an abrupt mechanical load or rapid temperature or pressure change to the part being tested. The resulting stress waves in turn generate short-lived, high frequency elastic waves in the form of small material displacements, or plastic deformation, on the part surface that are detected by sensors that have been attached to the part surface. When multiple sensors are used, the resulting data can be evaluated to locate discontinuities in the part [31].

1.2.5 Laser Testing Methods (LM)

Laser Testing includes 3 techniques: Holography, Shearography and Profilometry. As the method name implies, all three techniques user lasers to perform the inspections.

Holographic Testing uses a laser to detect changes to the surface of a part as it deforms under induced stress which can be applied as mechanical stress, heat, pressure, or vibrational energy. The laser beam scans across the surface of the part and reflects back to sensors that record the differences in the surface created by that stress. The resulting image will be a topographical map-like presentation that can reveal surface deformations in the order of 0.05 to 0.005 microns without damage to the part. By comparing the test results with an undamaged reference sample, holographic testing can be used to locate and evaluate cracks, delamination's, disbands, voids and residual stresses.

Laser Profilometry uses a high-speed rotating laser light source, miniature optics and a computer with high-speed digital signal processing software. The ID surface of a tube is scanned in two dimensions and the reflected light is passed through a lens that focuses that light onto a photo-detector, generating a signal that is proportional to the spot's position in its image plane. As the distance from the laser to the ID surface changes, the position of the focal spot on the photo-detector changes due to parallax, generating a high resolution three-dimensional image of the part surface that represents the surface topography of the part. This technique can be used to detect corrosion, pitting, erosion and cracks in pipes and tubes.

Laser Shearography applies laser light to the surface of the part being tested with the part at rest (non-stressed) and the resulting image is picked up by a charge-coupled device (CCD) and stored on a computer. The surface is then stressed and a new image is generated, recorded and stored. The computer then superimposes the two patterns and if defects such as voids or disbands are present, the defect can be revealed by the patterns developed. Discontinuities as small as a few micrometers in size can be detected in this manner [28].

1.3 Structural health monitoring

Structural Health Monitoring (SHM) aims to give, at every moment during the life of a structure, a diagnosis of the "state" of the constituent materials, of the different parts, and of the full assembly of these parts constituting the structure as a whole. The state of the structure must remain in the domain specified in the design, although this can be altered by normal aging due to usage, by the action of the environment, and by accidental events. Thanks to the time-dimension of monitoring, which makes it possible to consider the full history database of the structure, and with the help of Usage Monitoring, it can also provide a prognosis (evolution of damage, residual life, etc.). If we consider only the first function, the diagnosis, we could estimate that Structural Health Monitoring is a new and improved way to make a Non Destructive Evaluation. This is partially true, but SHM is much more. It involves the integration of sensors, possibly smart materials, data transmission, computational power, and processing ability inside the structures. It makes it possible to reconsider the design of the structure and the full management of the structure itself and of the structure considered as a part of wider systems [32].

1.3.1 Review of SHM principle

Knowing the integrity of in-service structures on a continuous real-time basis is a very important objective for manufacturers, end-users and maintenance teams. In effect, SHM: – allows an optimal use of the structure, a minimized downtime, and the avoidance of catastrophic failures, – gives the constructor an improvement in his products, – drastically changes the work organization of maintenance services:

i) by aiming to replace scheduled and periodic maintenance inspection with performance-based (or condition-based) maintenance (long term) or at least (short term) by reducing the present maintenance labor, in particular by avoiding dismounting parts where there is no hidden defect,

ii) by drastically minimizing the human involvement, and consequently reducing labor, downtime and human errors, and thus improving safety and reliability. These drastic changes in maintenance philosophy are described in several recent papers, in particular for military air vehicles, for Army systems ,for civil aircraft and for civil infrastructures

The improvement of safety seems to be a strong motivation, in particular after some spectacular accidents due to:

i) unsatisfactory maintenance, for example, in the aeronautic field, the accident of Aloha Airlines (Fig. 1.9a),

ii) Ill-controlled manufacturing process, for example, the collapse of the Mianus River bridge (Fig. 1.9b)). In both fields the problem of aging structures was discovered and subsequent programs were established. To pinpoint the importance of the problem of structural aging, the following statistic can be recalled: bridge inspection during the late 1980s revealed that on the 576,000 US highway bridges, 236,000 were rated deficient by present day standard [33,34].

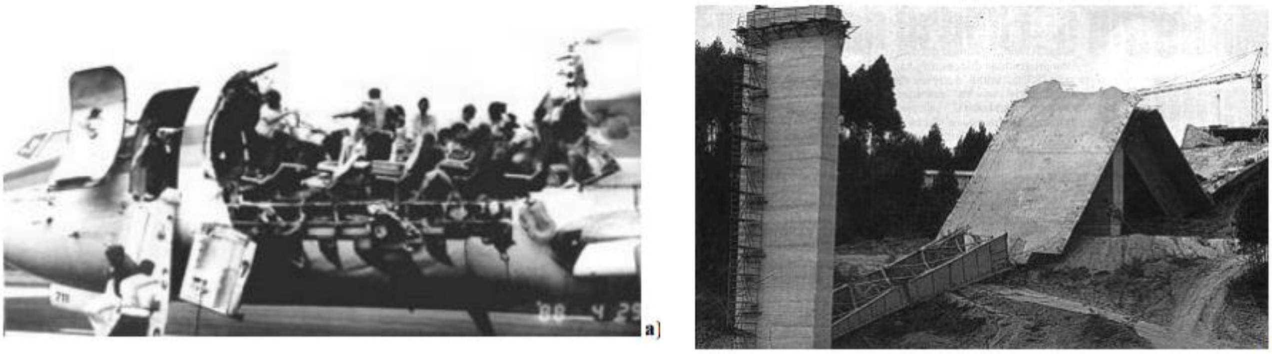

Figure 1.9. a) accident of Aloha Airlines, b) collapse of the Mianus River bridge

Maintenance is only responsible of 14% of hull loss. Furthermore, it should be noted that only 4% of all accidents are due to structural weakness. It can be concluded that, thanks to the introduction of SHM, even an improvement in maintenance and a decrease of structure-caused accidents by a factor of two would lead to a global reduction of accidents of less than 10%, which is far from what is needed to avoid a significant increase in the number of accidents in the near future if air traffic continues to increase. The economic motivation is stronger, principally for end-users. In effect, for structures with SHM systems, the envisaged benefits are constant maintenance costs and reliability, instead of increasing maintenance costs and decreasing reliability for classical structures without SHM (Fig. 1.10). The economic impact of the introduction of SHM for aircraft is not easy to evaluate. It depends on the usage conditions and, furthermore, it is difficult to appreciate the impact on the fabrication cost of the structure. The cost of SHM systems must not be so high as to cancel out the expected maintenance cost savings.

It is easier to evaluate the time saved by the new type of maintenance based on the introduction of SHM. Such an evaluation can be found, for military aircraft, in [BAR 97], who reports that, for a modern fighter aircraft featuring both metal and composite structure, an estimated 40% or more can be saved on inspection time through the use of smart monitoring systems. [35] [36]

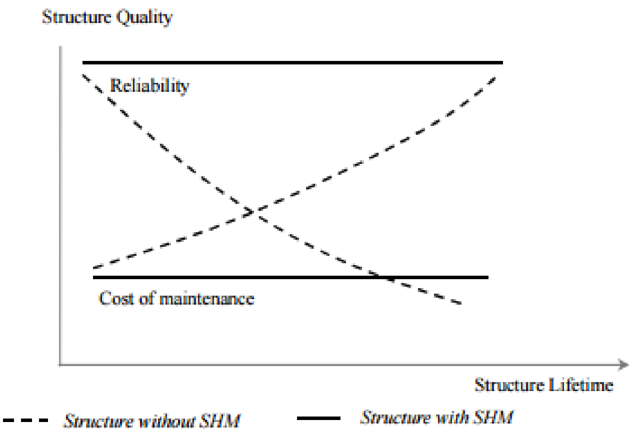

Figure 1.10. Economic impact of the introduction of SHM

1.3.2 Smart Materials/Structures

Since the end of the 1980s, the concept of smart or intelligent materials and structures has become more and more present in the minds of engineers. These new ideas were particularly welcome in the fields of aerospace and civil engineering. In fact, the concept is presently one of the driving forces for innovation in all domains. The concept of Smart Materials/Structures (SMS) can be considered as a step in the general evolution of man-made objects as shown in Figure 1.11. There is a continuous trend from simple to complex in human production, starting from the use of homogeneous materials, supplied by nature and accepted with their natural properties, followed by multi-materials (in particular, composite materials) allowing us.

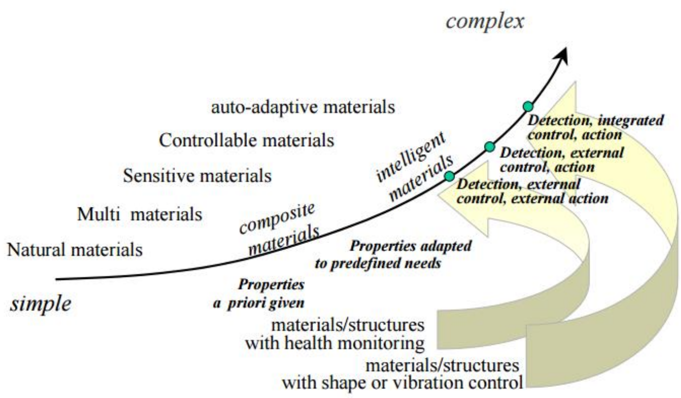

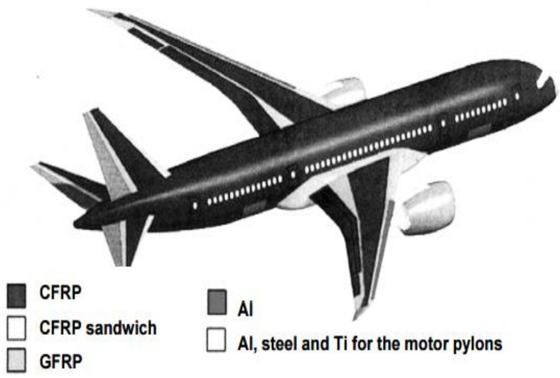

Figure 1.11. General Evolution of materials/structures used by people and place of smart material

Figure 1.12 Boing 787

To create structures with properties adapted to specific uses. In fact, composite materials and multi-materials are replacing homogeneous materials in more and more structures. This is particularly true in the aeronautic domain. For instance, composite parts are now currently used or envisaged for modern aircraft (see for instance in Fig. 1.12, Boeing's 787 Dreamliner project, which has 50% of its structures made of composites). It is worth noting that this aircraft is the first one in which it is clearly planned to embed SHM systems, in particular systems for impact detection.

The next step consists of making the properties of the materials and structures adapt to changing environmental conditions. This requires making them sensitive, controllable and active. The various levels of such "intelligence" correspond to the existence of one, two or all three qualities. Thus, sensitive, controllable and auto adaptive materials/structures can be distinguished. Classically, three types of SMS exist: SMS controlling their shape, SMS controlling their vibrations, and SMS controlling their health. It is clear that materials and structures integrating SHM systems belong, at least in the short term, to the less smart type of SMS. In effect, almost all achievements in this field are only intended to make materials/structures sensitive, by embedding sensors. The next step towards smarter structures would be to make self-repairing materials/structures, or at least materials/structures with embedded damage-mitigation properties. For damage mitigation, embedding actuators made of shape memory alloys (SMA) could be a solution that would induce strains in order to reduce the stresses in regions of strain concentration. These SMA actuators could be in the form of wires or films. As regards self-healing structures, very few attempts have been made. We could mention, in the field of civil engineering, the existence of self-healing concretes containing hollow adhesive-filled brittle fibers: the adhesive is released when the fibers are broken in the region where cracking occurs. A similar method can be applied to polymer matrix composites

As seen above, strong differences exist between structures with SHM and SMS controlling their shape and vibrations. Nevertheless, it is interesting to consider them as part of a whole since a really smart structure will integrate all three functionalities, and because they all rely on common basic researches aimed at:

- elaborating new sensitive materials to make sensors and actuators,
- developing technologies to miniaturize sensors and actuators, and to embed them without degradation of the host structures,
- conceiving systems for data reduction and diagnostic formulation.

This is the reason why, until recently, works on SHM were often presented at conferences and in journals devoted to the general topic of SMS [37].

1.3.3 Lamb wave ultrasonic testing

With advantages including capability of propagation over a significant distance and high sensitivity to abnormalities and inhomogeneity near the wave propagation path, elastic waves can be energised to disseminate in a structure, and any changes in material properties or structural geometry created by a discontinuity, boundary or structural damage can be identified by examining the scattered wave signals. In general, key questions to be answered by an elastic-wave-based damage identification approach, in terms of difficulty in implementation, are:

(i) Is there damage? (qualitative awareness of presence of damage)

(ii) Where is the damage? (quantitative localization of damage)

(iii) What is its size or severity? (quantitative assessment of damage).

Two basic configurations are usually used in elastic-wave-based damage identification, 'pitch-catch' and 'pulse-echo', in a manner similar to the human procedure of locating an object in terms of acoustic waves, as shown schematically in Fig. 1.13.

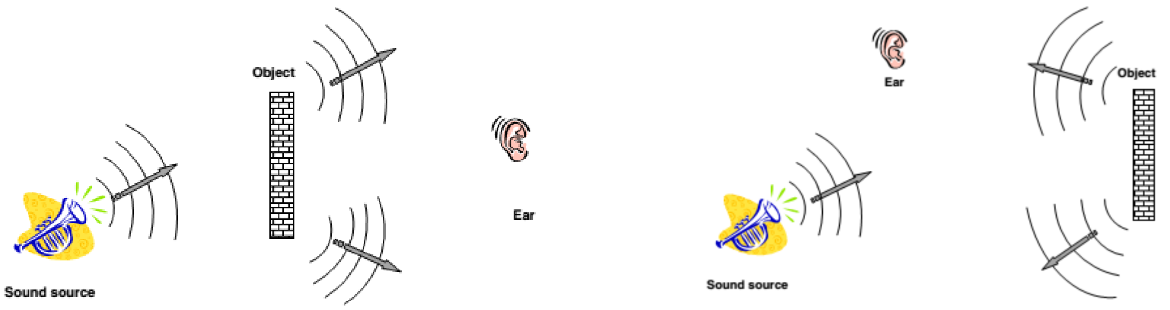

Figure 1.13. 'pitch-catch' and 'pulse-echo'

In a pitch-catch configuration, elastic waves activated by a source (e.g., wave actuator) travel across an object and are then captured by a sensor at the other end of the wave path. In a pulse-echo configuration, both source and sensor are located at the same side of the object, and the sensor receives the echoed wave signals from the object. Differences in the position and geometry of the object can modulate the activated wave signals to different extents, causing deferral of wave arrival, reduction of signal magnitude, dispersion of wave signal, dissipation of signal energy, etc. Thus elastic waves can provide ample information accumulated along their propagation paths for depicting the object.

The earliest exploration of elastic waves for the purpose of damage identification can be dated back to the distance measurement (a prototype of the sonar technique) and blemish detection used for ships and submarine hulls in the 19th century. The sinking of Titanicin 1912 and the desire to develop navigation techniques for submarines in World War I led to the famous experiment in 1915 by French physicist Paul Langévin, which was probably the inaugural of elastic wave-based damage identification in the ultrasonic range (the wave at a frequency of 150 kHz was used in the experiment). In the experiment, a transducer called a 'hydrophone' was invented, comprised of a mosaic of thin quartz crystals glued, between two steel plates, several of which were placed in conformity to a pulse echo configuration to generate and collect ultrasound signals. Hydrophones formed the basis of naval pulse-echo sonar in the following years. The introduction of quartz transducers and the clinical application of ultrasound in the middle of last century further propelled this technique. In recent years, researchers have increasingly become interested in taking advantage of elastic waves to develop novel damage identification techniques for various engineered structures and assets, based on mature understanding of elastic waves [38,39] and awareness of the potential of elastic waves for identifying damage in a cost-effective manner. In particular, Lamb waves – elastic waves in thin plate/shell structures – have been at the core of intensive efforts since the late 1980s. Lamb waves can propagate over a relatively long distance, even in materials with high attenuation ratios, such as polymer composites, and thus allow a broad area to be covered with only a few transducers.

Lamb waves have offered an intriguing avenue to develop novel damage identification and SHM techniques, in recognition of the observations that interaction of Lamb waves with structural damage can significantly influence their propagation properties, accompanying wave scattering and mode conversion. Rich information about damage is encoded in the Lamb waves scattered by that damage and Different locations and severity of damage cause unique scattering phenomena. As witnessed over the past two decades, there have been a number of pilot studies for developing damage identification techniques using Lamb waves [40-47] highlighted in some review articles in the literature [48] Through intensive researches in this area, Lamb waves have identified their superb niche for cost-effective damage identification and SHM. Actually, Lamb waves are now the most widely used acousto-ultrasonic guided waves for damage identification [49].

At a rudimentary level, successful damage identification using Lamb waves includes some essential steps

- Activating the desired diagnostic Lamb wave signal using an appropriate transmitter and capturing the damage-scattered wave signals using a sensor or a sensor network in accordance with either the pitch-catch or the pulse echo configuration,
- Extracting and evaluating the characteristics of the captured wave signals with appropriate signal processing tools
- Establishing quantitative or qualitative connections between the extracted signal characteristics and the damage parameters (presence, location, geometric identity, severity, etc.) through some sort of physical or mechanistic model, and
- Figuring out the damage parameters of interest in terms of captured signals, based on the quantitative connections established in step
- Note that in practice different approaches may not be strictly in line with this sequence.
- Though it appears straightforward, damage identification using Lamb waves is actually an inverse problem, in which the outcome (e.g., a damage-scattered wave signal) is known beforehand but the reason leading to such outcome

(e.g., the damage) is unknown. An inverse problem is often highly ill-posed and very difficult to solve.

In comparison with other NDE approaches, those capitalising on Lamb waves can offer faster and more cost-effective evaluation of various types of damage. For example, rather than using a single ultrasonic probe to inspect a long insulated pipe point by point, one can employ a wave transmitter and receiver pair at one location on the pipe, using the pulse-echo configuration to check the entire pipe instantaneously by examining the reflected wave signals without removing the insulating layer. Types of damage to which ultrasonic Lamb waves are particularly sensitive include voids, porosity, debonding, corrosion, cracking, hole, delamination, resin variation, broken fibre, fibre misalignment, resin crack, cure variation, inclusions and moisture, as summarised in details elsewhere [49].

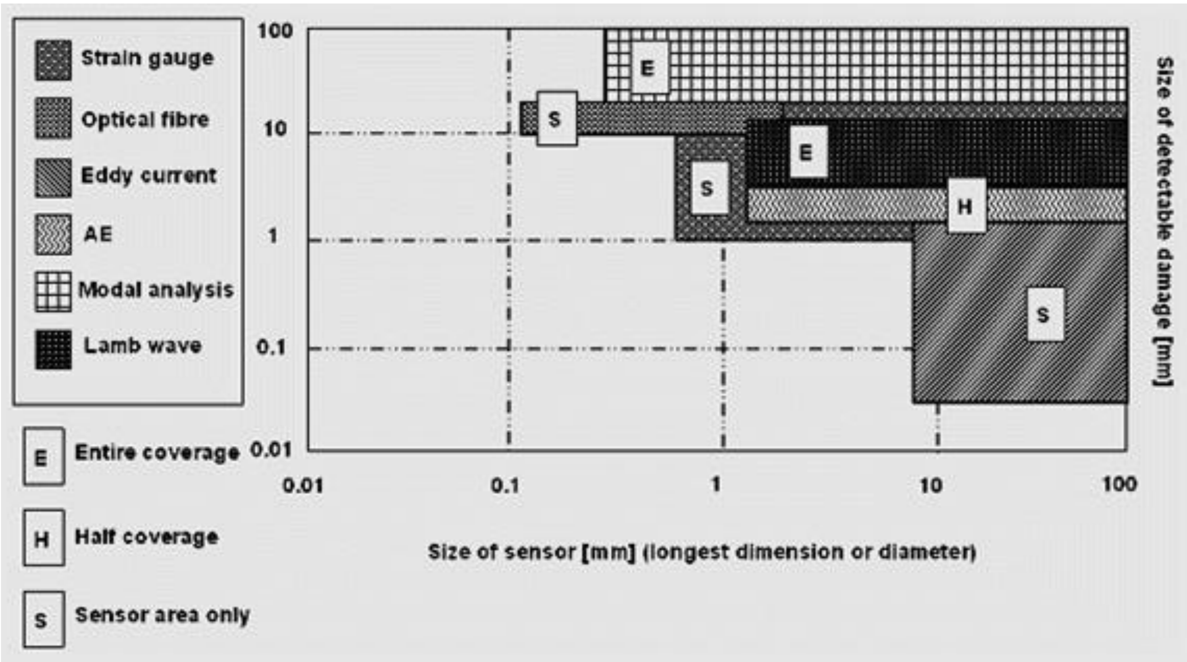

Figure 1.14. Comparison of lamb wave (damage size vs sensor size)

Smaller instances of damage down to a few millimetres can be accurately detected using Lamb waves in the frequency range from 1 to 10 MHz, as seen in Figure 1.14, than using other well established NDE techniques. Furthermore, less power is required by a Lamb wave transmitter for identifying damage than by other methods, Figure 1.15. However, because it is comprised of multiple wave modes which exist synchronously and overlap each other, a captured Lamb wave signal is often complex in appearance. Propagating at fast velocities (e.g., over 5000 m/s in an aluminium plate for example), wave packets reflected from structural boundaries can easily mask damage-scattered wave packets in the signal. Lamb waves are prone to contamination from a variety of interference sources including high-frequency ambient noise, low-frequency structural vibration, temperature fluctuation, inhomogeneity and anisotropy of materials.

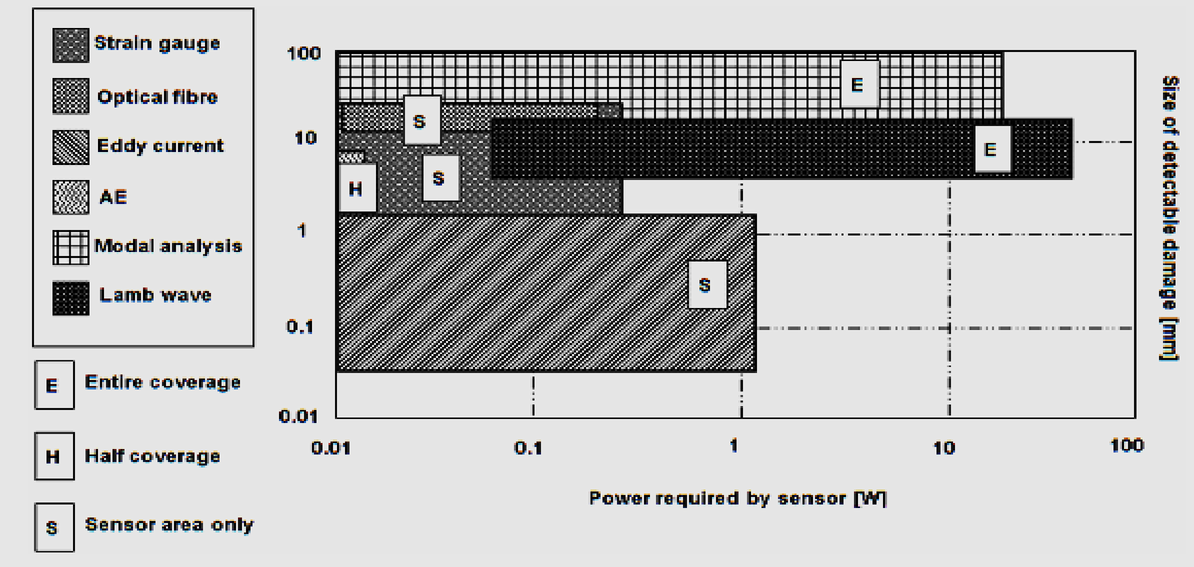

Figure 1.15. Comparison of lamb wave (damage size vs power requiered)

All these factors make damage identification using Lamb waves a multidisciplinary challenge for the community of researchers and engineers. In conclusion, damage identification techniques using Lamb waves are envisioned to be a promising method in lieu of traditional NDE approaches because

Lamb waves feature

- The capacity to inspect a large area using few transducers in a sparse configuration (it has been demonstrated that the ratio of the planar area of the plate
- that can be inspected to the area of a circular wave transducer can be about 3000:1,
- the ability to examine the entire cross-sectional area of the structure in terms of multiple wave modes, thereby detecting internal damage as well as surface defects,
- the capability of classifying various types of damage using different wave modes,
- high sensitivity to damage and therefore high identification precision,

- the possibility of inspecting coated or insulated structures such as pipeline under water/ground,
- the potential for integration with engineered structures and assets for developing online automated damage detection and SHM techniques, and
- low energy consumption with great cost-effectiveness, but complexity of signal appearance, requiring well-calibrated signal processing and interpretation techniques [50,51]

1.4 Aim of the study

We present an approach to determine the ultrasonic inspections for Structure health monitoring of aviation grade aluminum. the main purpose of investigation to develop the Technique for reliable NDT&E for aircraft, understand the propagations of lamb wave in during Structural life of components so we carried out static tension test and fatigue testing on AA2024 and AA7068 with three different stages - Without weld joints, Weld joints and ultrasonic impact treatments. The results which are more authenticated through Digital Image correlations method.

The lamb wave was invited in 1917, the English mathematician Horace Lamb published his classic analysis and description of acoustic waves of this type. After that there are number of publications are involved that are used lamb wave for Nondestructive inspections and evaluations. And lots of authors are recommended for investigation of lamb wave & the goal of our study are to understand the lamb wave and its behavior, this study deals methodology including transducer, activation of lamb wave, receiving of lamb wave, data processing and discussion of results, also Digital image correlation involved for accurately determinations of different stage of static and fatigue life.

The goal of the research is to develop a method to use PZT Ceramic Disc and Lamb wave for thin-wall structural health monitoring, and damage detection.

The scope of this dissertation is to address the issues of aviation’s industry quality control, Lamb wave propagations, the theoretical analysis of sensor-structure interaction (applying different epoxy), the investigation of suitable damage identification algorithms for data processing, and the Lamb wave propagation structural health monitoring methodology.

The objectives for this research is defined as follows:

- To present the detailed investigation of Lamb wave and its properties at various frequencies and modes. Validate the modeling through experimental testing, and address the issues of Lamb wave generation and detection.
- To develop analytical models and perform validation experiments for the sensor-structure interaction revealing the Lamb wave generating and sensing mechanism
- To present an arrangement that enables an array of transducers to interrogate a large area of structure.
- To demonstrate the applications of the transducer and Lamb wave propagation method for Structural Health Monitoring (SHM).

2 Materials and technique

2.1 Preparation of the specimens

We conducted invetigation on different Aerosacpec alluminum alloy (AA2024 &AA7068) but in different specimen like with surface treated, heat treatment, weld joints,Ultrasonic impact treatment and weldjoint with Ultrasonic impact treatment on static and fatiauge testing

2.1.1 AA2024

Alloy 2024 was introduced by first Al-Cu-Mg alloy to have a yield strength approaching 50,000-psi and generally replaced 2017-T4 (Duralumin) as the predominant 2XXX series aircraft alloy. With its relatively good fatigue resistance, especially in thick plate forms, alloy 2024 continues to be specified for many aerospace structural applications. 2024 variant alloys, such as higher purity 2124 and 2324, with improvements in strength and other specific characteristics, have also found application in critical aircraft structures. An improved sheet alloy for fuselage applications was introduced in 1991. Its offers improved fracture toughness and fatigue crack growth while maintaining the strength characteristics of 2024.

Alloy 2024 is available in bare and alclad sheet and plate product forms in the annealed state and several tempers of T3, T4, and T8 types.

Alloy 2024 plate products are used in fuselage structures, wing tension members, shear webs and ribs and structural areas where stiffness, fatigue performance and good strength are required. Sheet products, usually alclad, are used extensively in commercial and military aircraft for fuselage skins, wing skins and engine areas where elevated temperatures to 250°F (121°C) are often encountered.

Chemical composition limits (wt.%)

Containt	Fe	Cr	Si	Cu	Zn	Mn	Mg	Other	AL
Amount(%)	0.5	0.1	0.5	3.8-4.8	0.25	0.3-0.9	1.2-1.8	0.15	Re.

Without weld Joint Specimen

The investigation of proposed ultrasonic technique was performed during static uniaxial tensile testing and fatigue evaluation of the AA2024T3 (without weld joints) specimens. The drawing of the dogbone-shaped specimen used for testing is presented in Fig. 2.1.

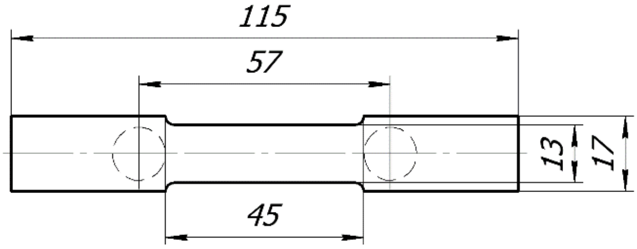

Figure 2.1. Specimen for AA2024Without weld joints

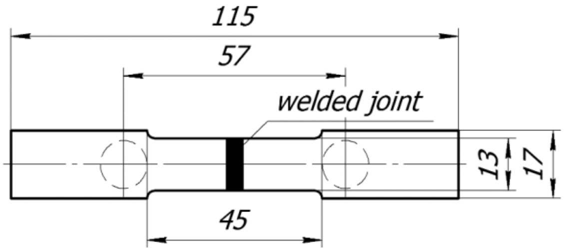

Figure 2.2. Specimen for AA2024 with weld joints

Weld Joint Specimen

Figure 2.3. Image of welded specimen.

The investigation of proposed ultrasonic technique was performed during static and cyclic uniaxial tensile testing of the AA2024T3 specimens with welded joints. The argon arc welding was used for joining process after which the specimens were treated with water quenching at 435°C to reduce residual stress and improve the strength properties of welded joint in Fig. 2.2 and 2.3.

2.1.2 AA7068

7068 alloy is a heat treatable wrought alloy with good fatigue strength, good anodizing response, and high thermal conductivity. It was designed as a higher strength alternative to aluminium 7075 for ordnance applications. It also provides the highest mechanical strength of all aluminium alloys.

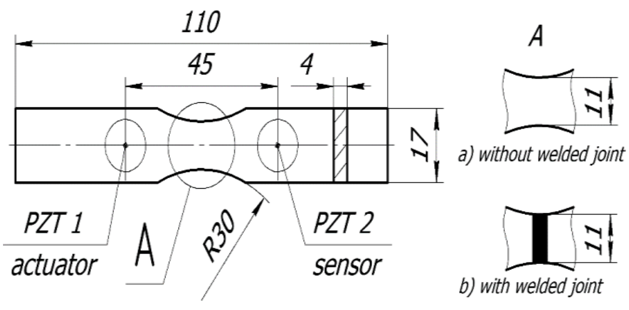

Figure 2.4. Dimension of Specimen

Figure 2.5. Speckle painted specimen

The specimens were cut in the dogbone shape (Fig. 2.4) from the 4 mm sheet. The specimens were split on three groups, the first was used for testing in the initial state, the specimens from the second group were cut across gage length and then welded using gas tungsten arc welding, Thired greoup was ultrasonic Impact treated, all of the specimen polished and clean before where the speakel paint apply for Digital Image correaltions show in Fig. 2.5.

Containt	Fe	Cr	Si	Cu	Zn	Mn	Mg	Other	AL
Min.Amount(%)	0.15	0.5	0.12	2.4	8.3	01-0.3	3%	0.15	Re.

2.2 Ultrasonic testing

The Sensor and actuator constitute the generic term transducer whci is more strictly defind as converter of one type of energy or physical attribute into another, sensors convert mecahnical motions induced by wave propogation in to electric signal while a Lamb wave actuator works in the opposite way yo convert elactrical excitations into the mechanical drive to active waves. The piezoelectric effect of natural monocrystalline materials such as quartz, tourmaline and Rochelle salt is relatively small. Polycrystalline ferroelectric ceramics such as barium titanate (BaTiO3) and lead zirconate titanate (PZT) exhibit larger displacements or induce larger electric voltages. PZT piezo ceramic materials are available in many variations and are most widely used for actuator or sensor applications. Special dopings of the PZT ceramics with e.g. Ni, Bi, La, Nd, Nb ions make it possible to specifically optimize piezoelectric and dielectric parameters.

Figure 2.6. PZT disc transducer

The PZT transducer can deliver wide frequency with low power consuption, low cost and small with ligh weight. Particullery sutaible in to integration into host structures with good coupling capcity but without significant intrusion. During the invertigationpiezoelectric transducers used as actuators and receivers are piezoceramic discs with diameter of 9 mm and thickness of 0.19 mm on steel substrate, mancufacture by Audiowell Corp.China, (product no - AW1E12G-190EFL1Z)

Surface Mounting

A PZT transducer as actuator or sensor can be either surface mounted on or embedded in a host structure. Either conductive glue (sliver powered added epoxy etc.,) or adhesive conductive / copper tap can be used for surface mounting PZT element on structure. Before applying glue, the surface of host structure should be light sending and thorough cleaning using acetone for getting rid of grease and dust.
During practice for AA2024 of static tensile testing and fatigue evaluation we use epoxy adhesive, most widely used for as structural adhesive.

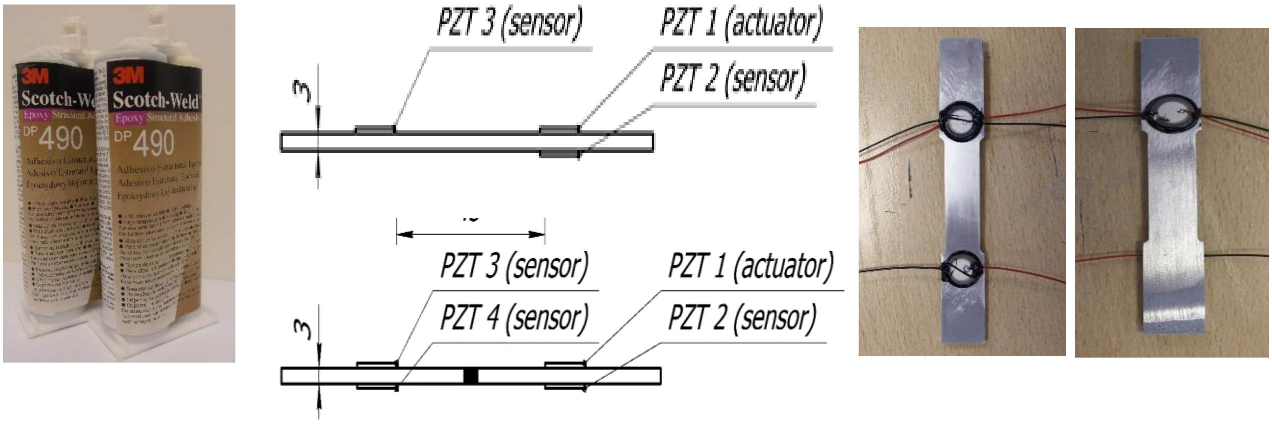

Figure 2.7. Epoxy and arrangment of Transduser for AA2024(with weld and without weld joits)

The adehsive 3M Scotch-weld DP490 is a black, thixotropic, gap filling two component epoxy adhesive with particularly good application characteristics
It is designed for use where toughness and high strength are required and shows special benefits in the construction of composite assemblies.
The product has excellent heat and environmental resistance Features. It is designed for use where toughness and high strength are required and shows special benefits in the construction of composite assemblies.

The product has excellent heat and environmental resistance, the investigation was carried out after full polymerization of the adhesive during 7 days because to minimze the visoelastic bhaviour of the adhesive,however the issue was conset to the practice was the applicablity of the glue for lamb wave propogation through the samples.

The 1st PZT was used as an actuator, the 2nd (to characterize the changes outside the highly stressed gage length of the specimen) and the 3rd (to evaluate the changes in the gage length) were used as receivers.

For welded AA 2024 alloy we used same epoxy adhesive 3M Scotch-weld DP490 but we make another arngment of trnasducer(add one more sensor) for analysis of lamb wave propogation in throuout the body as it was welded samples. The 1st piezoelectric transducer & The 2nd (to characterize the changes outside the highly stressed gage length of the specimen), the 3rd and the 4th (to evaluate the changes in the gage length) were used as receivers.

For AA7068 Alloy

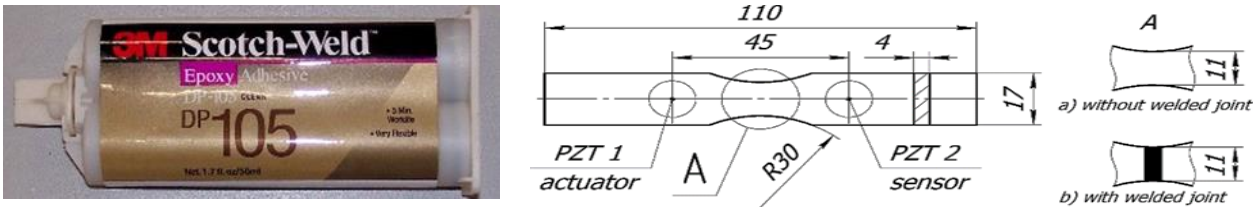

Figure 2.8. Eepoxy adhesive & arrangmet of transducers for AA7068

For investigation Alloy AA 7068 used 3M scotch-weld DP105 epoxy adhesive (high peel strength) Effective adhesive system for bonding, joining, gluing, attaching, assembling, encapsulating, potting, and sealing applications

It retains its clear colour even when cured in large masses where discolouration is often seen with other fast curing adhesive systems. The key features of DP105 are as follows: 4 minute work life, flexible, clear, high peel strength, convenient 1:1 mix ratio.

The arrangment of transducer were same for plain, with welded and ultrasonic treated samples, The 1st piezoelectric transducer (PZT) was used as an actuator. The 2nd (to characterize the changes outside the highly stressed gage length of the specimen), the 3rd and the 4th (to evaluate the changes in the gage length) were used as receivers.

2.2.1 Technique of wave generating and receiving

An arbitrary waveform generator (AWG) is a piece of electronic test equipment used to generate electrical waveforms. These waveforms can be either repetitive or single-shot (once only) in which case some kind of triggering source is required (internal or external). The resulting waveforms can be injected into a device under test and analyzed as they progress through it, confirming the proper operation of the device or pinpointing a fault in it.

Figure 2.9. AWG-4105

Throughout the investigation we used AWG-4105 Function/Arbitrary Waveform Generator 5MHz 2CH 16Kpts, Test equipment applications require signal stimuli varying from advanced communication signals to the playback of captured real-world analog signals. Signal source instruments generate the signal stimulus that is applied to a device under test (DUT). Consequently, signal sources comprise an important class of test instruments. AKTAKOM AWG-4105, AWG-4110 and AWG-4150 Series Function/Arbitrary Waveform Generators adopt the direct digital synthesis (DDS) technology, which can provide stable, high-precision, pure and low distortion signals. Its combination of excellent system features, easiness in usage and versatile functions makes this generator a perfect solution for your job now and in the future.

Standard Functions include the sine, square, pulse, triangle, and ramp waveforms that are commonly used in applications such as the testing of baseband, audio, sonar, ultrasound, and video components and circuits. Some tests that can be performed with standard function waveforms include frequency response characterization, device linearity characterization, digital logic generation, and DC-offset signal generation. The frequency response of a device under test (DUT) can be characterized by waveform responses. Arbitrary Waveforms involve the point-by-point user-defined waveform synthesis. This provides unlimited flexibility to the user to create custom waveforms.

The modulated waveform can be changed by modifying the parameters such as type, internal/external modulation, depth, frequency, waveform, etc. AWG Series can modulate waveform using AM, FM, PM, ASK and FSK. Sine, square, ramp or arbitrary waveforms can be modulated (pulse, noise and DC cannot be modulated). Pressing Sweep button, sine, square, ramp or arbitrary waveform can be swept (pulse, noise and DC cannot be swept). In the sweep mode, AWG Series generate signal with variable frequencies.

Pressing Burst button, burst for sine, square, ramp, pulse or arbitrary waveform can be generated. Output waveforms with set cycle times. Burst can last for certain times of waveform cycle (N-Cycle Burst) or be controlled by external gated signals (Gated Burst). Burst applies to all kinds of waveforms, but noise can only be used in gated burst. Generally, it is called burst function within every signal generator.

The 5-cycle sine modulated by Hanning-window signals were generated using arbitrary waveform generator AWG-4105 (bust mode) with the amplitude of 10 V and the frequency of 50 kHz.

Wave Receiver

Figure 2.10. Handyscope HS4 oscilloscope

This professional powerful computer controlled USB oscilloscope features four input channels. The Handyscope HS4 oscilloscope features a user selectable 12 bit, 14 bit or 16-bit resolution (14 bit effective, SNR 95 dB), 200 mV to 80 V full scale input range and 128 Ksamples record length per channel. Four Handyscope HS4 oscilloscope models are available, with a maximum sampling rate of respectively 5 MHz, 10 MHz, 25 MHz or 50 MHz on all four channels simultaneously

The signals were recorded using USB oscilloscope Handyscope HS4 with the sampling rate of 5 MHz and 12-bit resolution. To increase the S/N ratio the averaging of 100 recorded signals was performed. The signal recorded straightly from the generator by the channels (static evaluation was recorded through 3rd channel and fatigue testing was recorded from 2rd channel) of HS4 was used as the timing reference. The registered signals were processed using band-pass 10-800 kHz filtering. The signal acquisition from sensor PZTs was triggered by the reference signal.

2.2.2 Informative parameters

During the analysis the recorded ultrasonic signals were processes to calculate two parameters in order to characterize different state on specimen lifetime Maximum Envelope, Variance of two envelopes difference (or second central moment) & Normalized Correlation Coefficient [52]

The calculation of the maximum envelope of received ultrasonic signal was carried out using Hilbert transform procedure in the frequency domain [52] The signal amplitude is calculated as the maximum its envelope – MaxEnv (Amplitude of signal - envelope function of an oscillating signal is a smooth curve outlining its extremes [53]. The envelope thus generalizes the concept of a constant amplitude. The figure illustrates a modulated sine wave varying between an upper and a lower envelope. The envelope function may be a function of time, space, angle, or indeed of any variable.).

To evaluate the changes of the ultrasonic signal during cyclic loading the calculation of variance of two envelopes difference for initial and current states of the specimen was used. The first recorded signal corresponds to the undeformed state of the specimen. The following signals were registered during cyclic loading after the defined number of cycles. Then the envelopes difference is calculated by [54] The parameter is designated as m2 or the second central moment.

Normalized Correlation Coefficient measure of similarity of two series as a function of the lag of one relative to the other. This is also known as a sliding dot product or sliding inner-product [55].

There are two experiments performed for the uniaxial static tension. In the first the step mode loading was used and the signals were recorded when the specimen was fixed in grips but the load was withdrawn. Thus the influence of the adhesive layer deformation and residual strain of the specimen were assessed using ultrasonic evaluation. In the second the static uniaxial tensile loading was applied continuously with the stops in defined points for data acquisition (the specimen was fixed in grips and subjected to tensile load). So the dependence of the recoded signal amplitude on the stress-strain state was investigated.

To evaluate the changes of the ultrasonic signal during cyclic loading the calculation of variance of two envelopes difference for initial and current states of the specimen was used. The first recorded signal corresponds to the undeformed state of the specimen. The following signals were registered during cyclic loading after the defined number of cycles.

2.3 Static and fatigue testing

Static Tensile test

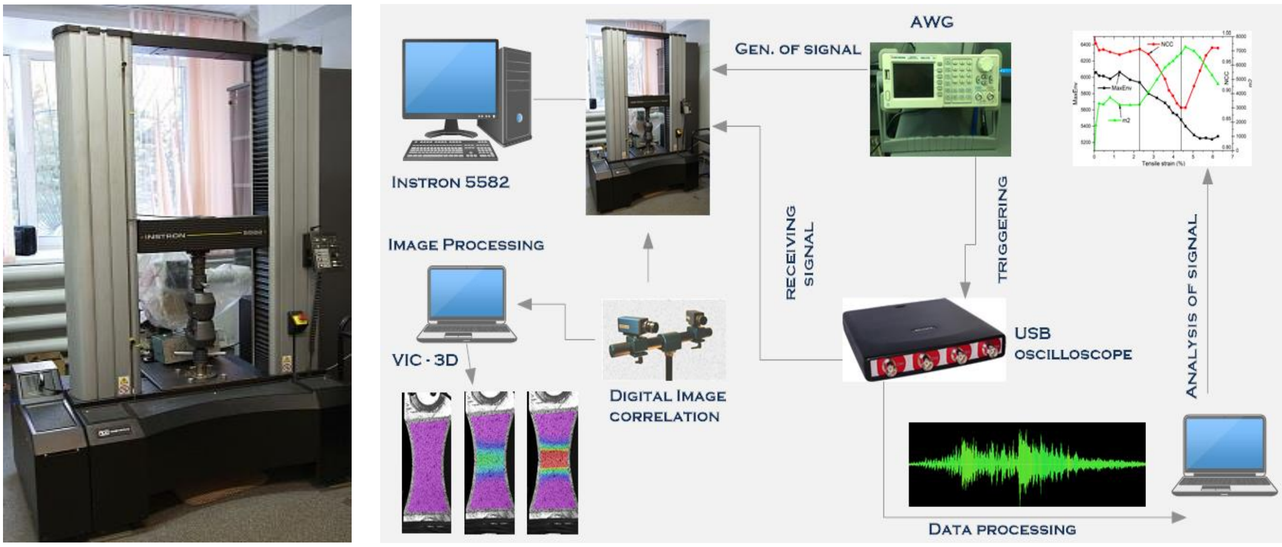

Figure 2.11. Instron 5582 and arrangement of static testing experiments

Uniaxial tensile test is known as a basic and universal engineering test to achieve material parameters such as ultimate strength, yield strength, % elongation, % area of reduction and Young's modulus. allow you to stretch (tensile), bend (flexural), squash (compression) or pull (shear) a sample until it breaks. These important parameters obtained from the standard tensile testing are useful for the selection of engineering materials for any applications required.

The tensile testing is carried out by applying longitudinal or axial load at a specific extension rate to a standard tensile specimen with known dimensions (gauge length and cross sectional area perpendicular to the load direction) till failure. The applied tensile load and extension are recorded during the test for the calculation of stress and strain as we see in the Fig. 2.11 the arrangement of experiment on Instron, where the static tension testing was carried out using electromechanically machine Instron 5582 the load rate of 0.3mm/min, AWG was use as generation of lamb wave and receive through USB oscilloscope, the lamb wave signal after data was procced by software's in computer for analysis of data,

Fatigue testing Universal Testing Machine BISS 150KN

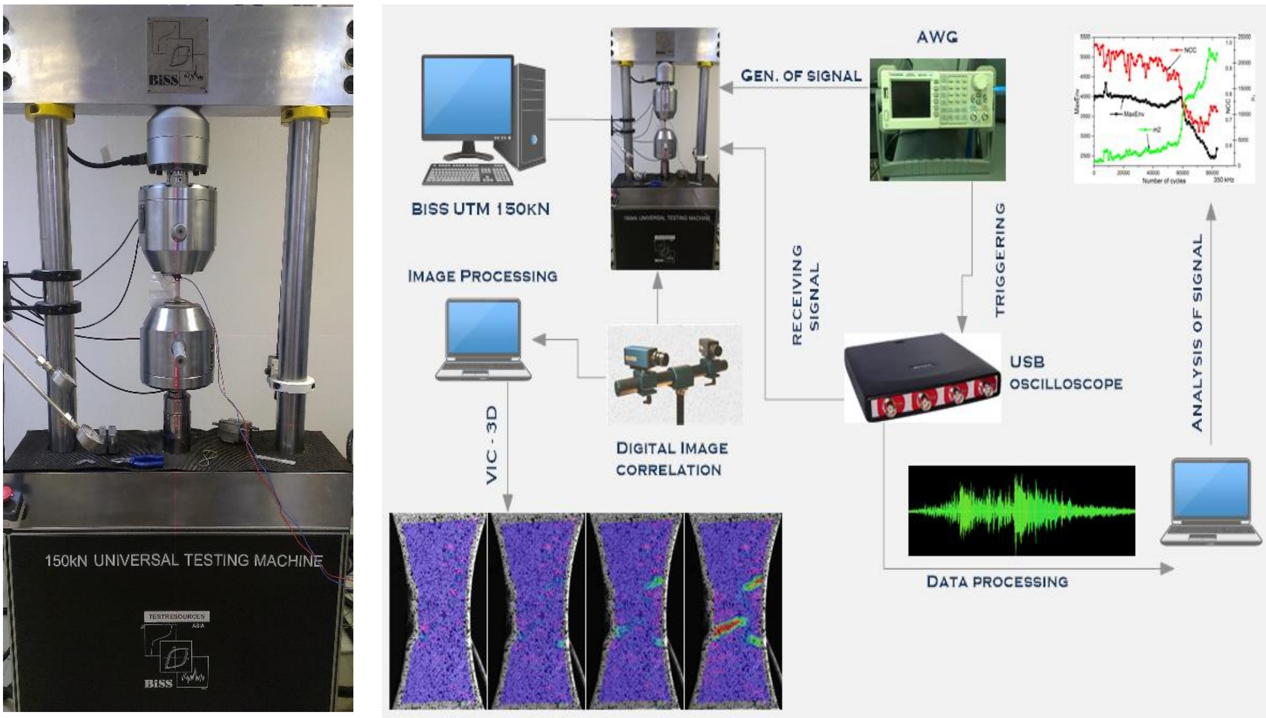

Figure 2.12. UTM BISS 150KN and arrangement of Fatigue testing experiments

Universal testing machines (UTMs) that test mechanical properties such as tensile, flexural, compressive and shear are among the most commonly used instruments plastics compounders are likely to buy when outfitting a lab. Product development is among the key reasons compounders and resin makers test compounds and resins with UTMs. Others include testing the material to determine its suitability for various plastics processes and whether its properties will meet the particular end-use application, as well as for quality control following development to ensure lot-to-lot consistency.

The loading was performed using servo hydraulic testing machine BiSS UTM 150kN with the load ratio R = 0.1, 10 Hz loading frequency and Pmax defined as 0.8σb. arrangement of the exterminate were like static tensile experiments

Note: - the Digital image correlation was carried out on the Alloy of AA7068 all specimens

2.4 Digital Image Correlation

The idea behind the method is to infer the displacement of the material under test by tracking the deformation of a random speckle pattern applied to the component's surface in digital images acquired during the loading. Mathematically, this is accomplished by finding the region in a deformed image that maximizes the normalized cross-correlation score with regard to a small subset of the image taken while no load was applied. By repeating this process for a large number of subsets, full-field deformation data can be obtained. [56]

The experimental setup for the DIC method is comparatively simple and illustrated in Figure 1. For test conditions where the specimen is either nonplanar, or the deformation is not pre-dominantly in-plane, the specimen shape and deformation can be measured using a two-camera setup. The two cameras are mounted on a rigid bar to avoid relative motion of the cameras.

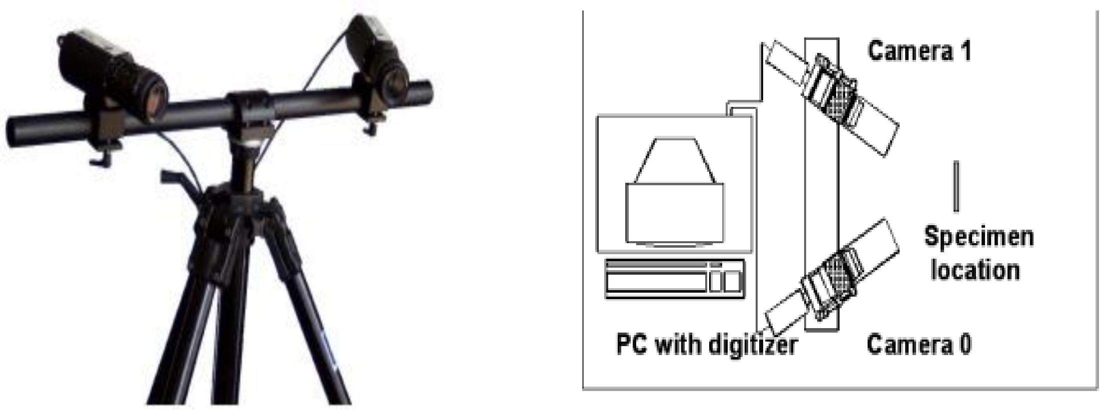

Figure 2.13. Arrangement of Digital Image correlations

The DIC method does not require the use of lasers and the specimen can be illuminated by means of a white-light source. However, the specimen surface must have a fairly uniform random pattern, which can either be naturally occurring or applied to the specimen before the test. Among the many methods for pattern application are self-adhesive, pre-printed patterns, stamps and application of paint speckles with air-brushes, spray cans or brushes [57,58].

3 Experimental results of AA2024 testing

3.1 Results of static testing of AA2024 and discussion

3.1.1 Specimens without welded joint

The choice of the frequency for ultrasonic tests was based on the results of preliminary study of the response of the actuator-sensor pairs glued on the specimen’s surface in the range from 10 to 400 kHz. The signal registration was performed with the frequency step of 1 kHz, the sensed signal amplitude was calculated and thus the two graphs were obtained (Fig. 3.1). They represent the signal sensed by the 2nd and the 3rd PZTs. First of all, this dependence was plotted to characterize the amplitude-frequency response of the PZTs used in the investigation. It is easily seen that the curves are similar to each other with respect to the decrease of the amplitude due to attenuation of the signal propagated through the gage length.

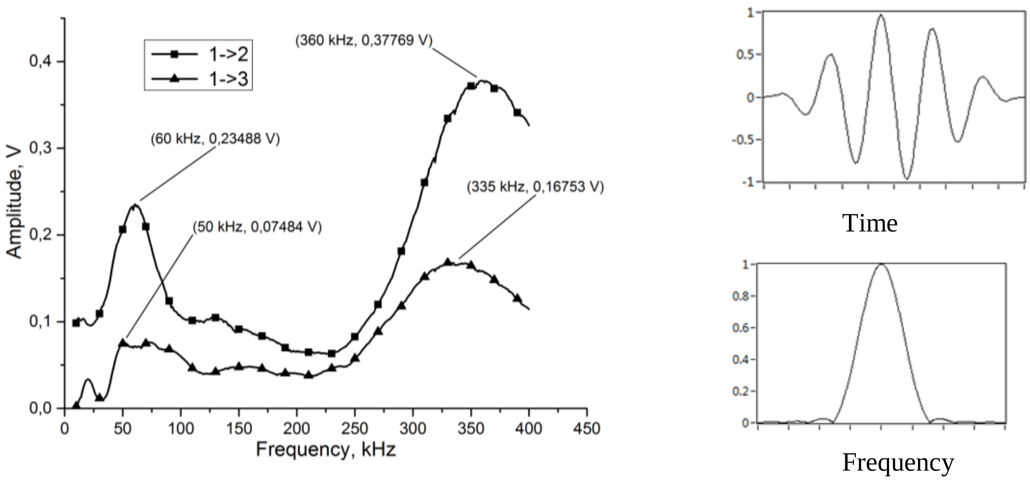

Figure. 3.1. The dependence of the sensed signal amplitude on the frequency. There are two actuator-sensor responses: from 1st PZT to 2nd (through thickness of the specimen) and from 1st to 3rd (through the gage length). The examples of the signal in time and frequency domains are shown.

This work deals with the investigation of the possibility of ultrasonic technique to characterize the changes of the specimen dimensions due to the deformation as well as microstructural changes of the material in the highly stressed gage length. Thus the frequency was chosen from the second curve (1→3): for the static testing the values of frequency corresponding to the peaks of 50 and 335 kHz were used.

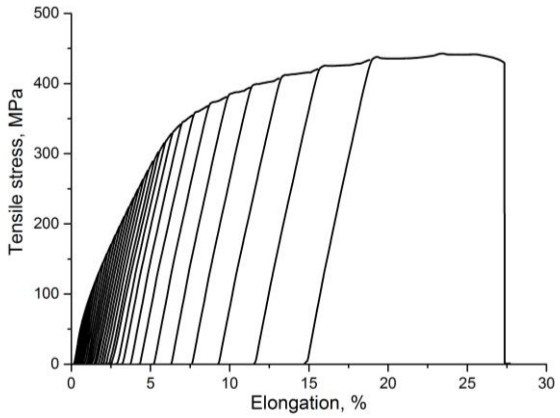

Figure 3.2. The stress-strain curve for the tension test of the AA2024T3 specimen.

Fig. 3.2 represents the stress-strain curve of the AA2024T3 specimen loaded in step mode until fracture: there are 34 points of defined load values where the loading has been stopped, the load was withdrawn and the ultrasound testing was performed. It should be noted that the elongation was measured using the embedded transducer of the testing machine and it is increased additionally due to the indentation of grips into the specimen, while the gage length for the elongation calculation doesn't consider this increment. The yield point is easily recognized at 300 MPa (4.5-5 % of elongation).

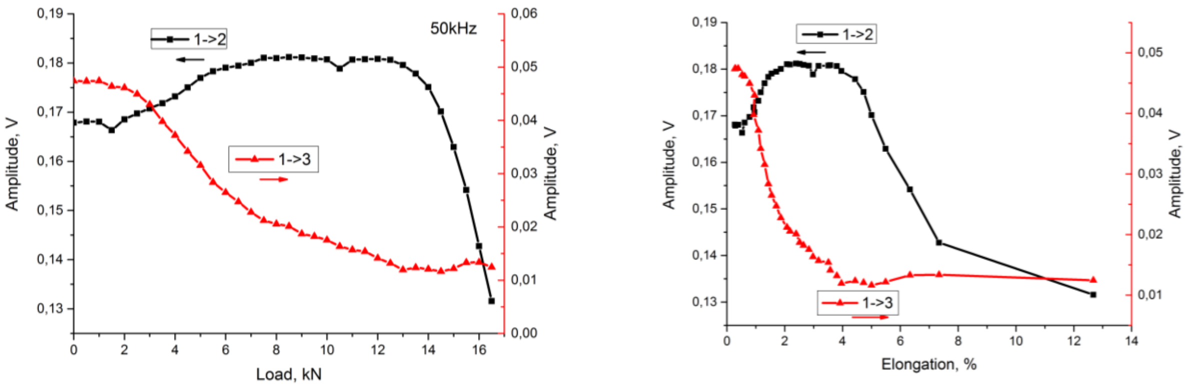

Figure 3.3. The graph of the dependence of the 50 kHz signal max amplitude on the load (a) and elongation (b) applied to the specimen.

It is easily seen that after the yield point the plastic strain starts to occur and the specimen is deformed irreversibly by plasticity. Fig. 3.3 represents the amplitude of the recorded 50 kHz signal (unloaded condition, the specimen is fixed in grips). The black curve (squares) is a graph of amplitude of the signal travelled through the thickness from 1st PZT to 2nd. The red curve (triangles) was recorded when the signals were sent from 1st to 3rd PZT through the gage length. The 1→2 signal amplitude increases slightly in the first stage of loading (up to 2 % of elongation) then it stays constant up to necking region after which the significant decrease of sensed amplitude is registered due to plastic deformation. The red curve behaves differently: the amplitude of the sensed signal decreases four times during elastic stage. This can be explained that the low frequency (50 kHz) Lamb waves are sensitive to the indentation of grips into the specimen surface during first stage of loading. Then after the yield point the amplitude stays constant until fracture.

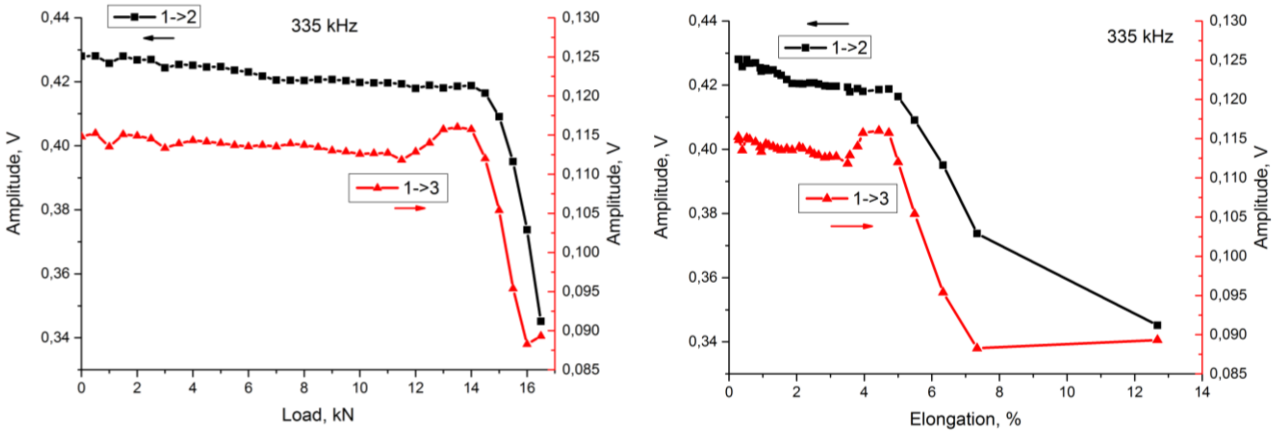

Figure 3.4. The graph of the dependence of the 335 kHz signal amplitude on the load (a) and elongation (b) applied to the specimen.

Fig. 3.4 shows the graphs of the sensed signal amplitude for the frequency of 335 kHz. The PZT on this frequency have the highest sensitivity (Fig. 2), thus the higher values of amplitude 0.42 V against of 0.18 V for the 50 kHz are obtained. The both curves behave similarly: before the yield point the amplitude doesn’t change at all. Then during further loading in the plasticity the sensed amplitude near the fracture point is decreased by ~20 %. This can be explained by the geometry changes of the specimen due to plastic deforming (necking) as well as microstructural changes in the material.

Fig. 3.5 shows the stress-strain curve recorded during the continuous tensile test (with the data acquisition without the specimen unloading) and the graph of the sensed signal amplitude. It is easily seen that the both curves are similar to each other. It can be concluded that the ultrasonic testing used is sensitive to the stress-strain state of material. During the elasticity the amplitude also increases linearly, to the yield point the shape changes to nonlinear because of the beginning of plastic deformation. Then the amplitude increases linearly up to fracture.

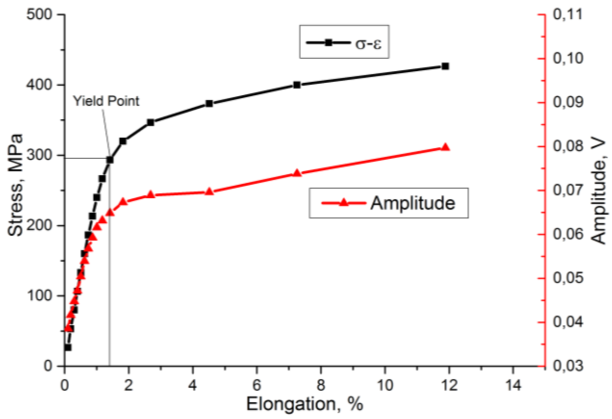

Figure 3.5. The combined graph of the stress-strain curve and the dependence of the 50 kHz signal amplitude on the elongation applied to the specimen.

3.1.2 Specimen with welded joint

Our previous work [59] was related to the investigation of the Lamb waves testing applied to unnotched AA2024T3 specimens tested with static and fatigue tension. Herein the same testing technique was applied and the same two testing frequencies (50 and 335 kHz) were used. The results of the present paper are quite similar to those obtained earlier.

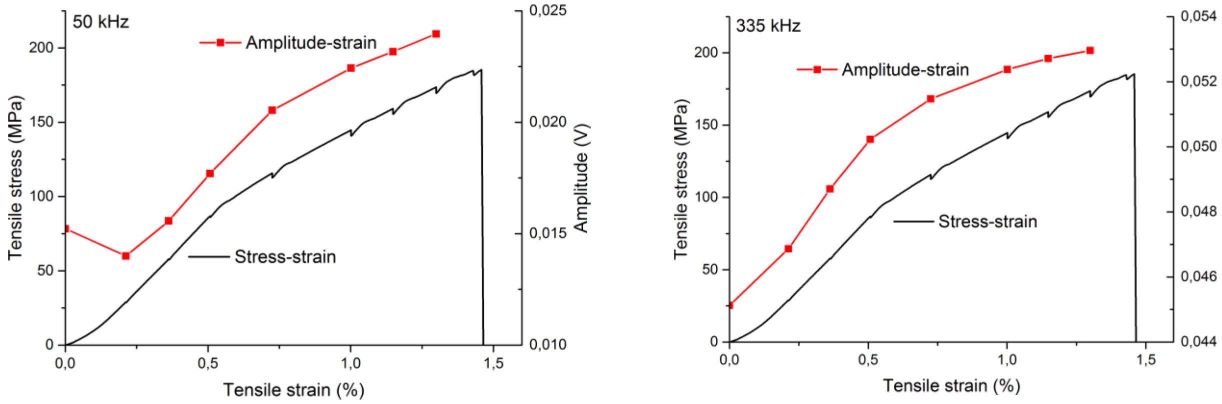

Figure 3.6. Combined stress-strain and amplitude-strain graphs for the continuous tension test of the welded AA2024T3 specimen.

Fig. 3.6 represents two combined graphs of the stress-strain curve of the AA2024T3 specimen with welded joint loaded continuously until fracture and the amplitude of the signal sensed by the 3rd PZT located on the same side with the generator along the gage section of the specimen. The signal sensed by the 4th PZT is almost the same with the 3rd except the reverse sign of the instantaneous sensed signal magnitude due to the propagation of A0 Lamb wave mode. There are 7 points of defined load values where the loading was stopped and the ultrasound testing was performed (these points are easily recognized as the teeth on the stress-strain curve due to the stress relaxation during data acquisition). The first graph (a) corresponds to the frequency of 50 kHz, the second (b) to the 335 kHz. It is seen that amplitude of both high and low frequency signals increases during loading of the specimen. This result is similar to one obtained in the previous our work that the ultrasound used is sensitive to the different stress-strain state. After the second experiment two sets of data were obtained because loading was performed in step mode with data acquisition at both loaded and unloaded conditions. The different testing procedure with the stress relaxation occurring during unloading of the specimen results in different propagation of ultrasound during whole experiment. Figure 3 presents two curves: while the specimen was in loaded (red square) and unloaded (black triangle) conditions. Graph (a) corresponds to the low frequency signal and (b) to the high frequency.

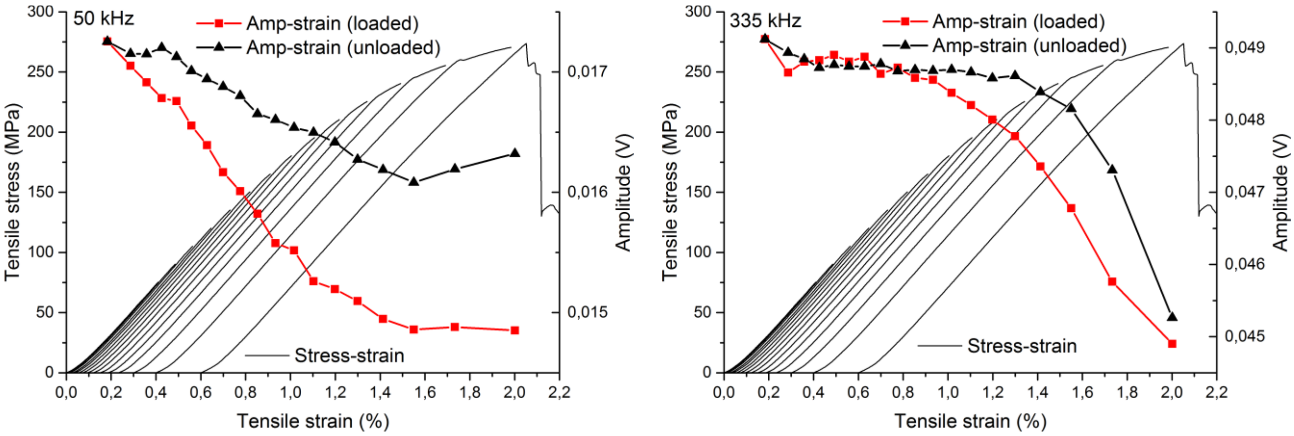

Figure 3.7. Combined stress-strain and amplitude-strain graphs for the step-mode tension test of the welded AA2024T3 specimen.

It is seen that in contrast to the first experiment the amplitude (loaded state – red square plot) for both high and low frequency testing decreases during extension of the specimen. The amplitude for the low frequency signal starts to decrease from the initial of loading with constant slope till the 1.1 % of tensile strain. Then short nonlinear stage is observed and finally there are three last points with constant amplitude value captured till the specimen fracture. The amplitude of the high frequency signal propagated along the gage length stays constant till 0.8 % of strain and then it starts to decrease nonlinearly up to fracture. The correspondent curves of amplitude recorded in the unloaded condition are plotted on the same graph (black triangle) and they have the same shape compare to the plots recorded in the loaded state. However there are small differences:

- the amplitude of high frequency signal start to decrease after the strain reaches higher values (~1.3 %),
- low frequency signal has lower amplitude throughout all the experiment and its amplitude increases slightly near fracture.

By analyzing the data obtained in our previous work [60] it can be noted that both high and low frequency signal propagation behavior during step mode loading of welded AA2024T3 specimen obtained in the present paper were the same compared to the unnotched specimen tested before. Low frequency signal amplitude decreases from the initial of loading and stays constant up to fracture while high frequency sensed signal decreases rapidly after the 2/3 of tensile strain.

3.2 Results of cyclic testing of AA2024 and discussion

3.2.1 Specimens without welded joint

The frequency of 50 kHz for ultrasonic tests was chosen based on our previous investigation of Lamb wave based technique for evaluation of AA2024T3 specimens during static tensile testing. The fatigue tests were carried out and the set of acoustic signals were obtained. Fig. 3.8 shows the shape of the received acoustic signal and their diagram of wavelet coefficients for two PZT sensors which were mounted on the different sides of the specimen. The signals represent the base signal in absentia of load application and cycling.

Time of arrival of the first package peak for PZT3 is 195,8 μs and for PZT2 – 180,9 μs, besides the valley point for the PZT2 was 195,8 μs. Such mutual time alignment of the first peak and valley on the both side of the specimen shows that the first wave package is zero symmetric Lamb wave mode (S_0). At the same time it is not possible to recognize the arrival of antisymmetric mode (A_0) due to its overlapping with S_0 mode. Longer distance, higher frequency or lower specimen thickness could enlarge the time difference in future experiments.

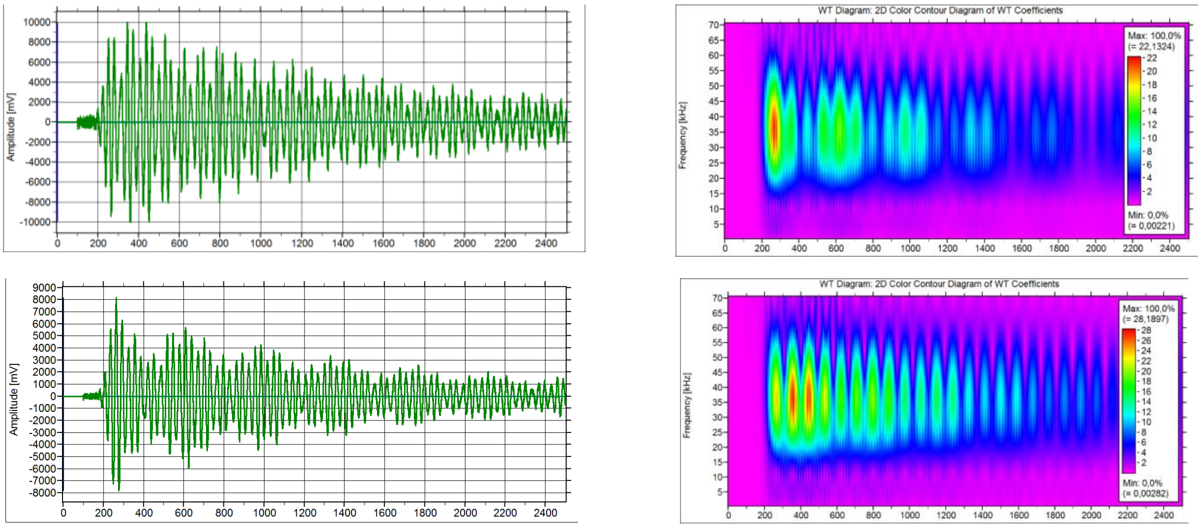

Figure 3.8. The shape of the received signal for PZT2 (on top) and PZT3 (at the bottom) at the left side and wavelet analysis of the received signal at the right side

Time of arrival for the S_0 mode changes during cyclic loading insufficiently thus it is impossible to make any precise analysis. Stable time position could be explained by small distance between actuator and receiver and long wavelength. As a result of two mentioned reasons the interaction of acoustic waves with fatigue induced defects is not enough to change the time of flight.

The signals were processed to obtain two informative parameters: Max Envelope and the 2nd central moment. The results for two specimens with the cyclic lifetime of 62000 (specimen A) and 55000 (specimen B) are presented in the paper.

The results of max envelope calculation for the two specimens are presented in Fig. 3.9. The graphs were smoothed using averaging.

Maximum envelope drops after 2000 cycles and then slightly decreases all the time up to the fatigue failure. It means that on the first stage the rate of damage accumulation is very high and defects significantly influence on the attenuation of acoustic waves. At the second stage the monotonic and smooth reducing of the amplitude take place till the end. The decreases of the maximum envelope from the initial values for different specimens and PZTs are:

- from 8590 to 7387 specimen A, PZT 2 1->2 (by 16%),
- from 11361 to 9625 specimen A, PZT3 1->3 (by 18%),
- from 5366 to 4828 specimen B, PZT 2 1->2 (by 11%),
- from 8694 to 7539 specimen B, PZT 3 1->3 (by 15%)

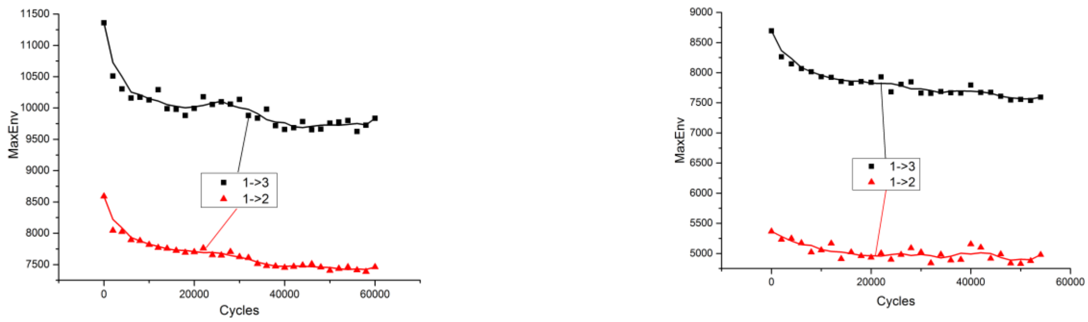

Figure 3.9. Maximum envelope vs number of cycles (specimen A – on the left, specimen B – on the right)

Additionally, it should be mentioned that amplitude for the transducers located on the opposite side from the actuator is higher than for the transducers located on the same side with the actuator.

The results for the 2nd central moment of envelope difference calculated for the two specimens are presented on Fig. 3.10. The graphs were smoothed using averaging.

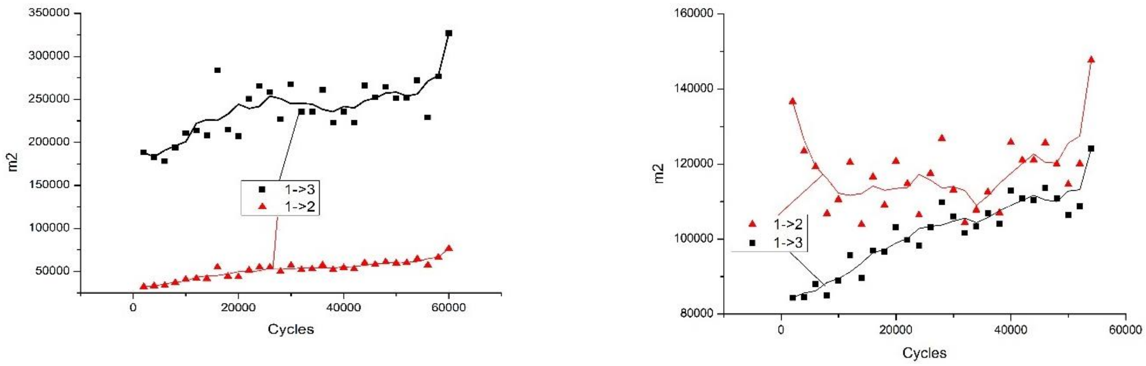

Figure 3.10. 2nd central moment of envelope difference vs number of cycles (specimen A – on the left, specimen B – on the right)

During cycling procedure, the specimen accumulates defects and it provides crack growth, thus initial signal will be distorted. The level of such distortion could be evaluated by 2nd central moment parameter. The 2nd moment characterizes the difference between original and current state signals at each step of cycling test. During the experiment crack growth and micro crack accumulation take place, therefore the signal distortions will increase. The phenomenon is directly visible on the curves of 2nd moment for the PZT3 and PZT4 (specimen A) and for the PZT3 (specimen B). These changes have the following absolute values:

- 32290 – 76534 specimen A, PZT2 1->2 (130%),

- 188312 – 327038 specimen A, PZT3 1->3 (70 %),
- 136671 – 147688 specimen B, PZT3 1->2 (10%),
- 84373 – 124108 specimen B, PZT3 1->3 (50%).

The curve of 2nd moment for the specimen B and PZT2 (1->2) does not demonstrate unequivocal behavior, though it has ascending trend.

3.2.2 Specimens with welded joint

Based on the results obtained during static tensile experiments the parameters for cyclic investigation were chosen. The average ultimate tensile stress for three specimens was obtained (210 MPa) and the maximum stress for cyclic was estimated as $0.4\sigma_u$=82 MPa. Thus three data sets for specimens with lifetime of 9000 cycles, 33500 cycles and 84000 cycles were captured. Such huge scatter of the lifetime is the result of poor quality of welded joints but it was not a problem for the present research where the ultrasonic testing technique was investigated. More over the presence of large welding defects such as pores or inclusions can give rise to the formation of large crack during cyclic loading in order to assess the Lamb wave testing technique sensitivity. The testing and data acquisition technique in this section are similar to ones used in static testing: there are two frequencies of testing 50 and 335 kHz, the amplitude of sensed signal corresponds to the 3rd transducer located on the same side with generator along the gage section of the specimen.

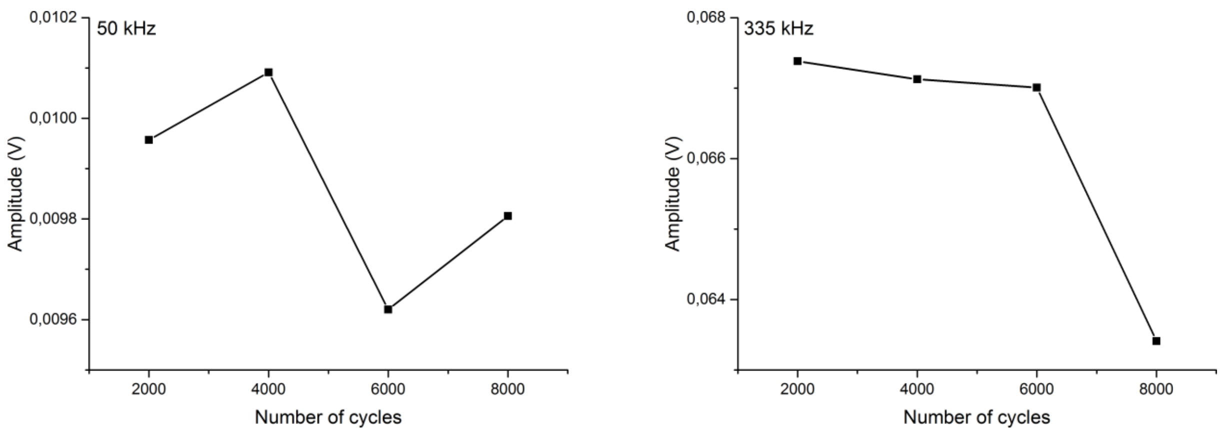

Figure 3.11. Sensed signal amplitude dependence on the different number of cycles for the specimen with lifetime of 9000 cycles.

Figure 3.11 presents two graphs of low (a) and high (b) frequency signal amplitude registered during cyclic loading of the specimen fractured after only 9000 cycles. Because the data acquisition interval was set to 2000 cycles there are only four points were captured. Low frequency signal amplitude behaves uncertainly while the high frequency amplitude remains constant at first three points and then large decrease is registered.

Low amount of data capturing points doesn't allow us to make any precise analysis of the propagated signal behavior so let's consider the second specimen with 33500 cycles of lifetime (Figure 3.12).

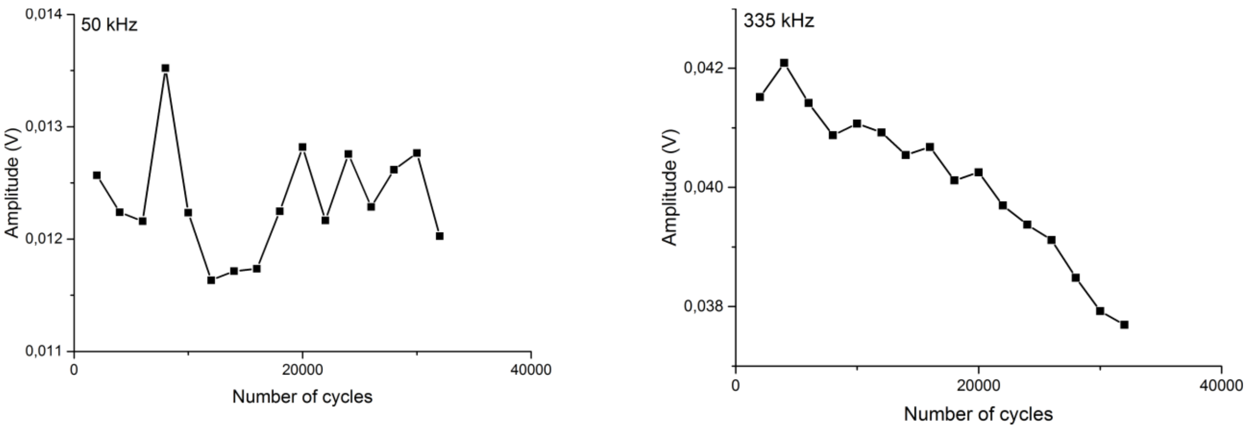

Figure 3.12. Sensed signal amplitude dependence on the different number of cycles for the specimen with lifetime of 33500 cycles.

It is seen that low frequency sensed signal graph doesn't have any precise trend during cyclic loading. The plot has large hops and drops of amplitude magnitude while the average value stays constant. In contrast to the low frequency behavior the high frequency signal amplitude decreases monotonically from the initial of the experiment till fatigue failure of the specimen.

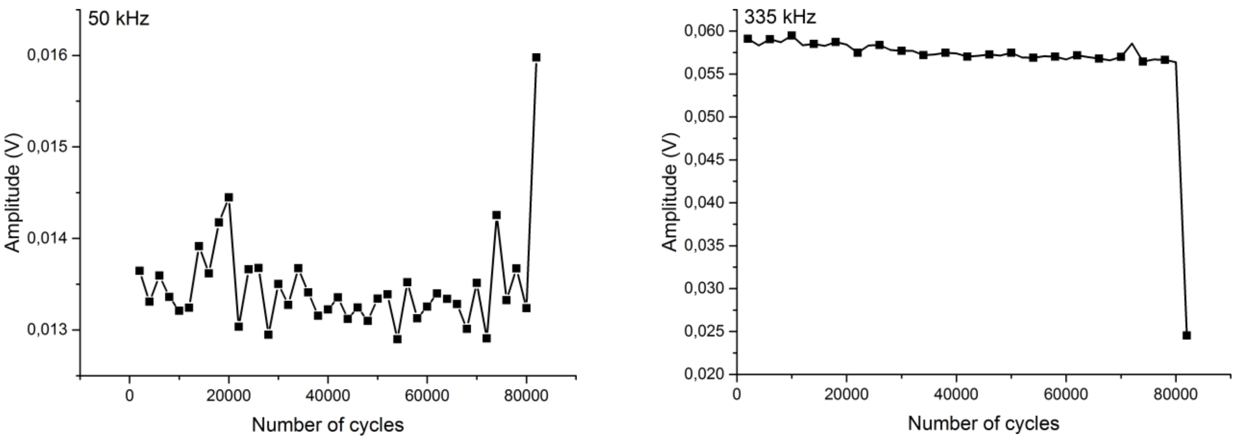

Figure 3.13. Sensed signal amplitude dependence on the different number of cycles for the specimen with lifetime of 84000 cycles.

Figure 3.13 presents the graphs of amplitude for the specimen with lifetime of 84000 cycles. The amplitude value for the low frequency testing stays near constant during entire experiment and at the last point near fracture the large jump is registered. This result differs with the explanation according to which the amplitude should decrease due to the higher signal attenuation owing to the micro damaging of the structure or the large crack formation. The second graph for high frequency confirms the assumption of higher attenuation with large drop of the sensed signal amplitude registered at the last point before fatigue failure. Also it should be noted that the specimen withstands more than 1500 cycles of load after the last data acquisition point.

4 Experimental results of AA7068 testing

4.1 Results of static testing of AA7068

4.1.1 Specimens without welded joint

The preliminary study was carried out in order to choose the frequency for further testing: the actuator-sensor response of the specimen fixed in grips was characterized in terms of maximum envelope of the signal depended on ultrasound frequency (in the range from 10 to 400 kHz, with the step of 1 kHz). The obtained graph is presented on the Fig. 4.1.

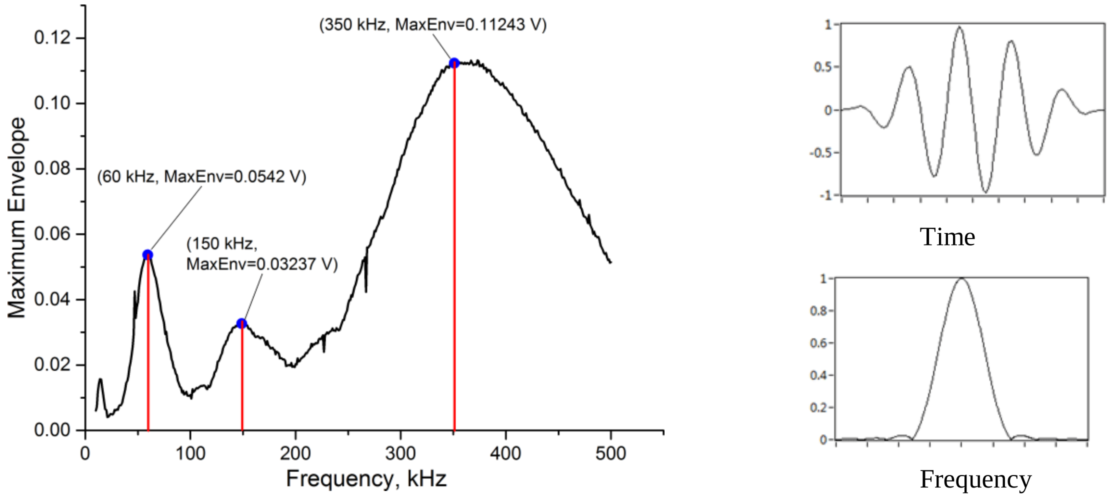

Figure 4.1. The dependence of the sensed signal amplitude on the frequency. The examples of the signal in time and frequency domains are shown.

It is easily seen that there are two main peaks of the maximum envelope corresponding to the frequencies of 60 kHz, 150 kHz and 350 kHz. The dispersion curves for aluminum plates obtained experimentally and theoretically allow calculating the group velocity and the wavelength of A_0 and S_0 modes for the investigated specimens with thickness of 4 mm. Thus it is seen that the first peak at 60 kHz corresponds to the A_0 mode while S_0 is negligible because it has long wavelength on this frequency. The third peak (350 kHz) corresponds to the mix of A_0 and S_0 modes – on high frequency they have quite similar sensed amplitude but arrive to the sensor at different time. The second peak at ~150 kHz is associated also with the mix of mainly A_0 and S_0. Actually the association of these peaks with different modes of Lamb waves are performed with an error about 5-15 % compared with the theoretical values. This discrepancy is related to the different boundary conditions of the specimen that is fixed in grips as well as due its small size where side reflections can greatly change the sensed signal.

This work deals with the investigation of the possibility of ultrasonic technique to characterize the changes of the specimen dimensions due to the deformation as well as microstructural changes of the material in the highly stressed gage length. Due to higher magnitude the first and the third peaks corresponding to the actuating frequency of 60 and 350 kHz were used during tensile testing. Thus the A_0 mode Lamb waves were generated using low frequency testing while S_0 mode with higher group velocity was used at high frequency.

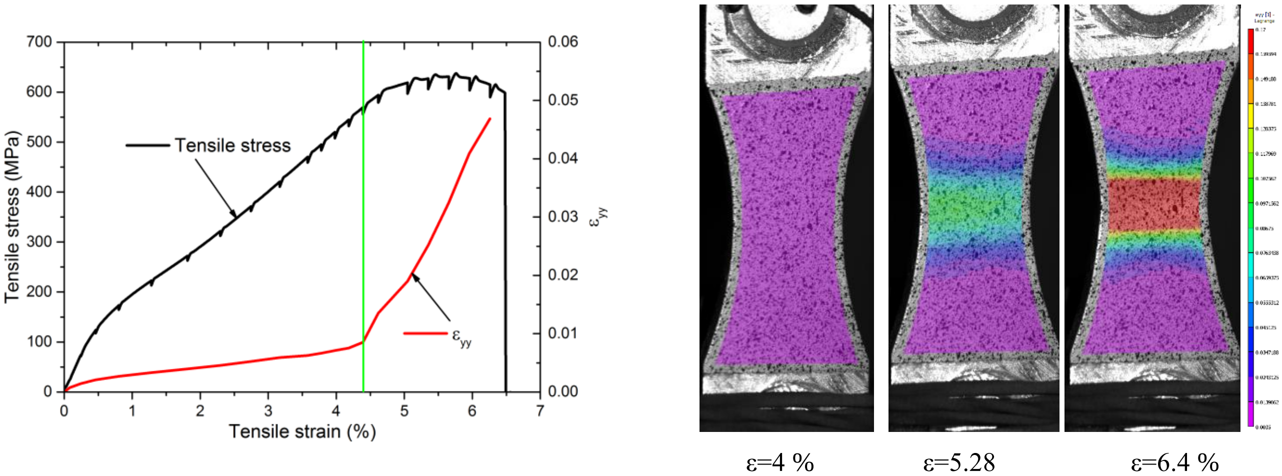

Figure 4.2. The stress-strain curve for the step mode tension test of the AA7068 specimen and normal strain εyy measured by Vic 3D. The images of εyy fields are shown on the right (corresponding strain value is shown).

Fig. 4.2 represents the stress-strain curve of the AA7068 specimen loaded in step mode until fracture: there are 21 points of defined load and strain where the loading was stopped and the ultrasound testing was performed. It is easily seen that after the yield point the plastic strain starts to occur and the specimen is deformed irreversibly by plasticity. The εyy graph was plotted by averaging of all εyy values in the calculation area shown on Fig. 3. It is easily seen that εyy plot can be divided on two parts (by the green vertical line). The first stage is characterized by the fully elastic straining of the specimen and the images of εyy fields look nearly the same (using the shown colorscale) while on the second stage the plasticity in the narrowest section of the specimen thus the εyy plot rises rapidly.

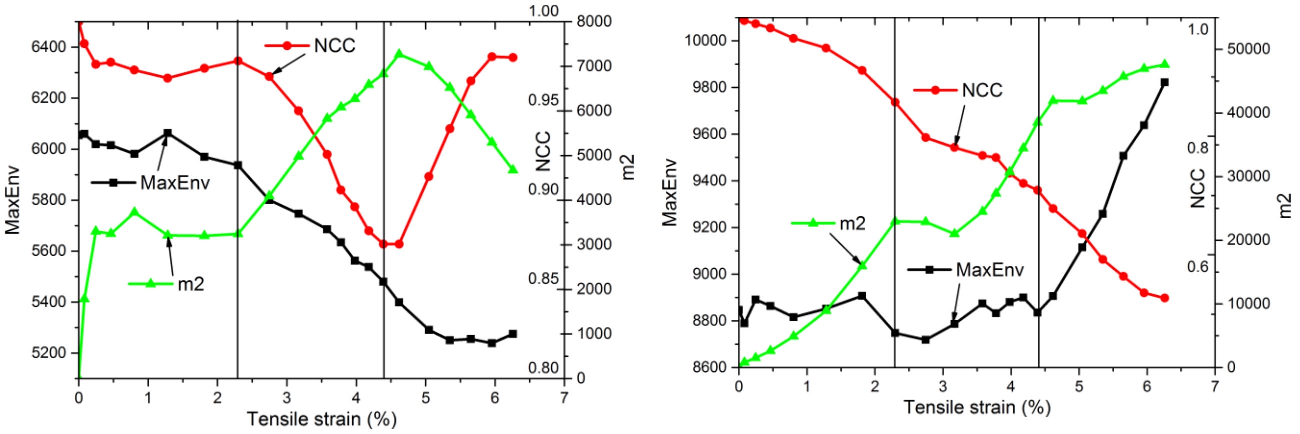

Figure 4.3. The plots of maximum of envelope (1), normalized correlation coefficient (2) and variance m2 (3) by the elongation for initial AA7068 specimen: (a) 60 kHz and (b) 350 kHz.

Fig. 4.3 displays the relationship between informative parameters and applied strain. For low frequency the max of envelope (MaxEnv) is decreasing during all straining process until fracture with a small region during plasticity where the values remain nearly constant. This change can be associated with the slight variation of the specimen dimensions due to elongation thus the lamb waves arrive to the sensor at different phase with boundary reflections and different interference pattern occurs. Two parameters characterizing the shape changes of signals (Variance m2 and NCC) have nearly the same behavior (with considering their reverse nature – m2 rises with the changes of compared signals while NCC decreases). Such relation is relevant to all of the sets of results presented in the paper so only the NCC parameter will be described and discussed. As for the Fig.4,a the normalized correlation coefficient after the first stage of constant values it decreases but during plasticity it goes back thus just before fracture the NCC is nearly the same that in the initial of the tensile test. Such controversial result doesn’t allow us to make a correct decision on the state of the specimen thus it should be concluded that entirely the low frequency testing provides not reliable results. The informative parameters obtained after the high frequency testing (Fig. 4.3,b) have a better explainable behavior: the NCC decreases during all the tensile test while MaxEnv stays nearly constant until the plasticity starts (after 4.4% elongation).

Fig. 4.4 shows the images of shapes of signals recorded during the continuous tensile test. By the joint analysis of the informative parameters data and these plots we can highlight following regularities: (1) the shape of the first packet of low frequency signal is almost unchanged during straining, there are only a minor changes of the “tail” of signal, (2) a close look to the first packet indicates that but the amplitude of received signal decreases that is confirmed by the MaxEnv, (3) the shape first packet of the high frequency signal (which corresponds to the S_0 mode) stays nearly unchanged and the MaxEnv increases on the last stage as well, (4) the second packet is produced most likely by the side reflections and decrease significantly during the test, (5) the “tail” of the high frequency sensed signals changes drastically throughout the tensile test, but it is quite difficult to make any precise assumption about this due to small size of the specimen and large amount of different reflected waves that interfere with each other.

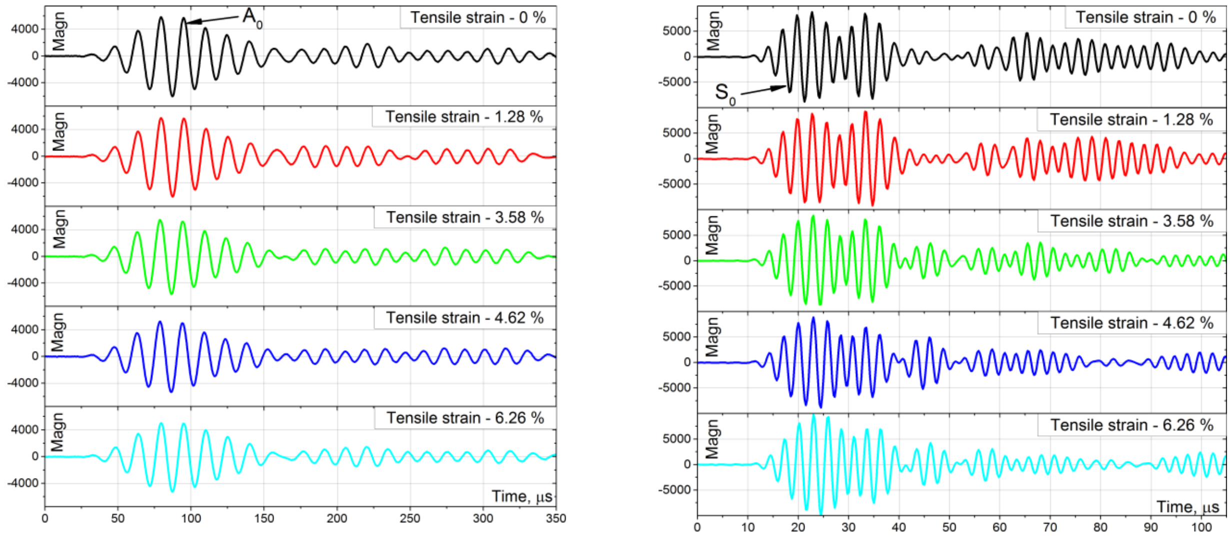

Figure 4.4. The images of shapes of signals captured for the specimen without welded joint(a) 60 kHz, (b) 350 kHz.

4.1.2 Specimens with welded joint

It can be seen (Fig. 4.5) that the welded joint drastically decreases the ultimate strength: σ_u of initial AA7068 alloy is about 627 MPa while welded specimen has about 290 MPa. Actually this alloy has low weldability using of methods of liquid state welding like tungsten arc welding. Present work deals with the investigation of the ultrasound testing technique thus high mechanical properties are not so important. Instead this weakened welded joint acts like a strain concentrator that can be seen from the stress-strain and εyy curves. While the specimen without welded joint has two easily identified stages on the εyy curve due to good plasticity of initial material the εyy curve for welded specimen is linear showing nearly elastic deformation behavior. The area of welded joint exhibits much higher strains but due lack of plasticity of welded material thus the averaged εyy curve is nearly linear.

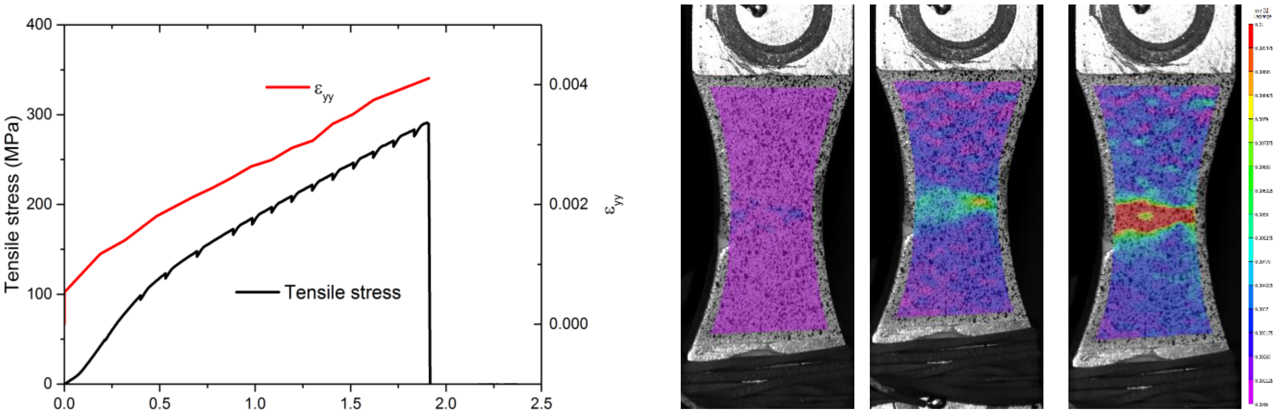

ε=0.32 % ε=1.2 % ε=1.87 %

Figure 4.5. The stress-strain curve for the step mode tension test of the welded AA7068 specimen and normal strain εyy measured by Vic 3D. The images of εyy fields are shown on the right (corresponding strain value is shown).

Fig. 4.6 shows the graphs of the informative parameters for the frequency of 60 kHz and 350 kHz. Due to low weldability of AA7068 the specimen fractured at low elongations (within 2-2.5% of elongation). This leads to the lower stressed state of the specimen just before fracture compared to the initial specimen.

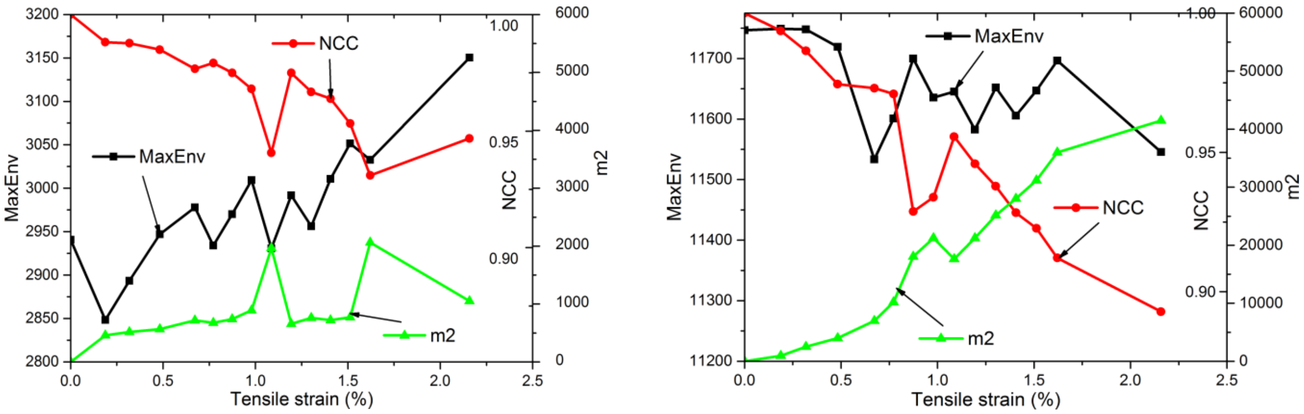

Figure 4.6. The plots of maximum of envelope (1), normalized correlation coefficient (2) and variance m2 (3) by the elongation for welded AA7068 specimen: (a) 60 kHz and (b) 350 kHz.

The analysis of the data gives the following conclusion: the behavior of the plots of the informative parameters for the welded specimen is nearly the same as for the first stage for the initial specimen without welding joint (this stage is shown by the vertical black line on Fig. 4.3). For the high frequency testing the MaxEnv stays nearly the same until fracture and NCC decreases during the entire tensile test. For low frequency it is more difficult to make the same conclusions because on the first stage for initial specimen all informative parameters have a sideway trend.

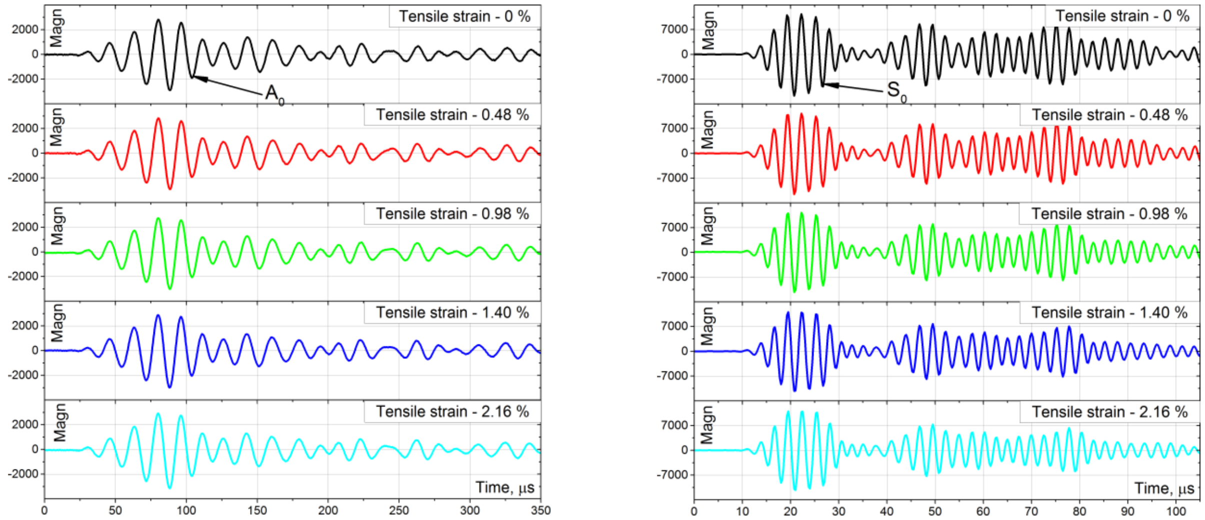

Figure 4.7. The images of shapes of signals captured for the specimen with welded joint (a) 60 kHz, (b) 350 kHz and for the specimen with welded joint.

Fig. 4.7 shows the variance of captured signals throughout the test of specimen with welded joint. The shapes of signals compared to those for the specimen without welded joint are nearly the same. On the low frequency plots the A_0 mode is easily distinguished and its shape doesn't changes up to fracture. The "tail" part also stays constant up to fracture. For the high frequency the first packet corresponds to S_0 mode but now second packet as for the initial specimen is observed. It confirms the assumption that this packet can be associated to the interference of side reflections. Also it can be seen that the "tail" part of the signal has higher amplitude compared to the initial specimen data.

4.2 Results of cyclic testing of AA7068

4.2.1 Specimens without welded joint

This section is devoted to results of fatigue tests for two aluminum specimens, one of which is monolithic (initial material), but the other contains welded joint. Strain distribution fields for different operating time and informative parameters computed for sensed signals for the specimen without welded joint are presented in

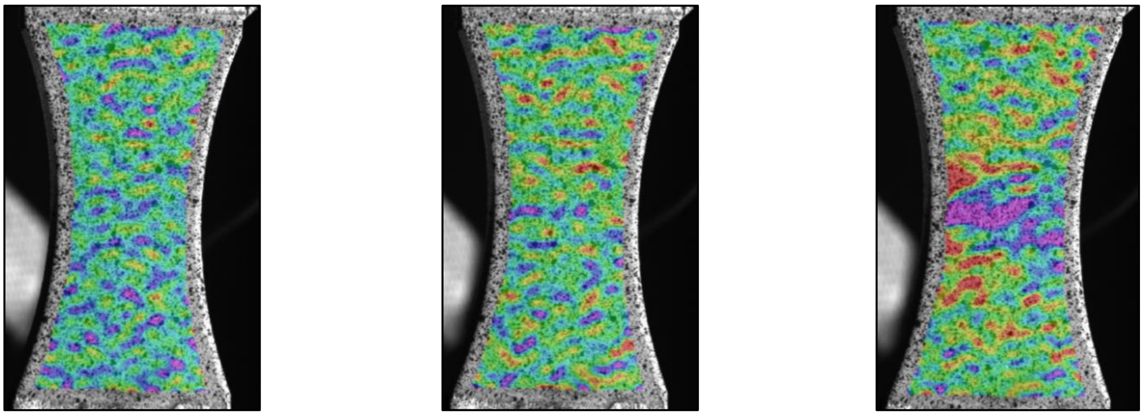

0 cycles | 94 000 cycles | 98 000 cycles

Figure 4.8. Aluminum specimen without welded joint. Vic-3D εyy strain distribution fields for different operating time.

Both specimens fractured in the middle of gauge length, but the fatigue crack growth process is significantly different. Thus for the specimen without welded joint the fatigue crack became distinguishable, according to the data captured via DIC system, not so far from the failure moment. The image capturing technique should be individually described. The images were captured with a step of 2k cycles at the load point of Pmax. Thus the DIC system is to be used to detect the changes in the specimen rigidity (due to the formation of micro- and macrocracks) resulting in higher tensile strains. Fig. 4.8 presents the images of εyy distribution and there are only two last images at 94k cycles and 98k cycles where the crack is detectable, while all previous images demonstrate uniform strain distribution field without localized deformations.

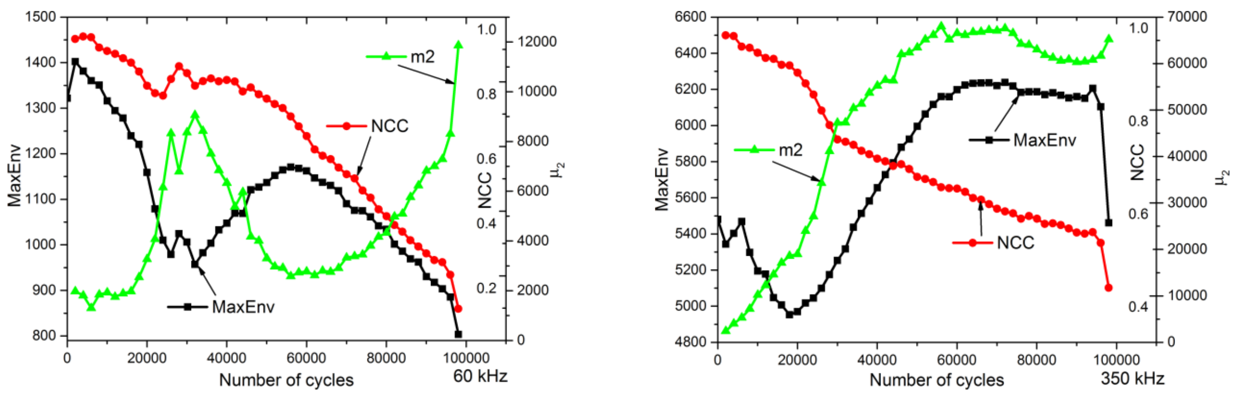

Figure 4.9. Aluminum specimen without welded joint. Variation of informative parameters for (a) 60 kHz and (b) 350 kHz with number of cycles.

The AA7068 is a high strength aluminum alloy thus the fracture toughness is low and the fatigue crack exhibits the fast brittle growth. But it should be noted that the mean value of εyy calculated over the area evaluated by DIC shows a small increase throughout the cyclic test. It is also can be seen from the visual comparison of images corresponding to 0 and 94k cycles that the field on the last image contains higher εyy values.

Fig. 4.9a,b shows the plots of informative parameters of ultrasonic data captured after the cyclic test of AA7068 specimen without welded joint. After the analysis of the data the following peculiarities can be highlighted:

- NCC for both frequencies exhibit downward trend till fracture,
- the values of all informative parameters just before fatigue failure "jump" in the direction of the local trend of the informative parameter allowing to relate it to the formation of fatigue crack and fast growth before fracture,
- for low frequency at 30k cycles there is a local peak (valley) on the plots of $\mu 2$ (MaxEnv) which is difficult to explain and that can be associated either with a calculation error or with the redistribution of Lamb waves propagation caused by small microstructural changes due to fatigue of AA7068, whereas NCC doesn't show such drastic changes.

4.2.2 Specimens with welded joint

Strain distribution fields for different operating time and informative parameters computed for sensed signals for the specimen with welded joint are presented in Fig. 4.10 and Fig. 4.11 correspondingly.

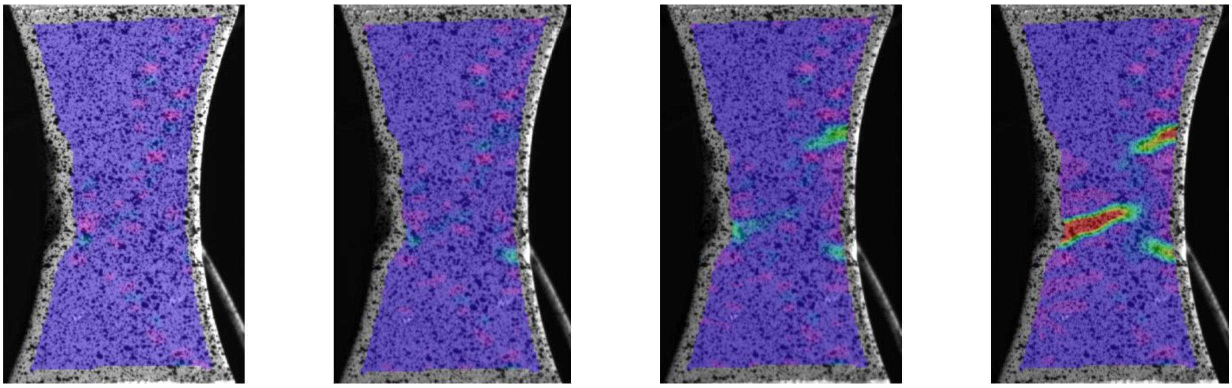

0 cycles 49 000 cycles 67 000 cycles 82 000 cycles

Figure 4.10. Aluminum specimen with welded joint. Vic-3D ε_{yy} strain distribution fields for different operating time.

The εyy strain distribution for the specimen with welded joint is shown in Fig. 4. The quality of the welded joint was poor thus it is seen that there are three macrocracks formed during cyclic loading at which the highest values of strain are observed by DIC method.

Also it should be noted that the formation of these cracks started much earlier than in the case of initial material without welding. Small areas with higher strain values corresponding to the nucleating cracks are observed at the ~45k-49k cycles then the cracks start to propagate until fatigue failure occurs. The plots of informative parameters in Fig. 4.11a,b have a different behavior compared to the non-welded specimen.

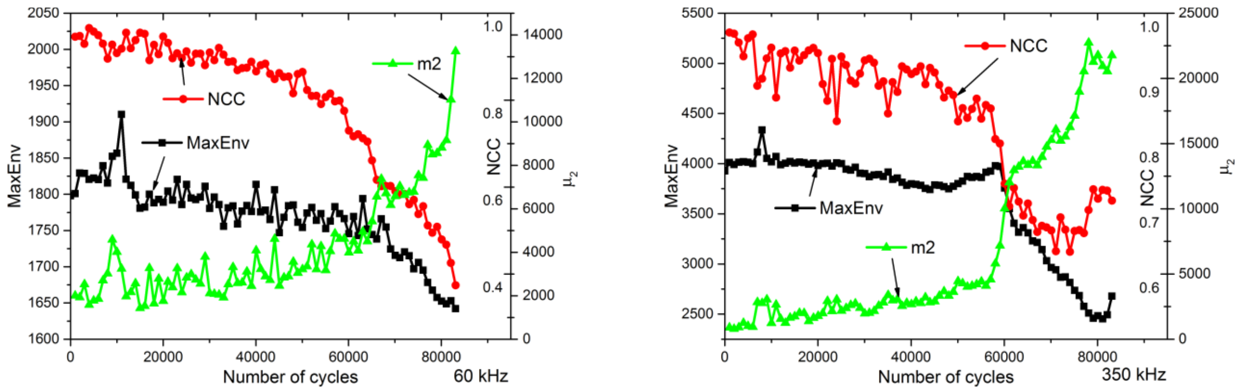

Figure 4.11. Aluminum specimen with welded joint. Variation of informative parameters for (a) 60 kHz and (b) 350 kHz with number of cycles.

The following features can be highlighted:

- The scatter of plots is higher than for the informative parameters without welded joint
- For the low frequency testing all parameters show the stable trend from the beginning of the experiment: MaxEnv decreases with a nearly constant rate until failure, μ2 rises in a similar way and NCC decreases constantly until ~50k cycles, but then the rate of growth increases
- For high frequency NCC curve behaves similarly to that for the low frequency except a small “jump” just before fatigue failure
- MaxEnv during cyclic testing stays nearly the same till 60k cycles after which it starts to go down

TASK FOR SECTION
«FINANCIAL MANAGEMENT, RESOURCE EFFICIENCY AND RESOURCE SAVING»

Student:

Group	Name
4BM4I	Shah Ronak Tushar

Institute	IHTP	**Department**	MSME
Level of education	magistracy	**Specialty**	22.04.01 Material science and technology of materials

Subject of research: «Investigation of Lamb wave ultrasonic technique for non-destructive evaluation of aluminum alloys»

Background to the section «Financial management, resource efficiency and resource saving»:	
The cost of resources for the research: logistics, energy, financial, information and human	*Scientific and technological research is carried out in the laboratory of mechanics of polymer composites ISPMS SB RAS, the project involves 3 workers: scientific adviser, student and researcher*
Norms and standards for resource consumption	*In accordance with GOST 14.322-83 "Rational consumption of materials" and GOST 51541-99 "Energy. Energy efficiency"*
The used system of taxation, tax rates, deductions, discounting and lending	*Deductions of insurance contributions - 30% of payroll*
The list of subjects for the study, design and development:	
1. Assessment of commercial potential, prospects and alternatives of research from the perspective of the resource efficiency	*- Potential consumers of research results,* *- SWOT-analysis of the project*
2. Development of the statute of scientific and technical research	*Not required*
3. Planning of research management process: the structure and schedule of the budget and the procurement organization	*- Planning research studies (purpose and result of epy research, a list of works, complexity of work and schedule)* *- Estimated costs for research*
4. Determination of the resource, financial, budgetary, social and economic efficiency of the project	*- Analysis and evaluation of the scientific and technical level of the project,* *- Evaluation of risks*

List of graphic material:

1. *SWOT Matrix*
2. *The schedule of estimated costs*
3. *Gantt chart*
4. *Evaluation of the resource, financial and economic efficiency*

Date of reference for this section on a line graph	

Task is issued by a consultant:

Position	Name	Degree	Signature	Date
Senior Lecturer, Department of Management	Gavrikova Nadezhda Alexandrovna			

Task is accepted by a student:

Group	Name	Signature	Date
4BM4I	Shah Ronak Tushar		

5 Financial management & Resource efficiency

Fatigue cracks are very dangerous in the aerospace industry, as they can lead to catastrophic failure. The presence of this factor leads to the creation of embedded control systems. There is a network of ultrasound sensors, integrated into the structure used for the detection of defects. The purpose of this section is to determine the viability and success of the research study. There are following tasks of the research:

- Assessment of the commercial potential of research and innovation,
- Drafting schedule and timetable,
- Valuation of logistical, human and financial resources research,
- Evaluation of the resource (resource-saving) and cost-effectiveness.

5.1 Evaluation of the commercial potential of research

5.1.1 Potential users of research results

Potential customers of this study are the enterprises of machine-building industry, located in the territory of the Russian Federation and foreign countries, including shipbuilding, automotive, aerospace, petrochemical, military-industrial complexes, etc. The method is intended to extend the range of the NDT of aircrafts, if the system does not register changes in excess of a certain threshold value. If the method will be used, it can be applied by Boeing, Airbus, etc.

5.1.2 SWOT-analysis

SWOT - (Strengths, Weaknesses, Opportunities and Threats) - is a comprehensive analysis of the study of external and internal environment of the research project. SWOT-analysis is used to study the external and internal environment of the project. SWOT - analysis of the study to evaluate the factors and events that facilitate or hinder the promotion of a method on the market (Table 5.1).

The strengths and weaknesses of the research are described, to identify opportunities and threats to its implementation, which appeared or may appear in its external environment.

The following the conclusions can be made on this information of the strengths, favor the development of the demand for the investigated method. Possible threats: the ability to create more affordable method of the built-in control

Table 5.1 - SWOT-analysis of the present research

Strengths	Possibilities in the environment
Method for SHM studied in this paper, Diagnostic technique is cost-effective & resource-efficient, Application procedure for most solid materials, Availability of qualified manager.	Can be used on a global level, The use in many industries, Adaptation of the method for different languages
Weak sides	Threats to the environment
Increased margins in the design, The possibility of a new method for the SHM, Lack of skilled workers for the application of the concept in industry.	The ability to create a more accessible method of embedded control Lack of demand for a new technique, Closing machine-building enterprises in Russia.

5.2 Planning of scientific and technical research

The proposed work is planned in the following order:

- Determination of the structure of work in the framework of a research study,
- Definition of participants in each phase of the work,
- The establishment of the duration of the work,
- Plotting research

5.2.1 The structure of the work

The complexity of the implementation of the research is estimated by experts in man-days and is probabilistic in nature, as it depends on many factors which are difficult to consider. The study is divided into stages (Table 2).

Determination of the complexity of work. The calculation of the complexity of the study is carried out by a statistical method based on the determination of the expected time of work:

$$t_{\exp i} = \frac{3 \times t_{\min i} + 2 \times t_{\max i}}{5},$$

where $t_{\exp i}$ - is the expected performance of the complexity of the i-th operation, $t_{\min i}$ - the minimum possible the complexity of implementation of a given i-th work (an optimistic estimate: to offer the most favorable conditions), $t_{\max i}$ - the maximum possible performance of the complexity of a given i-th operation (pessimistic estimate: assuming the most unfavorable combination of circumstances).

Table 5.2 – The list of main phases and works

Main phases	**№**	**Content**	**Performers**
Technical task	1	The arrangement of technical task	Panin S.V. – scientific adviser Shah Ronak – student Burkov M.V. - researcher
		Research	
Choice of research field	2	Study of Lamb waves and their implementation in SHM	Shah Ronak
	3	Choice of material to be tested	Burkov M.V., Shah Ronak
	4	Scheduling	Burkov M.V., Shah Ronak
Theoretical and experimental study	5	Scheduling and of experiment on AA2024 and AA7068	Burkov M.V., Shah Ronak
	6	Search for equipment	Panin S.V., Shah Ronak
	7	Experiment on AA2024 and AA7068	Burkov M.V., Shah Ronak
Analysis of results and conclusion	8	Analysis of results	Shah Ronak
	9	Evaluation of the effectiveness	Burkov M.V., Shah Ronak
Preparation of thesis	10	Delivery of report	Shah Ronak

The expected value of the time-consuming work is calculated:

In order to establish the duration of the work the formula in working days is used:

$$T_{wi} = \frac{t_{\exp i}}{N_i},$$

T_{wi} - the duration of one phase in days, $t_{\exp i}$ - the complexity of the expected performance of a work, person-days., N_i - the number of persons performing at the same job at this stage.

For the convenience of constructing a calendar schedule, the duration of the stages in working days is translated in calendar days and is calculated by formula:

$$T_{ki} = T_{wi} \times k,$$

where T_{ki} - the duration of the same work, calendar days, T_{wi} - the duration of a work, working day, k - calendar factor for the translation of working hours in the calendar hours.

Calendar factor is calculated as follows:

$$k = \frac{T_{cdy}}{T_{cdy} - T_{hy} - T_{hy}}$$

T_{cdy} - number of calendar days in a year, T_{wy} - the number of Saturdays and Sundays per year, T_{hy} - the number of holidays per year.

The duration of the stages in working days and the calendar factor:

$$k = \frac{T_{cdy}}{T_{cdy} - T_{hy} - T_{hy}} = \frac{365}{365 - 104 - 16} = 1{,}49$$

Then the length of the stages in working days is calculated (T_k be rounded to whole numbers). The calculation results are shown in Table 5.3.

Table 5.3 - Temporary indicators of research.

№	**Performers**	**Duration**				
		t_{min}, days	t_{max}, days	T_{exp}, days	T_w, w. days	T_k, cal. days
1	Panin S.V., Shah Ronak Burkov M.V.	1	3	2	1	2
2	Shah Ronak	16	36	24	24	30
3	Shah Ronak, Burkov M.V.	6	14	10	5	7
4	Shah Ronak, Burkov M.V.	4	14	8	4	6
5	Shah Ronak, Burkov M.V.	10	25	16	9	14
6	Shah Ronak, Panin S.V.	4	16	9	4	7
7	Shah Ronak, Burkov M.V.	4	14	8	4	6
8	Shah Ronak	1	10	5	2	4
9	Shah Ronak, Burkov M.V.	2	14	7	3	5
10	Shah Ronak	2	5	4	3	5
Summary						86

Table 5.3 shows that in the study of three people (scientific adviser, graduate student and researcher) involved for the job, there are 86 days to perform research

5.3 Scheduling of the research

The Gantt chart – is a horizontal belt graph that work on the topic presented in the extended length of time, characterized by start and end dates of work data. Schedule is built as part of Table 4 by month and week (7 days) for the time period of all the works. At the same time work on the graph are allocated different shading depending on the persons responsible for a particular stage of the work

Table 5.4 – Gant chart.

Phase	Performers	T_k	Feb	Mar	Apr	May	June
The arrangement of technical task	Panin S.V. Shah Ronak Burkov M.V.	2					
Study of Lamb waves and their implementation in SHM	Shah Ronak	30					
Choice of material to be tested	Shah Ronak Burkov M.V.	7					
Scheduling	Shah Ronak Burkov M.V.	6					
Scheduling and of experiment on AA2024 and AA7068	Shah Ronak Burkov M.V.	14					
Search for equipment	Shah Ronak Panin S.V.	7					
Experiment on AA2024 and AA7068	Shah Ronak Burkov M.V.	6					
Analysis of results	Shah Ronak	4					
Evaluation of the effectiveness	Shah Ronak Burkov M.V.	5					
Delivery of report	Shah Ronak	5					

5.4 Estimated costs of research

The costs are all manufacturing forms of consumption of money and measurable in monetary wealth that serve the immediate purpose of production. We expect the cost estimates, including the cost of purchasing the necessary equipment for the research and operating costs. Costs that form the cost of goods (works, services), grouped according to their economic content of the following elements:

$$К_{project} = Q_{mat} + Q_{am.tech} + Q_p + Q_{soc} + Q_{costs} + Q_{other}$$

Material costs reflect the cost of purchased materials and raw materials, which are part of products produced, forming its basis, and are essential components in the manufacture of products. In this study AA2024 and AA7068 specimens were used. Weight 0.1 kg per sample. Cost of 1 m^2 of sandpaper is 120 rubles. The costs of sandpaper, provided that a study is needed 1 m^2 amounted to 120 rubles.

Table 5.5 – Specimens costs

Price of AA7068 1 kg, Rub.	2000
Price of AA2024 1 kg, Rub.	1200
Specimen weight, kg	0.1
Abrasives, Rub.	120
Price of machining of specimen, Rub.	1000
Total costs of each specimen, Rub.	1440

To carry out scientific and technological project requires the following types of equipment: an Instron 5582 electromechanical testing machine, servo-hydraulic Machine Universal Testing Machine 150, the generator of ultrasonic signals AWG-4105 digital oscilloscope Handyscope HS-4, the optical system Vic-3D and PC.

The useful life of each type of equipment:

1) Set the Instron-5582, Universal Testing Machine 150, the generator of ultrasonic signals AWG-4105 digital oscilloscope Handyscope HS-4 and optical system Vic-3D - for the fifth group (test equipment): 10 years.

2) Computer - the third group: 5 years.

Expected material costs (Q_{mat}) are summarized in Table 5.6.

$$Q_{mat} = Q_{gen} + Q_{osc} + Q_{spec} = 35 + 25 + 14{,}4 = 74{,}4k\ Rub.$$

Table 5.6 – Expenses

Materials and equipment	**unit**	**Useful life**	**Amount**	**Price, Rub**	**Expenses, Rub**
Instron-5582	pc	10	1	15000000	15000000
UTM 150	pc	10	1	12000000	12000000
Generator AWG-4105	pc	10	1	35000	35000
Handyscope HS-4	pc	10	1	25000	25000
VIC-3D	pc	10	1	300000	300000
PC	pc	5	1	50000	50000
Specimens	pc	-	10	1440	14400
Summary:					74400

Depreciation of fixed assets - the amount of depreciation on the full restoration of fixed assets, calculated on the basis of their carrying amounts and the depreciation rates approved. The calculation of the costs is taken into account in the year of acquisition and in subsequent years, only the part of the cost, which comes from the aging of fixed assets each year. $Q_{dec.equip}$ is calculated as follows:

$$Q_{t.equip} = \left(\frac{\mathrm{T}_{oper}}{365}\right) \times \mathrm{K}_{equip} \times \mathrm{H}_{\mathrm{a}}$$

where $К_{equip}$ – price of equipment, $Н_a$ – depreciation coefficient.

$$Н_a = \frac{1}{Т_{u.life}}$$

where $Т_{u.life}$ – useful life of equipment

$$Q_{dec.equip} = \left(\frac{Т_{dec.equip}}{365}\right) \times К_{equip} \times Н_a = \left(\frac{5}{365}\right) \times 15000k \times \left(\frac{1}{10}\right) = 20547{,}5$$

$$Q_{dec.equip} = \left(\frac{Т_{dec.equip}}{365}\right) \times К_{dec.equip} \times Н_a = \left(\frac{10}{365}\right) \times 12000k \times \left(\frac{1}{10}\right) = 32875$$

$$Q_{dec.vic} = \left(\frac{Т_{dec.vic}}{365}\right) \times К_{vic.} \times Н_a = \left(\frac{15}{365}\right) \times 300k \times \left(\frac{1}{10}\right) = 1230$$

$$Q_{dec.pc} = \left(\frac{Т_{dec.pc}}{365}\right) \times К_{pc} \times Н_a = \left(\frac{70}{365}\right) \times 50k \times \left(\frac{1}{10}\right) = 956{,}7$$

$$\sum Q_{dec.equip} = Q_{dec.equip} + Q_{dec.equip} + Q_{dec.vic} + Q_{dec.pc}$$
$$= 20547{,}5 + 32875 + 1230 + 956{,}7 = 55609{,}7\ Rub.$$

Results are summarized in Table 5.7.

Table 5.7 – Depreciation of the equipment

Equipment	**$К_{equip}$, Rub.**	**$Т_{exp.equip}$, days**	**$Q_{dec.\ equip}$, Rub.**
Instron-5582	15000000	5	20547,5
UTM 150	12000000	10	32875
VIC-3D	300000	15	1230
PC	50000	70	956,7
Summary			55609,7

Payroll - wages calculated in accordance with the employment of performers, taking into account the district and implementing the tariff rates.

The structure of labor costs includes:

- payment of wages for the actual work performed,
- incentive payments for system regulations,
- The district payout ratio,
- compensation for unused leave,
- other types of payments

Let us assume that the total salary fund

$$S_{sf} = 5 * \frac{40000}{22} + 25 * \frac{30000}{22} + 59 * \frac{25000}{22} = 110200\ Rub$$

Social contributions are expressed as a single social tax, which includes: mandatory contributions by the standards established by the legislation organs of state social insurance, pension fund, state employment fund and medical insurance.

The unified social tax is 30%.

We expect social contributions ($Q_{soc.}$):

$$Q_{soc} = SCT = 0.3 \times S_{sf} = 0.3 \times 110200 = 33060\ Rub$$

Overheads are used for the following:

- maintenance costs,
- depreciation of fixed assets,
- the costs of labor protection and fire safety.

To design departments overhead costs are 200% of the total payroll, then:

$$Q_{ovh} = 2 \times S_{sf} = 2 \times 110200 = 220400\ Rub$$

Other costs - costs which include taxes, fees, contributions to a special non-budgetary funds, the payments on compulsory insurance of property, compensation for inventions and innovations for training, payment services, etc. These costs account for 2% of all costs and calculated using the formula:

$$Q_{other} = 0.02 \times \left(Q_{mat} + S_{sf} + Q_{dec.equip} + SCT\right),$$

$$Q_{other} = 0.02 \times (74400 + 110200 + 55609{,}7 + 33060) = 5465\ Rub$$

Cost of the project ($К_{proj}$):

$$К_{proj} = Q_{mat} + S_{sf} + Q_{dec.equip} + Q_{soc} + Q_{evh\text{х}} + Q_{other},$$

$$К_{proj} = 74400 + 110200 + 55609{,}7 + 33060 + 220400 + 5465 = 499135\ Rub$$

The planned accumulation (PA) is calculated. The project cost includes 30% of the profits, thus:

$$PA = 0.3 \times К_{proj} = 0.3 \times 499135 = 149740\ Rub$$

The project cost is:

$$C = К_{proj} + PA = 499135 + 149740 = 648875\ Rub$$

Table 5.8 summarizes the costs.

Table 5.8 - Estimated costs of the research project

Expense	Name	Sum
Material expenses	Q_{mat}	74400
Depreciation of equipment	$Q_{dec.equip}$	55609,7
Labour costs	P	110200
Social taxes	Q_{soc}	33060
Overheads	Q_{ovh}	220400
Other expenses	Q_{other}	5465
Estimated costs	K_{proj}	499135
Profit	PA	149740
project cost	C	648875

5.5 Determination of the resource and the financial efficiency of scientific and technical research

5.5.1 Analysis and assessment of the scientific and technical level of the project

To determine the scientific and technical level of the project, its scientific value, technical relevance and effectiveness it is necessary to calculate the rate of scientific and technological level (STL). STL ratio is calculated by the method of scores. The method consists in assigning a certain number of points on the scale adopted. The overall assessment of the result is calculated by the sum of the scores according to all indicators, taking into account the weight characteristics.

The formula for determining the overall assessment:

$$NTL = \sum_{i=1}^{n} k_i * M_i,$$

where k_i – weight coefficient *i*-th parameter, M_i – value of *i*-th parameter.

Table 5.9 – Weight coefficient of STL

Parameter	Weight coefficient
The level of novelty	0.5
Theoretical level	0.2
The possibility of implementing	0.3

Table 5.10 – Scale of novelty scores

Score	Level
1-4	Low STL
5-7	Average STL
8-10	Relatively high STL
11-14	High STL

Table 5.11 - The significance of the theoretical levels

Parameters of the importance of the theoretical levels	**Score**
Setting of the laws, the development of a new theory	10
A deep study of the problems, a comprehensive analysis, the interdependence between the factors	8
Development of a method (algorithm, device, programs)	6
The analysis of relationships between factors (availability hypothesis, explanation versions, practical advice)	2
Description of individual factors (material properties, experience, results)	0.5

Table 5.12 - Ability to implement in time and scope

Implementation period	**Score**
During the early years	10
From 5 to 10 years	7
More than 10 years	4
The scale of implementation	**Score**
One or more companies	2
Sector	7
National economy	10

STL calculation: $k_1=0.5$, $k_2=0.2$, $k_3=0.3$, $k_4=0.3$, $M_1=9$, $M_2=8$, $M_3=10$, $M_4=7$.

$$STL=0.5*9+0.2*8+0.3*10+0.3*7=11.2$$

According to the obtained values of the coefficient of the scientific and technical level can be said of quite a high STL of the project, its scientific value, technical relevance and effectiveness.

5.6 Risk assessment during project creation

Conducting a risk assessment is carried out by qualified experts on the basis of their views on the current situation in the country and the region, as well as the information about the suppliers and contractor’s equipment and their working conditions.

5.6.1 Description of risk groups

Project risks in their composition can be grouped into the following groups according to their nature (social, economic, environmental, technical, and political).

The social risks are:

- Loss and theft of property at the stage of production,
- Failure to comply with safety regulations,

- Lack of teamwork.

The economic risks are:

- The rise in prices,
- Unscrupulous vendors and performers,
- Changes in taxation,
- Unexpected expenses,

Technological risks include:

- Low quality components manufacturing,
- Faulty equipment,
- Danger of damage during transport equipment,
- Risk of damage to the components during installation.

Possible environmental risks:

- Pollution of the territory,
- Application and transportation of toxic materials,
- High level of injury.

Political risks:

- Criticism of the media,
- Violation of the existing regulatory legislation,
- Possible change of political course of the party and the government

5.6.2 Assessment of the importance of risk groups

In the risk importance is assessed by a probability of their occurrence. On a scale from 0 to 100 percent: 100 - will come exactly, 75 - is likely to occur, 50 - the situation of uncertainty, 25 - the risk is not likely to occur, 0 - the risk does not occur.

Risk assessment of the importance of estimated weighting factor (w_i). Importance is assessed on a scale b_i. Within each group score goes from simple to complex. The sum of the weighting coefficients must be equal to one.

Table 5.13 - Examination of social risks

№	Risks	Probability (p_i)	Importance (b_i)	Weight (w_i)	Total value (P_i*w_i)
1	Loss and theft of property at the stage of production	30	9	0.31	9.3
2	Failure to comply with safety regulations	10	7	0.24	2.4
3	Dissatisfaction of consumers with the high cost of final products	50	10	0.34	17
4	Lack of teamwork	15	3	0.11	1.65
Total			29	1	30.35

Table 5.14 - Examination of economic risks

№	Risks	Probability (p_i)	Importance (b_i)	Weight (w_i)	Total value (P_i*w_i)
1	Inflation	100	4	0.22	22
2	Unscrupulous vendors and performers	60	6	0.33	19.8
3	Changing tax	20	3	0.16	3.2
4	Unexpected expenses	70	5	0.29	20.3
Total			18	1	65.3

Table 5.15 - Examination of technological risks

№	Risks	Probability (p_i)	Importance (b_i)	Weight (w_i)	Total value (P_i*w_i)
1	Low quality components	50	10	0.31	15.5
2	Equipment failure	30	10	0.31	9.3
3	Risk of damage to equipment during transportation	30	6	0.19	5.7
4	Risk of component damage during installation	40	6	0.19	7.6
Итого			32	1	38.1

Table 5.16 - Examination of environmental risks

№	Risks	Probability (p_i)	Importance (b_i)	Weight (w_i)	Total value (P_i*w_i)
1	The pollution of the surrounding area	30	6	0.42	12.6
2	The use and handling of toxic materials	10	4	0.29	2.9
3	High injury level	10	4	0.29	2.9
Итого			14	1	18.4

Table 5.17 - Examination of political risks

№	**Risks**	**Probability (p_i)**	**Importance (b_i)**	**Weight (w_i)**	**Total value (P_i*w_i)**
1	Criticism in the mass media	4	4	0.2	0.8
2	Violation of the existing regulatory legislation	0	7	0.35	0
3	Possible change of political course of the party and the government	0	9	0.45	0
Итого			20	1	0.8

Table 5.18 - Identification of common project risks

№	**Risks**	**Rank (P_i)**	**Weight (W_i)**	**Probability (v_i)**	**Total value (w_i*v_i)**
1	Social	8	0.2	30.35	6.07
2	Economic	10	0.3	65.3	19.59
3	Technological	10	0.3	38.1	11.43
4	Ecological	5	0.1	18.4	1.84
5	Political	5	0.1	0.8	0.08
Итого		38			39.01

The final draft risk assessment is 39.01%. This value suggests that the risk of the project is considered acceptable, and it can be done. Based on the section "Financial management, resource efficiency and resource conservation" the following conclusions on the project can be made:

1. According to the assessment of commercial potential and innovative project opportunities, together with strengths, favor the development of the demand for the project. Possible threats: the ability to create more affordable method of SHM,

2. In drawing up the project schedule the required number of days of work was calculated - 86 days and for work 3 people involved on the project, as well as a Gantt chart that allows you to coordinate the work plan has been used,

3. The budget scientific and technological project totaled 648875 rubles,

4. The final draft risk assessment is 39.01%. This value suggests that the risk of the project is considered acceptable, and it can be done.

TASK FOR SECTION
«SOCIAL RESPONSIBILITY»

Student:

Group	Name
4BM4I	Shah Ronak Tushar

Institute	IHTP	**Department**	MSME
Level of education	magistracy	**Specialty**	22.04.01 Material science and technology of materials

Subject of research: «Investigation of Lamb wave ultrasonic technique for non-destructive evaluation of aluminum alloys»

Background to the section «Social responsibility»:	
1. Features the object of study and its scope	*The aim of this work is to conduct a test experiment on aluminum alloy using Lamb waves. The experiment was conducted in the laboratory of mechanics of polymer composites ISPMS SB RAS. In this work the following equipment was used: electromechanical tensile machine Instron 5582, servo-hydraulic machine 150 Universal Testing Machine, ultrasonic signal generator AWG-4105 digital oscilloscope Handyscope HS-4, the optical system VIC-3D, personal computer.*
The list of subjects for the study, design and development:	
1. Operational safety *1.1. The analysis of identified hazardous factors in the design and operation of the equipment used:* *1.2. The analysis of identified harmful factors in the design and operation of the equipment used:*	*Identify potential harmful and hazardous factors. Of the harmful the following have been identified: poor lighting in the room, industrial noise and microclimate with low humidity and low air movement. Among the hazards there are: the risk of electrical shock and fire occurrence*
2. Environmental Safety:	*Analyze the impact of the disposal of used aluminum alloy specimens, fluorescent lamps, on the electronic engineering: residential zone, the atmosphere and the hydrosphere. Describe the ways to address environmental safety.*
3. Safety in emergencies:	*Identify potential emergency situations and develop measures for their prevention and elimination of consequences:* *- Typical Siberian climate and possible sabotage*
4. Legal and organizational issues of security:	*Consider the legal norms of the labor legislation and organizational measures at the work area layout. The paper provides a list of state standards, building codes, etc.*

Date of reference for this section on a line graph	

Task is issued by consultant:

Position	Name	Degree	Signature	Date
Professor, Department of ecology and safety	Fedorchuk Yurii Mitrofanovich	PhD		

Task is accepted by student:

Group	Name	Signature	Date
4BM4I	Shah Ronak Tushar		

6 Social responsibility

In this final qualifying work is carried out research of a technique using Lamb waves to assess the status of AA2024 and AA7068 specimens. The paper used a number of methods for the preparation, testing and investigation of aluminum alloy specimens, but the working area is quite small. It includes:

- Room with electromechanical tensile machine Instron 5582 and servo-hydraulic testing machine Universal Testing Machine 150,
- Room with a personal computer for data processing, writing reports and articles.

In this section, the paper is being analyzed in the field of safety and standards for workers, society and the environment in the interaction and work on the presented equipment, developed a set of measures of technical, organizational, operating and legal nature, minimizing the negative effects of the planned activities, and will review the legislative and regulatory documents.

6.1 Operational safety

On the human dangerous (causing injury) can affect the process of his work, and harmful (disease-causing) factors of production.

Table 6.1 – Dangerous and harmful factors of research

Activity types	Factor *(GOST 12.0.003-74)*		Regulations
	Harmful	Hazardous	
Laboratory research: 1.Preparation for the test, the sample binding to the grips of the machine, 2. Run of the test, monitoring of the process of aluminum alloy straining 3. The processing of the data on a PC.	1. Low humidity, 2. Reduced air speed, 3.Insufficient lighting of the working area, 4. Excessive noise.	1. The electric current, 2. Flammability	General hygiene requirements for working zone air GOST 12.1.005-88. Hygienic requirements for the microclimate of industrial premises. SanPiN 2.2.4.548-96 Electrical safety. General requirements and nomenclature of species protection GOST R 12.1.019-2009 The parameters of natural and artificial lighting SNIP 23-05-2010 Noise. General safety requirements. GOST 12.1.003-83 Occupational Safety Standards System.

Hazardous production factor - a production factor whose impact on the worker, under certain conditions, lead to injury or other sudden health deterioration.

Harmful production factor - production factor, the impact of which on operating, under certain conditions, leads to a disease or a decrease in efficiency.

Harmful factor depending on the intensity and duration of exposure can be dangerous. Dangerous and harmful factors have a classification that is established and regulated by GOST 12.0.003-74.

6.2 Analysis of the identified hazards

Low humidity. During the work in the laboratory ISPMS RAS has been found that there is room in low humidity. Low humidity promotes intense evaporation of sweat from the body surface and, as a result, leads to a rapid heat transfer, and to excessive drying of the skin. Also, too low humidity leads to rapid fatigue human, as well as deterioration in the perception and memory. Low humidity in the room caused by the fact that the studies were carried out in the winter time, and that means acting heating season, when the air humidity is 20-25% instead of 40% standard. Special devices called air humidifiers are used to increase the humidity. As wetting agents can be used with open containers of water, wet tissue, as well as spraying water in the air.

Reduced mobility of air. Reduced mobility room air often causes stuffiness - it is associated with poor air circulation, reducing the amount of oxygen and increase in carbon dioxide. At this could affect the lack of ventilation and air conditioning systems. Solve the problem will help ventilation and installation in the workroom of fans or air conditioning systems, but should bear in mind that, according to SanPiN 2.2.4.548-96 increased speed of the air in the room is feeling a draft, so the mobility of air should not exceed 0.1 m / s.

Table 6.2 – Requirements for the microclimate

Period of the year	Job Category	Temperature, ° C	Relative humidity,%	Air speed, m / s
Cold	Light - Ia	22-24	40-60	0.1
	Light - Ib	21-23	40-60	0.1
Warm	Light - Ia	23-25	40-60	0.1
	Light - Ib	22-24	40-60	0.2

Works are divided into three categories based on the severity of the common energy body. Work related to the engineers - the developers considered the category of light work. Optimal and allowable temperature indicators, relative humidity and air velocity in the working area of industrial premises should be as given in Table 2 [GOST 12.1.005-88].

In the room where the tests were carried out, not all indicators agree with the regulations: temperature, relative humidity and air velocity are shown in Table 6.3.

Table 6.3 – Climate conditions in the laboratory of MPCM ISPMS

Period of the year	**Job Category**	**Temperature, ° C**	**Relative humidity,%**	**Air speed, m / s**
Cold	light	20	25	≤ 0.1

To ensure optimal performance and acceptable microclimate in the room during the cold season should be applied protection jobs from the glazed surfaces of window openings, so that was not cool, but since the new windows installed in the laboratory, the use of protective equipment is not required. During the warm period of the year must be protected from direct sunlight.

Insufficient illumination of the working area

According to the SP 52.13330.2011 in the laboratory, where there is a periodic monitoring of the progress of the production process, a constant presence of people in the room, lighting, while general lighting system, must not be less than 150 Lux, which did not fit with the actual lighting in the mechanics laboratory IMPA RAS. Inadequate lighting affects the functioning of the visual apparatus, that is, determines the visual performance, on the human psyche and its emotional state causes fatigue of the central nervous system, resulting from ongoing efforts to identify a clear or doubtful signals. It is therefore necessary to make the design of artificial lighting for uniform distribution.

The room in which the work was conducted fluorescent lamps for artificial lighting were used. Natural light is provided by two side windows. It is important to emphasize that the lack of illumination of the working space can lead to poor eye health, such as myopia.

Calculation of the total artificial lighting uniform horizontal work surface is performed by the coefficient of luminous flux, which takes into account the luminous flux reflected from the ceiling and walls. A space length is 6 m, width B is 5 m, height is 3 m. Working height above the floor surface h_p is 1 m. According to the SP 52.13330.2011 the illuminance not lower than E = 150 lux is to be made, under discharge visual work.

Area: $S = A \times B$, where A – length, m, B – width, m. So $S = 6 \times 5 = 30\ m^2$

Reflectance of walls with windows without curtains p_W=50%, ceiling p_C=70%. Safety factor, which takes into account the pollution luminaire for rooms with low dust release, is K_1=1.5. Ratio of non-uniformity of lamps for Z=1.1.

Choosing fluorescent lamp LD-80, which is equal to the luminous flux is 4800 lm, the power is 80 watts. Choose fixtures with fluorescent lamps type LPO-01-2h35. This lamp has two lamps of 36 watts each, lamp length is 1235 mm, width - 145 mm.

Integral optimality criterion lamps location is the value of λ, which for fluorescent lamps with protective grille is in the range 1.1-1.3. Accepting λ=1,2, distance from ceiling fixtures (overhang) is h_c=0.05 m.

The height of the lamp above the work surface is defined by the formula:

$$\mathrm{h} = \mathrm{h_l} - \mathrm{h_p} - \mathrm{h_c},$$

h_l – height of the lamp above the ground, the height of the suspension. The lowest permissible height of suspension above the floor for two-lamp fixtures LPO-01: h_l=2.5 m.

The height of the lamp above the work surface is defined by the equation:

$$\mathrm{h} = \mathrm{h_l} - \mathrm{h_p} - \mathrm{h_c} = 3 - 1 - 0.05 = 1{,}95\ m$$

Distance between the two lamps or rows is calculated by:

$$\mathrm{L} = \lambda \times \mathrm{h} = 1{,}2 \times 1{,}95 = 2{,}34 \text{ m.}$$

Number of lamps in the room:

$$\mathrm{Nb} = \frac{\mathrm{B}}{\mathrm{L}} = \frac{5}{2{,}34} = 2{,}14 \approx 2 \text{ pc.}$$

Number of lamps in a row:

$$\mathrm{Na} = \frac{\mathrm{A}}{\mathrm{L}} = \frac{6}{2{,}34} = 2{,}56 \approx 2 \text{ pc.}$$

Total amount of lamps:

$$\mathrm{N} = \mathrm{Na} \times \mathrm{Nb} = 2 \times 2 = 4 \text{ pc.}$$

Distance from lamps to walls is calculated by:

$$\mathrm{l} = \frac{\mathrm{L}}{3} = \frac{2{,}34}{3} = 0{,}78 \text{ m.}$$

The lamps are placed in two rows. Fig 6.1 presents the plan of the room and allocation of the fluorescent lamps.

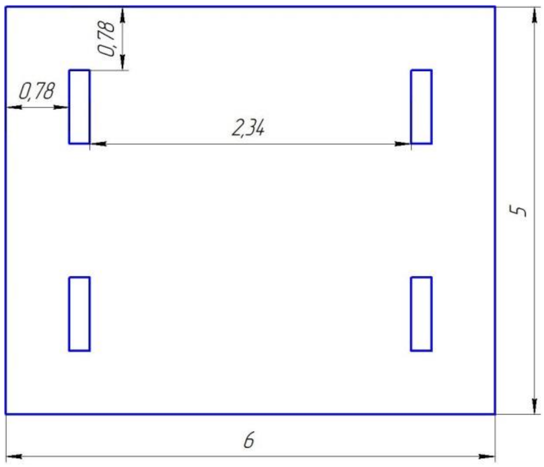

Figure 6.1 – Plan of room and lamps.

Index of the room is calculated by the equation:

$$i = \frac{A \times B}{h \times (A + B)} = \frac{6 \times 5}{1.95 \times (6 + 5)} = 1.2$$

The coefficient of flux use that shows a part of flux which goes to the working place for the LPO-01 at p_p= 70%, p_S=50% and i = 1.2 is η=0.47.

The demanded flux for fluorescent lamps is calculated by the equation:

$$F_d = \frac{\mathrm{E} \times \mathrm{A} \times \mathrm{B} \times \mathrm{K}_з \times Z}{N \times \eta} = \frac{150 \times 6 \times 5 \times 1.5 \times 1.1}{4 \times 0{,}47} = 3949{,}5\ lm$$

The following condition is performed:

$$-10\% \leq \frac{F_{ld} - F_d}{F_{ld}} \times 100\% \leq 20\%$$

$$\frac{4800 - 3949.5}{4800} \times 100\% = 17\%$$

Thus: -10% ≤17%≤ 20% , the flux of the lamp is enough for illumination.

Noise excess

Noise is a fluctuation of various physical nature with complex spectral and temporal structure. Noise creates a significant burden on the human nervous system, giving him a psychological impact. It provokes an increase in the background noise of blood stress hormones such as norepinephrine and epinephrine, cortisol. The noise can slow down the reaction and inhibit the human central nervous system, causing changes in heart rate and breathing rate, and provokes cardio - vascular disease, hypertension and gastric ulcer.

Background noise premises create six concurrent computers. Periodically there is noise coming from the printer or telephones. The permissible noise levels for the programmer, according to SanPiN 2.2.4 / 2.1.8.562-96 presented in Table 4.

Table 4 - Maximum permissible sound pressure levels

Type of working activity Frequency	**Levels of sound pressure, dB, at different frequency, Hz**								
	1,5	3	25	50	00	000	000	000	000
Work with high accuracy in laboratories with noisy equipment in rooms with noisy calculation computers	103	91	83	77	73	70	68	66	64

Background noise premises create six concurrent computers. Periodically there is noise coming from the printer or telephones. The permissible noise levels for the programmer, according to SanPiN 2.2.4 / 2.1.8.562-96 presented in Table 4.

6.3 Analysis of identified hazards projected production environment

Electricity. Electrical safety is a system of organizational and technical measures and means to ensure the protection of people from harmful and dangerous effects of electric current, electric arc, electromagnetic fields and static electricity.

Electrical installations are classified by voltage: with a nominal voltage up to 1000 V (room without heightened risk) up to 1000 with the presence of an aggressive environment (rooms with increased risk) and more than 1000 V (especially dangerous).

With regard to the danger of electric shock to persons distinguished:

1. Premises without heightened risk in which there are no conditions that create an increased or special danger,

2. Premises with increased risk, which are characterized by the presence of one of the following conditions, which create an increased risk of: humidity, conductive dust, conductive flooring (metal, excavation, concrete, brick, etc.), high fever, the possibility of simultaneous touches human to have a connection to the land of steel structures, technological devices, on the one hand, and the metal housings of electrical equipment - on the other,

3. Particularly dangerous areas, which are characterized by the presence of equipment over 1000 and one of the following conditions, which create a particular

danger: extreme dampness, or reactive organic medium, at the same time two or more high-risk conditions. Territory placing external electrical installations against the danger of electric shock to persons equated to particularly hazardous areas.

The room in which the test is a laboratory, and falls into the category without heightened risk of electric shock, as the humidity in the room is 25% and the air temperature 20 ° C, in addition, there are no conductive floors, conductive dust. But, nevertheless, in a room, the following measures of protection against electric shock: lack of access to live parts to accidental contact, all live parts isolated and protected. The inaccessibility of live parts is achieved by their reliable isolation, the use of protective enclosures (housings, covers, corrugated, etc.), the location of the live parts on the inaccessible heights.

Flammability. Explosion and fire hazard premises are divided into categories A, B, B1 - B4, D and E, and building - into categories A, B, C, D and E. As fire danger exterior installation are divided into categories of AN, BN, BH, Gn and Dn.

According to NPB 105-03 Laboratory Mechanics in IMPA RAS refers to the category B4 - combustible materials that can burn in contact with oxygen. Examples of such materials in the laboratory are - office paper, paper wallpaper, plastic, from which the PC case is made and its components, and testing machine, linoleum and other fire cause could serve as a short-circuiting the electrical fire, which could spill over from neighboring premises arising, for one reason or another, and we should not exclude the possibility of sabotage, namely arson.

According to the degree of fire resistance, this room belongs to the 1st degree of fire resistance according to SNIP 2.01.02-85 (made of brick, which refers to the difficult combustible materials).

In order to eliminate the causes of fires and localization in the room the following measures must be carried out of the laboratory: a) Use only serviceable equipment, b) the holding of periodic briefings on fire safety, c) disconnect electrical power and lighting when the alleged lack of staff or at the end of work, d) smoking in strictly designated area, e) not to block the escape routes and emergency exits.

Localization and liquidation deck is used in the initial stage for primary fire extinguishing. Primary extinguishing agents usually applied to the fire brigade arrived.

Fire extinguishers, water-foam (OHVP-10) can be used to extinguish fires without the presence of electricity. Carbon dioxide (OU-2) and powder extinguishers are designed to extinguish electrical installations under voltage up to 1000 V. In addition, powder extinguishers are used to extinguish the documents. To extinguish the live parts of electrical installations and portable use dry chemical, such as OP-10.

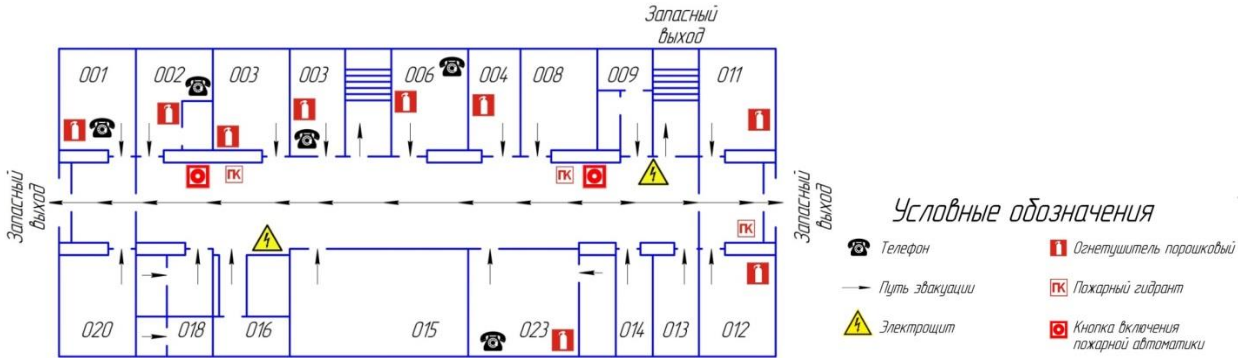

Figure 6.2 – Evacuation plan of ISPMS SB RAS building N1

In public buildings and facilities on each floor should be placed at least two portable fire extinguishers. Fire extinguishers should be located in prominent places near the exits of the premises at a height of not more than 1.35 m. Placement of primary fire extinguishing equipment in the corridors, passages should not interfere with the safe evacuation of people.

The building of IMPA RAS complies with fire safety requirements, namely, the presence of security and fire alarms, evacuation plan, combinations of powder and carbon dioxide fire extinguishers, plates indicating the direction to the emergency (evacuation) exit. Figure 6.2 shows an evacuation plan, the laboratory room in which the tests were conducted, №001.

6.4 Ecological safety

The presented research work does not directly have any negative factors that could affect the ecology of our planet. However, it is worth considering the disposal, namely, a waste of aluminum alloy specimens, fluorescent lamps and electronic equipment (computers, printers, etc). Disposal of such equipment is quite complex, since such waste have a complex structure. The immediate processing of most of the components includes sorting them, the subsequent homogenization and sent for reuse, i.e., preliminary grinding or remelting.

Fluorescent lamps are "extremely dangerous" types of waste. The content of mercury in all fluorescent lamps is three to five milligrams of mercury. In view of this need to provide certain storage conditions, their use and disposal. According to the sanitary norms store mercury-containing waste must be sealed in special containers, access to unauthorized persons in such containers should be banned. Transporting lamps storage area shall be carried out organizations that specialize in disposing of hazardous waste. It is strictly prohibited publication of such waste, such as fluorescent lamps, on the landfill of municipal solid waste. For the processing of aluminum alloy specimens it is necessary to address the metallurgy to further melting and processing.

Metallurgical production has a considerable influence on the environment for venting the combustion products of fuels in the blast furnaces. Thus emitted into the atmosphere of carbon dioxide and hydrogen sulfide, as well as the dust from the graphite content of different light or heavy metals (aluminum, antimony, arsenic, mercury, lead, tin and the like. D.), Depending on the nature and purpose of metallurgical production.

Harmful substances are oxides of carbon, sulfur and nitrogen. The annual flow in the atmosphere of sulfur dioxide measured environmental experts in the amount of 100-150 million tonnes. With its emissions associated with the formation of so-called acid rain, which cause great harm to the flora and fauna, destroy various buildings, monuments. Pollution steelworks is due to the wastewater that come different chemical compounds formed during the smelting of metals. Water metallurgical production consumes large quantities, so it is always companies are building in the vicinity of rivers and lakes, or create special hydraulic structures, in which it is stored.

As a result of pollution of the environment the health is deteriorating, life expectancy reduces and mortality increases.

Proceeding from the above the company in accordance with the SanPiN 2.2.1 / 2.1.1.1200-03 necessary to organize the sanitary protection zones, that will reduce the impact of pollution on the air (chemical, biological, physical) to the values established hygienic standards.

The buffer zone is not allowed to post: residential development, including individual houses, landscape and recreational areas, recreational areas, etc...

Allowed to place within the boundaries of the sanitary protection zone of an industrial facility or building production facilities and for maintenance workers and the specified object for the operation of an industrial facility (production).

It is also necessary to limit the amount of harmful emissions into the atmosphere, soil and water.

6.5 Protection in Emergencies

The study presented in this thesis work, conducted in the city of Tomsk with a continental-cyclonic climate. Natural phenomena (earthquakes, floods, droughts, hurricanes and so on. D.) In this city are very rare.

Possible emergency situations at the facility in this case, can be: cold or sabotage.

To Siberia in the winter season is characterized by frost. Achieving critical low temperature leads to accidents and life-support systems of heating, the suspension of work, frostbite, and even loss of life. In the case of frozen pipes replacement heaters must be provided. Their number and power should be enough to work in the production is not stopped.

Emergencies arising from acts of sabotage, there are more and more often.

Often, these threats are false. But there are explosions and in reality. According to GOST R 22.3.03-94 to prevent the likelihood of the diversion, the company should be equipped with video surveillance, round the clock security, system throughput, a reliable communications system, and to avoid the dissemination of information about the system of the object, location, facilities and equipment in the rooms, security systems, warning devices their place of installation and the amount. Officials carried out every six months training to simulate the action in the event of an emergency evacuation

6.5.1 Legal and organizational issues of security

SanPiN 2.2.4.548-96. Hygienic requirements for the microclimate of industrial premises, SanPiN 2.2.1 / 2.1.1.1278-03. Hygienic requirements for natural, artificial and combined coverage of residential and public buildings, SNIP 21-01-97. Fire regulations, SanPiN 2.2.1 / 2.1.1.1200-03. Sanitary protection zones and sanitary classification of enterprises, structures and other objects, SanPiN 2.2.2 / 2.4.1340-03. The sanitary and epidemiological rules and norms "Hygienic requirements for personal computers and the organization of work." SP 60.13330.2012 Heating, ventilation and air conditioning, PND F 12.13.1-03. Guidelines. Safety at work in analytical laboratories (general provisions), GOST 12.1.005-88. OSSS General hygiene requirements for working zone air, GOST R 12.1.019-2009. Electrical safety. General requirements and nomenclature of species protection, GOST 12.1.004-91. Fire safety. General requirements, GOST 17.1.3.06-82. Protection of Nature. Hydrosphere. General requirements for the protection of groundwater, GOST 30775-2001 Resources saving. Waste management. Classification, identification and coding of waste, GOST R 22.0.07-95. Safety in emergencies. The sources of man-made emergencies. Classification and nomenclature of damaging factors and their parameters. Federal law of December 21, 1994 № 68-FZ. On protection of population and territories from emergency situations of natural and technogenic character, GOST 12.2.049-80 Occupational Safety Standards System. Production equipment. Are common ergonomic requirements, GOST 12.2.032-78. Occupational safety standards system. Workplace when sitting. General ergonomic requirements, GOST 21889-76. The system of "man-machine". The chair of the human operator. General ergonomic requirements.

Conclusions

Static testing

Investigations for static test of AA2024 confine that the lamb wave propagations are sensitively through the changing of properties, we enclose the studying of lamb wave behavior for with weld joints and without welded joints specimens during different stage of strain. Also confine the test technique are accessible for Fatigue test. The result graphs (Fig. 3.4 & 3.5) shows that epoxy layers and PZTs are not affected by strain due to loading within the yield stress. The loading for fatigue testing lie below the yield point,

The static tensile tests of AA7068 specimens were performed with acquisition of ultrasonic data. After the digital processing of raw data, the set of informative parameters was calculated including MaxEnv and NCC characterizing the changes in propagated signal amplitude and its shape correspondingly. After the analysis of the results we can conclude following:

1) Small size of the specimen leads to the very complex and inexplicable results. There are a lot of boundary reflections from sides of the specimen as well as the influence of grips of testing machine which is very difficult to assess.

2) It is seen that low frequency testing (using A0 mode of Lamb waves) doesn't provide good results of quantitative analysis of signals. High frequency tests (mainly S0 mode) provide better explainable results allowing it to be used for characterizing the changes of stress-strain state of the specimen during loading.

3) The first packet of the signal for all specimens was used to calculate the MaxEnv parameter, while the entire signal was analyzed by NCC and m2. But according to the plots the last parameters allow to make better conclusions about the state of the specimen. Thus it is necessary to make a close look investigation of variance of the shape of the first packet of sensed signal, because now NCC and m2 are influenced by "tail" of the signal which behavior is difficult to explain in contrast to the first travelled packet that is less influenced by the side reflections and grips.

Fatigue Testing

Analysis of AA2024 obtained results shows that proposed technic for integral structural damage and health evaluation is sensitive during cycling test. The dependence of signal characteristic parameters on the number of cycles was determined and the behavior of these parameters is not linear and allows once to characterize the state and processes, which are arise within the material from cycling load.

According to the alignment of sensor-generator it could be concluded that the pass generator-PZT3 (on the opposite side of the specimen) is more sensitive to defects accumulation processes and crack growth as the pass generator-PZT2 (on the same side of the specimen).

Summing up all obtained results from fatigue testing of AA7068 specimens, it could be concluded that combined implementation of optical and Ultrasonic NDT methods results in consolidation of their advantages and allows overcoming the limitations. Optical methods provide the information of the specimen surface and cannot go inside the materials. However, inspection based on Lamb wave in a case of small specimen and large wavelength does not acquire the information about small damages and cannot identify their location. Moreover, it is not convenient in the case of result analysis by a human and requires complicated interpretation techniques and mapping algorithm, where optical methods, which provide desirable information without significant issues would be helpful.

It should be noted that due to small size of the specimens the analysis of ultrasonic results is complicated because of boundary reflections from specimen edges and the influence of the testing machine grips.

After the analysis of the results obtained for the AA7068 specimens without welded joint the following should be concluded – NCC for both frequencies exhibits the downward trend till fracture indicating that signal changes throughout the test and just before fatigue failure the values of informative “jump” in the direction of the local trend of the informative parameter allowing to relate it to the formation of fatigue crack and fast growth before fracture, On the specimen with welded joint, it could be concluded due to the earlier crack forming (compared to the initial specimen) in the poor quality weldability, informative parameters have slightly different behavior. It emerges in the more consistent parameters trends without considerable ambiguities. The amplitude smoothly decreases throughout the fatigue test until the point of crack initiation after which the amplitude drops allowing us to conclude about the major influence of the crack growth process on ultrasonic signal propagation.

List of publications

There are four International publications created during the research

1. Investigation of Lamb Wave Based Ultrasonic Technique for AA2024 Evaluation at Static Tensile Loading by A.V. Byakov, A.V. Eremin, M.V. Burkov, R.T. Shah, P.S. Lyubutin, S.V. Panin // Key Engineering Materials, ISSN: 1662-9795, Vol. 685, pp 394-398
2. Lamb Wave Based Ultrasonic Technique for AA2024 Fatigue Evaluation by A.V. Byakov, A.V. Eremin, M.V. Burkov, R.T. Shah, P.S. Lyubutin, S.V. Panin // Key Engineering Materials ISSN: 1662-9795, Vol. 685, pp 399-402,
3. Lamb wave ultrasonic evaluation of welded AA2024 specimens at tensile static and fatigue testing by M V Burkov, A V Byakov, R T Shah, P S Lyubutin, S V Panin // IOP Conf. Series: Materials Science and Engineering 93 (2015) 012025
4. Numerical analysis of processes of deformation and fracture of AA7068 using Lamb wave technique, Pichugov V.V., Shah R.T. Burkov M.V. // Proceeding of “Materials and technologies of new generations in modern materials science”, June 9-11, 2016, Tomsk, Russia.

List of references

1 Aerospace & space materials by M.peter s & C.leyens , Institute of material research, Germen aerospace center, Germany

2 http://www.aluminiumleader.com/history/industry_history/

3 http://aerospaceengineering.aero/advancements-in-aerospace-engineering-materials/

4 Varin, R.A. Intermetallics: Crystal structures. In Concise Encyclopedia of Structure of Materials, Martin, J., Ed., Elsevier: Amsterdam, The Netherlands, 2007, pp. 235–238. [Google Scholar]

5 https://eh.net/encyclopedia/the-history-of-the-aerospace-industry/

6 Why aircraft fail? by S. J. Findlay and N. D. Harrison

7 Campbell, G.S., and Lahey, R.T.C., (1983) A survey of serious aircraft accidents involving fatigue fracture, Vol. 1 Fixed-wing aircraft, National Aeronautical Establishment, Canada

8 Campbell, G.S., and Lahey, R.T.C., (1983) A survey of serious aircraft accidents involving fatigue fracture, Vol. 2 Rotary-wing aircraft, National Aeronautical Establishment, Canada

9 Sp. G. Pantelakis and Al Th. Kermanidis Multiscale Fatigue Crack Initiation and Propagation of Engineering Materials, 2008, Springer

10 Suresh S. Fatigue of Materials, second ed., Cambridge University Press,1998, ISBN 0521578477, 700 pages

11 Schijve J. Fatigue Cracks, Plasticity Effects and Crack Closure, Four Lectures on Fracture Mechanics, 1l. No. 1-L, (1978)

12 Elber W. Damage Tolerance in Aircraft Structures, ASTM Spec. Tech.Publ.486, (1981) 230

13 Minakawa K. and McEvily AJ. On Crack Closure in the near Threshold Region, Scripta Metallurgica, 15 (1981) 633-636

14 Matrukanitz RP (1990) Selection and weldability of heat-treatable Aluminium alloys. ASM Handbook-Welding, Brazing and Soldering 6:528–536

15 Knipstrom KE, Pekkari B (1997) Friction stir welding process goes commercial. Weld J 76:55–57

16 Maggiolino S, Schmid C (2007) Corrosion resistance in FSW and in MIG welding techniques of AA6XXX. J Mater Process Technol (in press)

17 Moreira PMGP, de Figueiredo MAV, de Castro PMST (2007) Fatigue behaviour of FSW and MIG weldments for two aluminium alloys. Theor Appl Fract Mech 48:169–177

18 Ma ZY, Mishra RS (2003) Cavitation in super plastic 7075 aluminium alloys and prepared via friction stir processing. Acta Mater 51:3551–3569
AWS Welding Hand book (1996) 3:232–235

19 M. Eibl, C. M. Sonsino, H. Kaufmann and G. Zhang (2003) Fatigue assessment of laser welded thin sheet aluminium, International Journal of Fatigue, 25(8), 719–731.

20 A. Ali, X. An, C. A. Rodopoulos, M. W. Brown, P. O'Hara, A. Levers and S. Gardiner (2007) The effect of controlled shot peening on the fatigue behaviour of 2024-T3 aluminium friction stir welds, International Journal of Fatigue, 29.(8), 1531–1545.

21 O. Hatamleh, J. Lyons and R. Forman (2007) Laser and shot peening effects on fatigue crack growth in friction stir welded 7075-T7351 aluminium alloy joints, International Journal of Fatigue, 29(3), 421–434].

22 E. Sh. Statnikov, V. N. Vityazev and O. V. Korolkov, Study of Comparative Characteristics of Ultrasonic Impact and Optimization of Deformation Treatment Processes, 5th World Congress on Ultrasonics, Paris, France, 2003.

23 S. Pilli and C. A. Rodopoulos (2007) Use of Ultrasonic Impact Treatment as an Effective Surface Engineering Treatment to Improve the Corrosion-Fatigue Properties of Al-2024-T351, EUROMAT 2007, 10–13 Sept, 2007, DGM.

24 E. Sh. Statnikov, V. N. Vityazev and O. V. Korolkov, Study of Comparative Characteristics of Ultrasonic Impact and Optimization of Deformation Treatment Processes, 5th World Congress on Ultrasonics, Paris, France, 2003.

25 I. I. Mukhanov and Yu.M. Golubev, Strengthening Steel Components by

Ultrasonically Vibrating Ball, Vestn. Mashin., No 11, 1966 (in Russian).
26 C. A. Rodopoulos, A. Th. Kermanidis, E. Statnikov, V. Vityazev and O. Korolkov (2007) The effect of surface engineering treatments on the fatigue behaviour of 2024-T351 Aluminium alloy, Journal of Materials Engineering and Performance, 16,1 30–34
27 ASTM E709 - 15 Standard Guide for Magnetic Particle Testing
28 https://www.asnt.org/MinorSiteSections/AboutASNT/Intro-to-NDT
29 https://www.nde-ed.org/index_flash.htm
30 A Brief Description of NDT Techniques A Paper By Mark Willcox & George Downes
31 http://nde.edu/
32 http://www.iste.co.uk/
33 State of the Practice and Art for Structural Health Monitoring of Bridge Substructures
34 An introduction to structural health monitoring by Charles R. Farrar and Keith Worden Engineering Science and Applications Division, Los Alamos National Laboratory Los Alamos, Los Alamos, NM 87545, USA 2 Department of Mechanical Engineering, University of Sheffield, Mappin Street, Sheffield S1 3JD, UK
35 Bently, D. E. & Hatch, C. T. 2003 Fundamentals of rotating machinery diagnostics. New York, NY: ASME Press.
36 Boller, C. & Buderath, M. 2007 Fatigue in aerostructures—where structural health monitoring can contribute to a complex subject. Phil. Trans. R. Soc. A 365, 561–587. (doi:10.1098/rsta.2006.1924
37 Ch. 1 Introduction to SHM by Daniel BALAGEAS
38 Cheeke, J.D.N.: Fundamentals and Applications of Ultrasonic Waves. CRC Press, Boca Raton (2002)) 9. (Montalvão, D., Maia, N.M.M., Ribeiro, A.M.R.: A review of vibration-based structural health monitoring with special emphasis on composite materials. The Shock and Vibration Digest 38(4), 295–324 (2006)

39 Rose, J.L.: Ultrasonic Waves in Solid Media. Cambridge University Press, New York (1999)

40 Wang, C.S., Chang, F.-K.: Built-in diagnostics for impact damage identification of composite structures. In: Chang, F.-K. (ed.) Proceedings of the 2nd International Workshop on Structural Health Monitoring, Stanford, CA, USA, September 8-10, 1999, pp. 612–621. Technomic Publishing Co (1999)

41 Tang, B., Henneke, E.G.: Lamb-wave monitoring of axial stiffness reduction of laminated composite plates. Materials Evaluation 47, 928–934 (1991)

42 Tan, K.S., Guo, N., Wong, B.S., Tui, C.G.: Experimental evaluation of delaminations in composite plates by the use of Lamb waves. Composites Science and Technology 53, 77–84 (1995)

43 Alleyne, D.N., Cawley, P.: The interaction of Lamb waves with defects. IEEE Transactions on Ultrasonics, Ferroelectrics and Frequency Control 39(3), 381–397 (1992)

44 Guo, N., Cawley, P.: Lamb waves for the NDE of composite laminates. In: Thompson, D.O., Chimenti, D.E. Review of Progress in Quantitative NDE, vol. 11, pp. 1443–1450. Plenum Press, New York (1992)

45 Cawley, P., Alleyne, D.: The use of Lamb waves for the long range inspection of large structures. Ultrasonics 34, 287–290 (1996)

46 Alleyne, D.N., Cawley, P.: Optimisation of Lamb wave inspection techniques. NDT&E International 25(1), 11–22 (1992)

47 Roh, Y.-S., Chang, F.-K.: Effect of impact damage on Lamb wave propagation in laminated composites. In: Sun, C. (ed.) Proceedings of the ASME International Mechanical Engineering Congress and Exposition (Dynamic Responses and Behavior of Composites), San Francisco, CA, USA, November 12-17, 1995, pp. 127–138 (1995)

48 Rose, J.L.: Guided wave nuances for ultrasonic nondestructive evaluation. IEEE Transactions on Ultrasonics, Ferroelectrics and Frequency Control 47(3), 575–583 (2000)

49 Lee, B.C., Staszewski, W.J.: Modelling of Lamb waves for damage detection in metallic structures: part I - wave propagation. Smart Materials and Structures 12, 804– 814 (2003)

50 National Institute for Occupational Safety and Health, http://www.cdc.gov/NIOSH/

51 The National Aeronautics and Space Administration (NASA): Derailed. System Failure Case Studies 1(5), 1-4 (2007)

52 Hahn, S. L. Hilbert Transforms in Signal Processing (1996), Artech House, Norwood, USA

53 https://en.wikipedia.org/wiki/Envelope_(waves)

54 M. Choi, B. Sweetman Efficient Calculation of Statistical Moments for Structural Health Monitoring, Department of Civil Engineering, Texas A&M University, USA

55 https://en.wikipedia.org/wiki/Cross-correlation

56 Peters, W.H. and Ransom, W.F., Digital imaging techniques in experimental stress analysis, Opt. Eng., 21(3), pp. 427-431, 1892

57 Schreier, H.W., Braasch, J.R. and Sutton, M.A., Systematic Errors in digital image correlation caused by gray-value interpolation, Opt. Eng., 39(11), pp. 2915-2921, 2000

58 Contactless and fullfield 3d-deformation measurement for impact and crash tests Ralf Lichtenberger, Hubert Schreier LIMESS Messtechnik u. Software GmbH, D-75180 Pforzheim

59 Investigation of Lamb Wave Based Ultrasonic Technique for AA2024 Evaluation at Static Tensile Loading by A.V. Byakov, A.V. Eremin, M.V. Burkov, R.T. Shah, P.S. Lyubutin, S.V. Panin // Key Engineering Materials, ISSN: 1662-9795, Vol. 685, pp 394-398

60 Lamb Wave Based Ultrasonic Technique for AA2024 Fatigue Evaluation by A.V. Byakov, A.V. Eremin, M.V. Burkov, R.T. Shah, P.S. Lyubutin, S.V. Panin // Key Engineering Materials ISSN: 1662-9795, Vol. 685, pp 399-402,